

Variability and accuracy of shear strength measurements in soft soils

Master Thesis

Variability and accuracy of shear strength measurements in soft soils

Master Research GE04-1520

Part of: Master Programme Earth Surface, and Water at Utrecht University
Student: Alexander van Duinen (student number 5771307)
UU Supervision: Esther Stouthamer (UU) and Gilles Erkens (UU / Deltares)
Date: May 5, 2019 (version 2)

Content

Abstract	1
1 Introduction	3
1.1 Background	3
1.2 Objective of the project	4
1.3 Outline	4
2 Literature review	5
2.1 WBI 2017 approach	5
2.2 Sources of uncertainty	6
2.2.1 Uncertainties CPT	6
2.2.2 Uncertainties laboratory tests	7
2.2.3 Sample disturbance	8
2.2.4 Transformation uncertainty	10
2.3 Statistical models to describe spatial variability	10
2.3.1 Dutch practice	10
2.3.2 International literature	12
2.3.3 Spatial variability based on finite scale models	12
2.3.4 Spatial variability based on fractal models	15
2.3.5 Summary	16
2.4 Knowledge gaps	16
3 Study areas	17
3.1 Measurement sites	17
3.2 Geological setting	17
4 Methods	21
4.1 Introduction	21
4.2 In situ tests	22
4.3 Laboratory tests	23
4.4 Spatial variability	26
4.5 Undrained shear strength behaviour	26
4.6 Cone penetration tests	27
4.7 Dissipation tests	29
4.8 Field vane tests	31
4.9 Sensitivity framework	36
5 Results: Natural variability	41
5.1 Introduction	41
5.2 Stratigraphy derived from CPT data	41
5.3 Correction and normalization of CPT data	47
5.4 Variability cone penetration resistance	49
5.5 Correlation length	54
6 Results: Sample disturbance	61
6.1 Introduction	61
6.2 General soil properties	61
6.3 Coefficient of consolidation from dissipation tests	63
6.4 Undrained shear strength from field vane tests	65
6.5 Sample length and determination of soil unit weight	69

6.6	Intrinsic undrained shear strength ratios from reconstituted samples	72
6.7	Undrained shear strength ratios from intact natural samples	74
6.8	Comparison of undrained shear strength ratios from reconstituted and natural samples	76
6.9	Intrinsic compression parameters from reconstituted samples	79
6.10	Compression parameters and stress sensitivity from intact natural samples	81
6.11	Sensitivity from field vane tests, triaxial tests and constant rate of strain tests	82
6.12	Undrained shear strength ratio from field vane tests and triaxial tests	85
6.13	Effect of natural variability	90
7	Discussion	95
7.1	Natural variability	95
7.2	Sample disturbance	96
7.3	Implications	98
8	Conclusions	101
9	Recommendations	103
9.1	Natural variability	103
9.2	Sample disturbance	104
	References	107
	Appendices	
A	Measurement sites	111
B	Legend borehole descriptions	115

Figures

Figure 2.1	Correlation between the undrained shear strength s_u from laboratory tests and the net cone penetration resistance q_{net} to derive the empirical correlation factor N_{kt} .	6
Figure 2.2	Differences in shear strength and stiffness of Lierstranda clay (Norway) for Block sampler, 54 mm Piston sampler and 75 mm Piston sampler.	9
Figure 2.3	Differences in measured shear strength for Bothkennar Clay due to various reasons of disturbance.	9
Figure 2.4	Effect of sampling systems on compression behaviour and yield stress of Bothkennar Clay.	10
Figure 2.5	Relation between variance reduction factor, number of tests and characteristic lower bound value.	12
Figure 2.6	Example of empirical correlation function and fitted theoretical correlation function.	13
Figure 2.7	Semivariogram with lag distance on the x-axis, range and sill.	14
Figure 2.8	Fractal model with recurring pattern of variability.	16
Figure 3.1	Locations of the research sites.	18
Figure 3.2	Longitudinal section through the Rhine-Meuse delta.	19
Figure 4.1	Derivation of the coefficient of consolidation from CPTu dissipation tests.	29
Figure 4.2	Relationship between normalised pore water pressure and dimensionless time factor T^* .	31
Figure 4.3	Relationship between β and plasticity index I_p .	33
Figure 4.4	Observed excess pore water pressures during and following vane insertion.	34
Figure 4.5	Correction factor to adjust FVT measurements.	35
Figure 4.6	Graph of the void index I_v and vertical effective stress with the position of the Intrinsic Compression Line (ICL) and the Sedimentation Compression Line (SCL).	37
Figure 4.7	Compression lines from three sites plotted with the Intrinsic Compression Line (ICL).	38
Figure 4.8	Sensitivity framework.	39
Figure 5.1	Measured cone penetration resistance q_c at location AC 075.	41
Figure 5.2	Measured cone penetration resistance q_c at location AC 090.	42
Figure 5.3	Measured cone penetration resistance q_c at location AC 251.	42
Figure 5.4	Photo of samples from borehole B-100 at location AC 251.	43
Figure 5.5	Begemann classification based on friction ratio R_f at location AC 251 and borehole B-100.	44
Figure 5.6	Been and Jefferies(1992) classification based on soil type behaviour index I_c .	44
Figure 5.7	Interpreted stratigraphy at location AC 075.	45
Figure 5.8	Interpreted stratigraphy at location AC 090.	46
Figure 5.9	Interpreted stratigraphy at location AC 251.	46
Figure 5.10	Corrected cone penetration resistance q_{net} at location AC 251.	47
Figure 5.11	Normalized dimensionless cone penetration resistance Q_t at location AC 251.	48
Figure 5.12	Measured cone penetration resistance q_c per soil layer at location AC 075.	48
Figure 5.13	Normalized dimensionless cone penetration resistance Q_t per soil layer at location AC 075.	49
Figure 5.14	Variability of the corrected cone penetration resistance q_{net} at location AC 075.	50
Figure 5.15	Variability of the corrected cone penetration resistance q_{net} at location AC 090.	50
Figure 5.16	Variability of the corrected cone penetration resistance q_{net} at location AC 251.	51

Figure 5.17	Variability of the corrected cone penetration resistance q_{net} of clays versus the vertical effective stress σ'_{vi} .	51
Figure 5.18	Variability of the corrected cone penetration resistance q_{net} of humic clays versus the vertical effective stress σ'_{vi} .	52
Figure 5.19	Variability of the corrected cone penetration resistance q_{net} of peat versus the vertical effective stress σ'_{vi} .	52
Figure 5.20	Variability of the corrected cone penetration resistance q_{net} of peat versus the vertical effective stress σ'_{vi} .	53
Figure 5.21	Semivariogram of the measured cone penetration resistance V_{qc} versus lag distance τ of various clays.	55
Figure 5.22	Semivariogram of the normalized cone penetration resistance V_{Qt} versus lag distance τ of various clays.	55
Figure 5.23	Correlation function of the measured cone penetration resistance ρ_{qc} versus lag distance τ of various clays.	56
Figure 5.24	Correlation function of the normalized cone penetration resistance ρ_{Qt} versus lag distance τ of various clays.	56
Figure 5.25	Correlation function of the measured cone penetration resistance ρ_{qc} versus lag distance τ of various peat.	57
Figure 6.1	General soil properties of the Lekdijk site near Schalkwijk.	62
Figure 6.2	General soil properties of the Waaldijk site at Waardenburg.	62
Figure 6.3	General soil properties of the Achterwaterschap AC 251 site.	62
Figure 6.4	Measured dissipation behaviour and fit of the dissipation behaviour.	63
Figure 6.5	Coefficient of consolidation c_h from dissipation tests compared with coefficient of consolidation from oedometer tests for the Lekdijk near Schalkwijk.	64
Figure 6.6	Coefficient of consolidation c_h from dissipation tests for the Achterwaterschap.	64
Figure 6.7	Normalised velocity V of the FVT compared with the normalised velocity of the CPT for the Lekdijk near Schalkwijk.	65
Figure 6.8	Normalised time to failure T_f of the FVT for the Lekdijk near Schalkwijk.	66
Figure 6.9	Normalised velocity V of the FVT compared with the normalised velocity of the CPT for the Achterwaterschap.	66
Figure 6.10	Normalised time to failure T_f of the FVT for the Achterwaterschap.	67
Figure 6.11	$s_{u,measured}$ of the FVT for the Lekdijk near Schalkwijk.	67
Figure 6.12	$s_{u,measured}$ of the FVT for the Achterwaterschap.	68
Figure 6.13	$s_{u,corrected}$ of the FVT for the Achterwaterschap.	69
Figure 6.14	Sample length in the field and in the laboratory before and after extrusion of the samples at the Lekdijk near Schalkwijk.	70
Figure 6.15	Variability of soil unit weight for the Lekdijk near Schalkwijk.	71
Figure 6.16	Variability of soil unit weight for the Achterwaterschap.	71
Figure 6.17	$s_{u,peak}/\sigma'_{vc}$ and $s_{u,ultimate}/\sigma'_{vc}$ versus soil unit weight from triaxial compression tests on reconstituted samples.	72
Figure 6.18	$s_{u,peak}/\sigma'_{vc}$ versus plasticity index I_p and organic matter content OC from triaxial compression tests on reconstituted samples.	73
Figure 6.19	Strength gain of reconstituted samples measured by laboratory vane tests on reconstituted samples.	74
Figure 6.20	s_u/σ'_{vi} versus soil unit weight from triaxial compression tests on reconstituted and intact samples.	75
Figure 6.21	s_u/σ'_{vi} versus soil unit weight from triaxial compression tests on reconstituted and intact samples; $s_{u,ult}/\sigma'_{vi}$ of the intact samples compared with $s_{u,ult}/\sigma'_{vi}$ of the reconstituted samples.	75
Figure 6.22	s_u/σ'_{vi} versus soil unit weight from triaxial compression tests on reconstituted and intact samples; $s_{u,peak}/\sigma'_{vi}$ of the intact samples compared with $s_{u,ult}/\sigma'_{vi}$ of the reconstituted samples.	76

Figure 6.23	s_u/σ'_{vi} versus soil unit weight from triaxial compression tests on reconstituted and intact samples; $s_{u,ult}/\sigma'_{vi}$ of the intact samples compared with $s_{u,ult}/\sigma'_{vi}$ of the reconstituted samples.	77
Figure 6.24	s_u/σ'_{vc} versus soil unit weight from triaxial compression tests on reconstituted and intact samples; $s_{u,peak}/\sigma'_{vc}$ of the intact samples compared with $s_{u,ult}/\sigma'_{vc}$ of the reconstituted samples.	78
Figure 6.25	s_u/σ'_{vi} versus plasticity index I_p from triaxial compression tests on reconstituted and intact samples; $s_{u,peak}/\sigma'_{vi}$ of the intact samples compared with $s_{u,ult}/\sigma'_{vi}$ of the reconstituted samples.	78
Figure 6.26	s_u/σ'_{vi} versus organic matter content OC from triaxial compression tests on reconstituted and intact samples; $s_{u,peak}/\sigma'_{vi}$ of the intact samples compared with $s_{u,ult}/\sigma'_{vi}$ of the reconstituted samples.	79
Figure 6.27	Constant rate of strain tests on reconstituted samples interpreted within the sensitivity framework.	80
Figure 6.28	Values of the intrinsic compression index C_c^* and e_{100}^* derived from the CRS tests on reconstituted samples.	80
Figure 6.29	Values of the intrinsic compression index C_c^* and e_{100}^* derived from the CRS tests on reconstituted samples plotted against organic matter content OC.	81
Figure 6.30	Values of the intrinsic compression index C_c^* and e_{100}^* derived from the CRS tests on reconstituted samples plotted against dry unit weight.	81
Figure 6.31	Constant rate of strain tests on intact sample 31 at NAP +0.92 m from the Waaldijk.	82
Figure 6.32	Constant rate of strain tests on intact sample 2 at NAP -5.70 m from the Achterwaterschap.	82
Figure 6.33	Comparison of S_t from the FVT and triaxial compression tests (TXC) on intact samples and S_σ from the constant rate of strain tests (CRS) at the Lekdijk	83
Figure 6.34	Comparison of S_t from the FVT and triaxial compression tests (TXC) on intact samples and S_σ from the constant rate of strain tests (CRS) at the Waaldijk.	84
Figure 6.35	Comparison of S_t from the FVT and triaxial compression tests (TXC) on intact samples and S_σ from the constant rate of strain tests (CRS) at the Achterwaterschap.	84
Figure 6.36	Comparison of S_t from the FVT and triaxial compression tests (TX) on intact samples for three sites.	85
Figure 6.37	Comparison of s_u/σ'_{vi} from the FVT ($s_{u,peak_corr}$) and triaxial compression tests (TXC) on intact samples at the Lekdijk near Schalkwijk.	86
Figure 6.38	Comparison of s_u/σ'_{vi} from the FVT ($s_{u,peak_corr}$) and triaxial compression tests (TXC) on intact samples at the Waaldijk at Waardenburg.	87
Figure 6.39	Comparison of s_u/σ'_{vi} from the FVT ($s_{u,peak_corr}$) and triaxial compression tests (TXC) on intact samples at the Achterwaterschap.	88
Figure 6.40	Comparison of s_u/σ'_{vi} from the FVT and triaxial tests (TX) for three sites.	89
Figure 6.41	Comparison of s_u/σ'_{vi} versus plasticity index I_p from the FVT and triaxial tests (TX) for three sites.	90
Figure 6.42	Comparison of s_u/σ'_{vi} versus organic matter content OC from the FVT and triaxial tests (TX) for three sites.	90
Figure 6.43	Comparison of s_u derived from FVT ($s_{u,peak_corr}$), CPTs and triaxial tests (TXC) for the Lekdijk site.	91
Figure 6.44	Comparison of s_u derived from FVT ($s_{u,peak_corr}$), CPTs and triaxial tests (TXC) for the Waaldijk site.	92
Figure 6.45	Comparison of s_u derived from FVT ($s_{u,peak_corr}$), CPTs and triaxial tests (TXC) for the Achterwaterschap AC 251 site.	93
Figure A.1	Location Lekdijk at S44_239_00 near Schalkwijk.	111
Figure A.2	Location Waaldijk at TG198+015 in Waardenburg.	112
Figure A.3	Location Achterwaterschap at AC 251 near Alblisserdam.	112
Figure A.4	Location AC 075 at the north dike of the drainage canal Achterwaterschap.	113

Figure A.5 Location AC 090 at the north dike of the drainage canal Achterwaterschap. 113

Tables

Table 4.1	Overview of the performed field tests.	23
Table 4.2	Specifications of the performed Field vane tests.	23
Table 4.3	Overview of the performed laboratory tests.	25
Table 4.4	Boundaries of the soil types according to Been and Jefferies (1992).	28
Table 5.1	Statistics of the cone penetration resistance per soil layer for class 1 cone and class 1+ cone.	54
Table 5.2	Derived horizontal correlation lengths of the measured cone penetration resistance q_c based on the class 1 cones and class 1+ cones. The related variance reduction factor is also given.	58
Table 6.1	Mean values of the intrinsic undrained shear strength ratios from triaxial compression tests on reconstituted samples.	73

Abstract

Spatial variability and uncertainty regarding the subsoil play an important role in assessment and design of water defences, public infrastructure and houses. The objective of this research was to quantify the uncertainties of the shear strength of the subsoil due to spatial variability in horizontal direction and sample disturbance to optimize the characteristic lower bound of the shear strength and to improve the reliability of assessments of slope stability of dikes.

Characteristic lower bound values of the soil parameters, in which the uncertainties are taken into account, are usually applied in assessment and design analyses. In this research spatial variability and sample disturbance are studied. These are two aspects which are important in the common Dutch approach for the assessment of slope stability of water defences in The Netherlands (WBI 2017; I&M, 2017), which uses CPTs and empirical correlations between the cone penetration resistance of CPTs and the undrained shear strength obtained from laboratory tests. CPTs with correlations are used as it is thought that the in situ state of the soil (stress history) is important for the operational shear strength. As the in situ state is very variable CPTs are applied to determine the local in situ state and shear strength. It is common practice for infrastructure projects to perform CPTs with an interval of 100 m or more. For the assessment of slope stability of a dike the nearest CPT or the CPT with the lowest shear strength are used to estimate the undrained shear strength for the slope stability analysis of a cross section of a dike.

In this research three series of 15 CPTs with a distance interval of 7 m are performed along the Achterwaterschap. The CPT logs give a detailed insight in the variability of the stratigraphy and cone penetration resistance on the scale of a potential slip failure (50-100 m). It is found that the stratigraphy and cone penetration resistance vary considerably. Calculated horizontal correlation lengths vary between 3 and 33 m, dependent on deposits and location. So the correlation length is not a characteristic of a depositional environment, but it is a stochastic variable. Measurement accuracy of the CPT cones and uncertainty about pore water pressure and soil unit weight also play a role in the analyses. Based on these findings it is concluded that one CPT is only an absolute arbitrary measure of the shear strength. The characteristic lower bound values of the in situ state of the soil and the undrained shear strength have to be derived from a series of CPTs. This series of CPTs can belong to a dike section for example.

Sample disturbance is important in the WBI 2017 approach as the CPT correlations rely on the results of laboratory tests. The CPT correlations often show substantial uncertainty, and sample disturbance is thought to be a relevant aspect regarding to this uncertainty. Sample disturbance is studied with a comparison of the sensitivity and undrained shear strength from field vane tests with the sensitivity and undrained shear strength derived from intact samples. This is done for three sites: Waaldijk at Waardenburg, Lekdijk near Schalkwijk and Achterwaterschap. It is concluded that sample disturbance occurs for clayey soils with a soil unit weight of 16 to 19 kN/m³. These clayey soils are found below the dikes at the Waaldijk and Lekdijk sites. At these sites the sensitivity and undrained shear strength based on the laboratory tests is low compared to the results from the field vane tests. Sample disturbance is also determined from the recovery ratio of the samples and the volume changes of the samples in the laboratory due to extrusion of the samples from the sample tubes. At the Achterwaterschap site no effect of sample disturbance is found. When the effect of sample disturbance on the undrained shear strength is compared with the spatial variability of the undrained shear strength based on four CPTs close to the boreholes and the field vane tests, it is concluded that the spatial variability of the undrained shear strength is larger than the effect of sample disturbance. Therefore the relative low shear strength of the intact samples can be partly explained by spatial variability. As sample disturbance cannot be indicated as a very important factor for the uncertainty of CPT correlations, it is likely that various other aspects contribute to this uncertainty. Therefore it is recommended for the

derivation of CPT correlations to improve the sampling techniques, to apply cross checks and to analyse the involved data carefully. Field vane tests can play an important role in these cross checks, however further study of the interpretation regarding the drainage conditions and the corrections for strain rate is needed.

1 Introduction

1.1 Background

Uncertainties of geotechnical soil parameters are an important issue in the assessment of failure mechanisms of water defences (dikes), public infrastructure and houses. Different failure mechanisms that are the result of the behaviour of the subsurface can cause failures of water defences, public infrastructure and houses. Repairing such failures and the resulting damage are costly for water boards, Ministry of Public Works and local authorities, but not least can lead to flooding of inhabited areas. Reduction of the uncertainties will lead to higher reliability of the assessment of the failure mechanisms.

It is well known that the strength, stiffness and compressibility of the (commonly) Holocene deposits are important variables in the assessment of these failure mechanisms. It is therefore worrying that from site investigations and laboratory tests it becomes clear that these geotechnical soil parameters considerably vary. The in situ state of the soil (often called stress history, which can be described by the void ratio, yield stress, overconsolidation ratio, state parameter or relative density) is highly variable. The in situ state of the soil is often the most variable parameter in geotechnical engineering problems, like liquefaction (sandy layers), slope instability (clayey and peaty layers), settlement and subsidence. The in situ state depends on the depositional environment and soil forming processes (Mitchell & Soga, 2005). The in situ strength, stiffness and compressibility are strongly connected with the in situ state of the soil.

The observed spatial variability of the geotechnical soil parameters is a result of the heterogeneity in the depositional and post-depositional processes. Commonly the spatial variability in horizontal direction is however not investigated in geotechnical practice, as it is assumed that a strong horizontal correlation results in a conservative design (Cao et al., 2017; Fenton, 1999). Measurement errors and interpretation uncertainties also contribute to the variability. Test devices which are used in the field and the laboratory have measurement errors (Deltares, 2009; Peuchen & Terwindt, 2014). At least for very soft soils these measurement errors can be relatively large compared to the strength and stiffness of the soil. Laboratory tests are dealing with sample disturbances (Tanaka, 2000; Hight et al., 2003; Lunne et al., 2006; L'Heureux et al., 2018). Interpretation of the field tests, such as the cone penetration test (CPT) and Field Vane Test (FVT), and laboratory tests is not always straightforward (Chandler, 1988; Teh & Houlsby, 1988; Lu et al., 2004; Morris & Williams, 2000; Schnaid, 2008 and many others). For example, when using CPTs in site investigations the interpretation of these tests is complex because of alternating mm or cm thin layers with different geotechnical soil properties or differences in drainage conditions resulting in drained or undrained or partially drained soil behaviour or differences in stiffness in different layers and much more.

These different sources of uncertainty in the soil parameters are responsible for a large part of the reliability of the assessment of the different failure mechanisms. To prevent for the occurrence of the different failure mechanisms usually a conservative estimate (characteristic lower bound) of the soil parameters is taken into account. With a statistical approach a safe estimate is made in order to deal with the variability of the soil parameters and to overcome the interpretation difficulties and other errors. As far as this variability of the soil parameters is a real property of the soil this common approach is correct. This approach is however too conservative when the soil parameters are underestimated, leading to expensive solutions for the infrastructural constructions.

For the assessment of slope stability of water defences in The Netherlands guidelines are made available by the Dutch Ministry of Infrastructure and Water Management (WBI 2017; I&M, 2017). CPTs are an important tool in these guidelines to derive the shear strength and the in situ state of the subsoil. These guidelines are used in this study as a reference for the common approach in The Netherlands to derive geotechnical soil parameters from field and laboratory tests and to determine characteristic lower bound values of the shear strength.

1.2 Objective of the project

The objective of this research is to quantify the uncertainties of the shear strength of the subsoil due to spatial variability in horizontal direction and sample disturbance to optimize the characteristic lower bound of the shear strength and to improve the reliability of assessments of slope stability of dikes.

With regard to the spatial variability the sub objective of the research is to compose an instruction for the schematization of the spatial variability of soil layers based on one or more CPTs for the purpose of the assessment of the slope stability of flood defences. The instruction will be fitted onto the WBI 2017 system. Starting point is the natural variability of the subsoil, i.e. variability induced by differences in the sedimentary environment, variability of soil properties, effects of creep, ripening and variability in pore water pressures etc. The effect of a coincidental pre-loading of the soil in a dike section in the past due to human activities is outside the scope of this research.

Concerning sample disturbance the sub objective of the research is to verify whether sample disturbance is an important aspect which introduces uncertainty in the derivation of the empirical correlation factor N_{kt} which correlates the cone penetration resistance of CPTs to the undrained shear strength of triaxial tests performed in the laboratory. The underlying goal of the project is to optimize the field and laboratory research in order to reduce the uncertainty in the correlation factor N_{kt} . Another goal is to improve the Protocol CPT testing for s_u determination (Deltares, 2016a) and the Protocol for laboratory tests for investigations on flood defences (Deltares, 2016b).

1.3 Outline

Chapter 2 contains a literature review. This chapter describes the WBI 2017 approach regarding the determination of the shear strength of the subsoil based on CPTs and laboratory tests. The literature review also examines the sources of uncertainty concerning CPTs, laboratory tests and sample disturbance. Furthermore chapter 2 gives a review of existing statistical models to describe spatial variability.

The research is conducted at the Lekdijk near Schalkwijk, Waaldijk at Waardenburg and the Achterwaterschap near Alblasterdam. These measurement sites and their geological setting are described in Chapter 3. In the field CPTs, CPTs with dissipation tests, Field Vane Tests (FVT) and boreholes are conducted. In the laboratory classification tests, constant rate of strain tests and triaxial tests on reconstituted samples and intact samples are performed.

In Chapter 4 the applied methods for the interpretation of the field and laboratory tests are given.

In Chapter 5 the interpretation and analysis of the CPT data from the site investigation regarding the spatial variability of the subsoil is described. Based on the CPTs and boreholes the stratigraphy is deduced. For the most important layers where sufficient data is available the spatial variability in horizontal direction is quantified using the semivariogram and correlation function.

In Chapter 6 the results of the in situ tests and the laboratory tests concerning sample disturbance are discussed, as well as the comparison of the results from the in situ tests and the laboratory tests. The comparison of the in situ tests and laboratory tests is based on the stress sensitivity S_σ , strength sensitivity S_t and undrained shear strength s_u . These parameters are used to assess the effect of sample disturbance. In Paragraph 6.13 the relevance of sample disturbance in the context of spatial variability on very short distances (meter scale) is evaluated.

Chapter 7 gives the discussion of the obtained results of the research and the implications for the engineering practice. Important points of discussion are the interpretation of the FVT and the determination of the stress sensitivity S_σ and strength sensitivity S_t .

Chapter 8 and 9 give the conclusions and recommendations respectively.

2 Literature review

2.1 WBI 2017 approach

In The Netherlands the WBI 2017 guideline for slope stability (I&M, 2016) gives guidance for the assessment of flood defences regarding the stability of slopes. For assessments (and design) of slope stability of flood defences cone penetration tests (CPTs) are important tests for soil investigation. CPTs can be applied both for interpretation of the stratigraphy and determination of stress history and shear strength.

The idea behind application of CPTs to determine the in situ undrained shear strength and stress history (in situ state) of soft soils is that the spatial variability of the undrained shear strength and stress history is such large, that a high density of local measurements (horizontal and vertical) is needed to avoid prohibitively conservative choices. Executing boreholes with large distances between the boreholes and laboratory tests on samples from these boreholes is thought to be insufficient for an accurate and reliable insight in the spatial variability of the parameters.

CPT readings do not provide a direct measurement of undrained shear strength or stress history. Therefore the net cone penetration resistance q_{net} is correlated with the empirical correlation factor N_{kt} to the undrained shear strength s_u from triaxial tests or direct simple shear tests performed in the laboratory. The laboratory tests are conducted on samples extracted from boreholes. The laboratory tests are used as reference strength for the interpretation of the CPTs. It is evident that these samples from the boreholes have to be intact undisturbed samples. An accurate determination of the correlation factor is essential because a large coefficient of variation of this correlation factor leads to low characteristic lower bound values and calculation values of the undrained shear strength. The accuracy of the assessment depends on the accuracy of all parts of the site investigation and interpretation.

In the 'Dijken op Veen' ('Dikes on peat') project (Deltares, 2014) an approach is developed where CPTs should be carried out in each cross section where a slope stability analysis has to be performed. About the required interval between these cross sections or CPTs within the dike section no instruction is given. In practice the distance between two CPTs will be 100 meters or more. Using CPT data to calculate a characteristic lower bound value of the undrained shear strength this characteristic lower bound value is about 35% lower than the mean value of the undrained shear strength. This is likely due to the effect of the uncertainty due to spatial variability and the effect of the transformation uncertainty of the correlation factor N_{kt} . This transformation uncertainty causes the majority of the gap between mean value and characteristic lower bound. Transformation uncertainty is estimated to be about two times the uncertainty due to heterogeneity (Deltares, 2014).

Within the WBI 2017 guideline the same approach is adopted. However, within the WBI system one works with dike sections, which are defined as stretches of a dike with more or less homogeneous dike geometry, hydraulic boundary conditions, subsoil etc. In such a dike section several CPTs can be available. The variability of the shear strength within a dike section based on a number of CPTs has been showed to be considerable. Within the WBI guidelines it is not specified yet how to deal with this variability of the soil properties in the assessment of a dike section. Within the WBI system it is the aim to determine a realistic probability of failure for a dike section. So it is not intended to determine the probability of failure based on worst case estimations and combinations of worst case estimations, but to find characteristic lower bound values and design values or distributions of shear strength parameters that reflect the dike behaviour well.

Figure 2.1 gives an example of the correlation between the undrained shear strength s_u from laboratory tests and the net cone penetration resistance q_{net} to derive the empirical correlation factor N_{kt} . The data is obtained from four different sites along a dike, with CPTs and boreholes performed at the crest, berm and inner toe of the dike. With the purple and

blue lines the mean and 95% confidence interval of N_{kt} are given. The mean value is 14.5, the coefficient of variation is 0.25, the upper bound is 9.7 and the lower bound is 40.0. As can be seen in Figure 2.1 there is some scatter over the whole range of cone penetration resistances. Data from the various sites are not equally distributed over the 95% confidence interval, but cover on average about 50% of the confidence interval. This measure is used in the 'Dijken op Veen' project and the WBI 2017 guideline as a measure for the systematic part of the transformation uncertainty. This is an important measure, because in the statistical analysis to derive the characteristic lower bound value of the undrained shear strength only the non-systematic errors average out and the systematic errors affect the characteristic lower bound value.

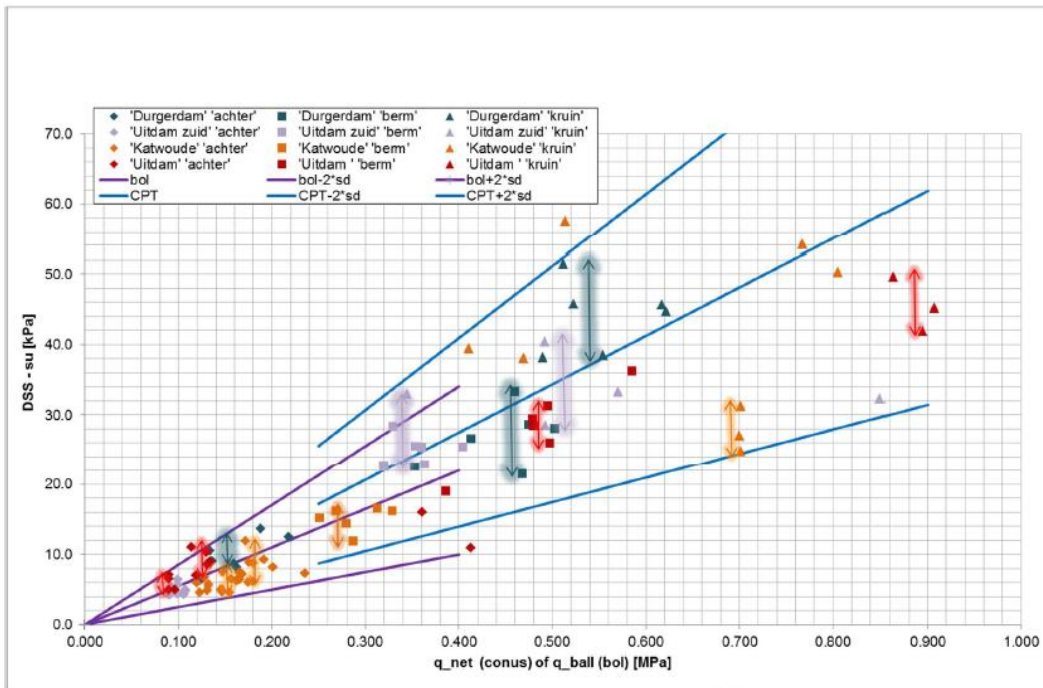


Figure 2.1 Correlation between the undrained shear strength s_u from laboratory tests and the net cone penetration resistance q_{net} to derive the empirical correlation factor N_{kt} (Deltares, 2014). The purple and blue lines are the mean and 95% confidence interval of N_{kt} .

2.2 Sources of uncertainty

For the derivation of the empirical correlation factor N_{kt} a large number of uncertainties can be identified. The uncertainties can be divided in several groups of sources of uncertainties: spatial variability, measurement uncertainty, statistical uncertainty (insufficient number of tests), transformation uncertainty and epistemic uncertainty (Cao et al., 2017; Van der Krogt et al., 2018). As noted before it is important to distinguish between non-systematic errors and systematic errors. Non-systematic errors average out on the scale of a large failure mechanism and systematic errors do not. Systematic errors affect the characteristic lower bound value. In practice all possible sources of uncertainties may be partly systematic and partly non-systematic.

2.2.1 Uncertainties CPT

CPTs are performed in The Netherlands in accordance with NEN-EN-ISO 22476 according to different classes. This standard distinguishes the application classes 1 to 4, where per class requirements are set for the minimum measurement accuracy. For class 1, the highest requirements for measuring accuracy apply. The standard sets requirements for the

measurement accuracy of the cone penetration resistance q_c , local friction f_s , pore water pressure u_2 , inclination and penetration depth.

In the Protocol CPT testing for s_u determination (Deltares, 2016a), a class 1+ CPT is defined for CPT testing in soils with very low cone penetration resistances (<0.2 MPa). In practice, cones are used which can measure sufficiently accurately to cone penetration resistances of 0.1 MPa. Particularly in the hinterland of dikes, however, cone penetration resistances of 0.3 to 0.03 MPa also occur in weak clay and peat layers. In the case of the CPT classes defined in NEN-EN-ISO 22476 and the applicable minimum measurement accuracy, the measurement uncertainty in such cases is equal to or larger than the cone penetration resistance to be measured. This is not considered acceptable. In the aforementioned protocol, the various options for the specifications of the cones from the prevailing NEN ISO standard are made more stringent and requirements are set for the execution of tests.

NEN-EN-ISO 22476 mentions various uncertainties regarding cone penetrometer testing: ambient and transient temperature effects, incorrect calibration parameters, e.g. loss of calibration due to bending or damage, lack of or poor saturation, improper transfer of loads due to dirt in gaps and seals, error in the data acquisition system, deviation of the geometry of the cone and zero shifts.

An investigation of the accuracy of CPT testing is performed by Peuchen & Terwindt (2014), who identified and quantified a large number of measurement uncertainties. The measurement uncertainty of the cone penetration resistance q_c can be considered as relatively small and non-systematic in normal conditions; much smaller than the requirements of NEN-EN-ISO 22476. This measurement uncertainty may result in a coefficient of variation (CoV) of 0.02 for a class 1 cone at high stress level to 0.20 for a class 2 cone at very low stress level. The cone penetration resistance can be uncertain due to hysteresis effects when penetrating in a soft layer just beneath a strong layer. Wear of a cone penetrometer can be an important issue for accurate measurements. In normal conditions however a worn cone tip has to be replaced. Temperature effects can also affect CPT readings. Boylan et al. (2008) showed that a cone will perform not correct in soft soils when the temperature of the soil is substantially lower than the temperature of the cone. This will result in significant positive or negative shift of the measured values. In case of non-vertical penetration the cone penetration readings can also be influenced. For an inclination below 15 degrees the effect is less than 5% (Peuchen & Terwindt, 2014).

According to Peuchen & Terwindt (2014) measuring the pore water pressure u_2 is a major challenge in practice. In laboratory conditions the uncertainty of u_2 measurements is random and small. The performance of u_2 measurements depends strongly on operational procedures and adequacy of saturation. Loss of saturation leads to slow pore pressure response and pore pressure data may be unreliable. In adverse in situ conditions with free gas or dissolved gas accurate measurement of u_2 can be very problematic. According to the ASTM D 5778 standard the piezocone fluid system can cavitate when penetrating through unsaturated soil or in dilating sand layers below the water table. This can adversely affect dynamic response of the measurement system. The saturation may recover during further penetration as air bubbles go back into solution. ASTM D 5778 mentions a standard deviation of 2% of the full scale output (FSO) in case of careful operation.

In the correction of the measured cone penetration resistance q_c to the net cone penetration resistance q_{net} an additional uncertainty occurs due to the uncertainty of total stress of the soil.

Overall most of the regular measurement uncertainties of the CPT seem to be non-systematic and relatively small.

2.2.2 Uncertainties laboratory tests

In the context of assessments and design of water defences in The Netherlands laboratory tests are performed according to a protocol (Deltares, 2016b). This protocol gives guidance to

perform triaxial tests, direct simple shear tests, oedometer tests and constant rate of strain tests. Where national and international standards leave some issues open or are not specific enough this protocol fills these lacunae. The idea behind this protocol is to minimize uncertainties due to differences in procedures between different projects and laboratory. The protocol supplies various instructions, such as about the saturation of samples, consolidation procedure, strain rates, corrections for membrane and drainage strips, accuracy of pressure transducers etc.

A number of these issues regarding the accuracy of triaxial tests and direct simple shear tests are discussed in (Deltares, 2009). Various uncertainties are quantified. For a consolidation stress of 30 kPa and application of an accurate pressure transducer the total systematic measurement uncertainties are about 2 kPa and the total non-systematic measurement uncertainties are also about 2 kPa for the triaxial test and about 3 kPa for the direct simple shear test. However, when the protocol (Deltares, 2016b) is used corrections for membrane and drainage strips of triaxial tests and friction of the direct simple shear apparatus are applied, and thus the systematic measurement uncertainties are smaller.

Based on (Deltares, 2009) and the protocol (Deltares, 2016b) the CoV due to uncertainties in laboratory tests can be estimated as 0.02 to 0.04 for high stress levels and 0.06 to 0.12 for low stress levels.

Temperature is also an issue which affects soil behaviour. Mitchell & Soga (2005) cite various authors who highlight that shear strength, stiffness and yield stress are temperature dependent, with a decreasing strength and stiffness for higher temperatures. In the laboratory the tests are usually carried out at room temperature. This results in relatively low shear strength, stiffness and yield stress as the in situ soil temperature is about 10° C lower than room temperature.

2.2.3 Sample disturbance

The issue of sample disturbance is described in many papers. Sample disturbance can occur due to sampling, transport and handling of the samples, trimming and preparation of the samples in the laboratory and so on. Sample disturbance affects the in situ soil structure, resulting in loss of strength, decrease of stiffness and lower yield stress.

Regarding the sampling system the Sherbrooke block sampler (Tanaka, 2000; Hight et al., 2003; Lunne et al., 2006; L'Heureux et al., 2018) and Laval system (Hight et al., 2003) are often proposed to give the best quality samples. In The Netherlands the Ackermann tube sampler is the most common sampling system. The thin-walled stainless steel tubes have a length of 440 mm, an inner diameter of 67 mm, a sharp cutting edge and can be hammered or pushed into the soil. The Stationary Piston sampler is also used in The Netherlands. This sampling system uses a 1000 m long aluminium liner with an inner diameter of 100 mm. Samples from the Piston sampler have to be trimmed to a smaller diameter of 50 or 65 mm to perform the laboratory tests. The sample quality derived by this type of sampling systems is assessed to be less by the aforementioned authors.

Figure 2.2, Figure 2.3 and Figure 2.4 give some examples of sample disturbance due to the sampling system and other actions with the samples.

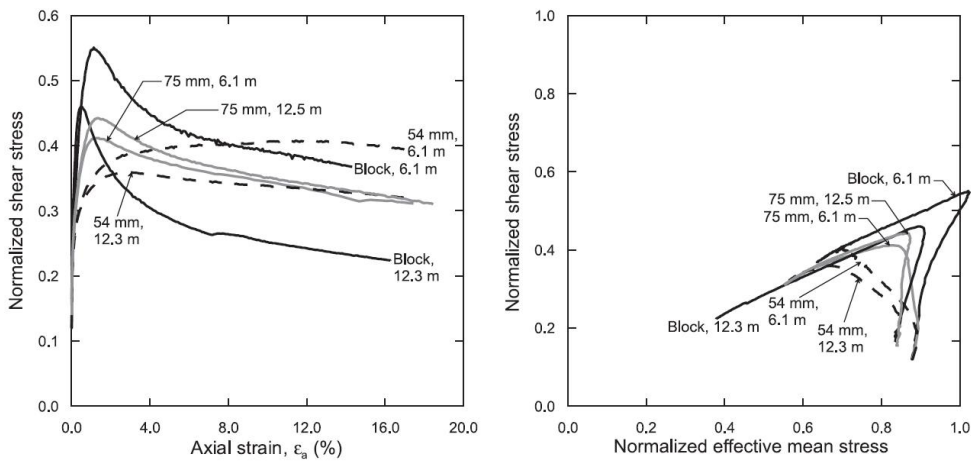


Figure 2.2 Differences in shear strength and stiffness of Lierstranda clay (Norway) for Block sampler, 54 mm Piston sampler and 75 mm Piston sampler (Lunne et al., 2006). The block samples show higher peak shear strength and stiffer behaviour than the other samples.

Figure 2.2 shows that samples from the Sherbrooke block sampler give very different behaviour compared to Piston sampler (54 mm and 75 mm). Peak strength and stiffness are much lower using the Piston sampler. With the 54 mm Piston sampler the peak strength has been fully disappeared.

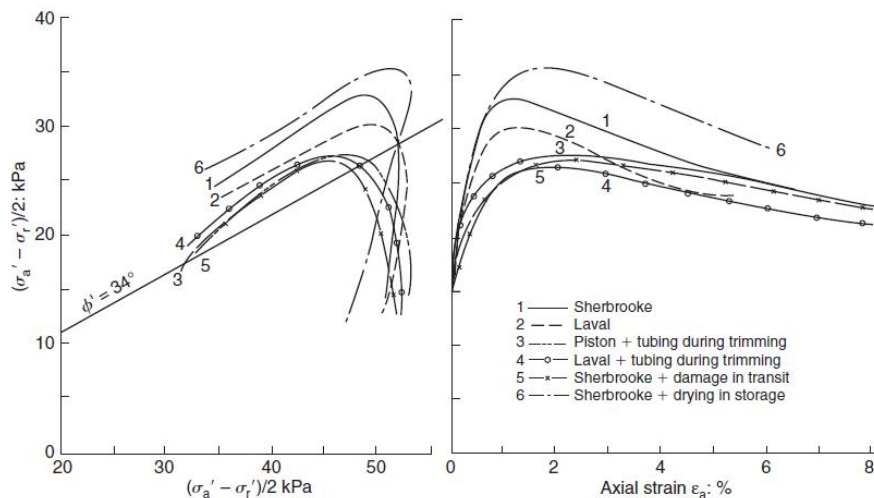


Figure 2.3 Differences in measured shear strength for Bothkennar Clay due to various reasons of disturbance (Hight et al., 2003). The disturbance also affects peak shear strength (up to 15%) and stiffness.

In Figure 2.3 it is demonstrated that several actions with samples affects the sample quality too. With the Sherbrooke and Laval samples as references tubing during trimming and damage in transit disturb a sample and reduces the peak strength and stiffness. The strength reduction due to damage in transit is about 15% for the Sherbrooke samples. Drying out the sample during storage gives an increase in peak strength.

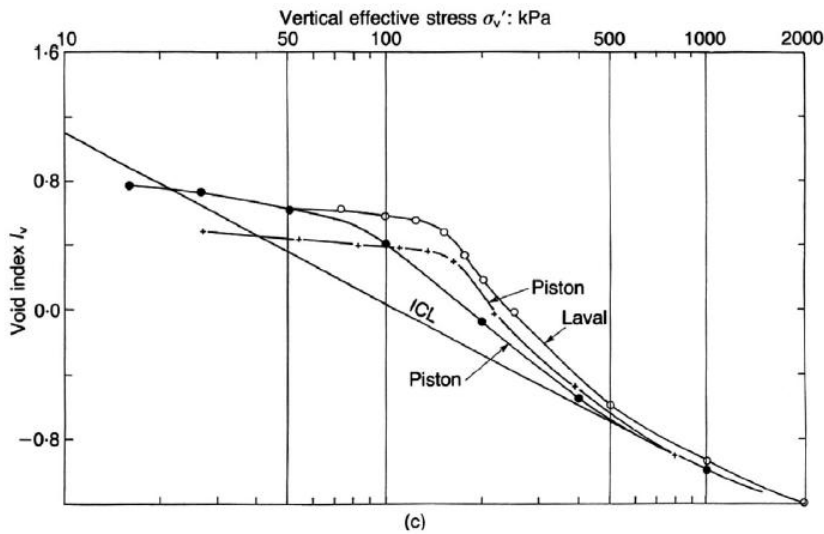


Figure 2.4 Effect of sampling systems on compression behaviour and yield stress of Bothkennar Clay (Hight et al., 2003).

Compression behaviour also depends on sample quality, as shown in Figure 2.4. The yield stress from the sample derived with the Piston sampler is about 80 kPa, whereas the yield stress of the other samples is about 150 kPa.

2.2.4 Transformation uncertainty

As discussed before the CPT does not give a direct measurement of shear strength, nor the yield stress. So, a correlation has to be used to relate the cone penetration resistance to the undrained shear strength or yield stress. In the WBI 2017 approach the undrained shear strength is derived from laboratory tests. The correlation between the undrained shear strength from laboratory tests and the cone penetration resistance causes transformation uncertainty. This transformation uncertainty occurs due to differences between the direct and indirect measurements. This uncertainty is also related to the transformation models that are used. Some of the relevant aspects are differences in strain rate, drainage conditions, failure mode and differences in mobilized shear strength due to anisotropy of the undrained shear strength due to differences in importance of horizontal stress between the direct and indirect measurement. The transformation uncertainty is difficult to determine, because it is not easy to deduce this uncertainty independent from other uncertainties.

Regarding the transformation model, usually a linear relation between the direct and indirect measurements is used, but also a non-linear model, for example with correction for OCR (Larsson & Åhnberg, 2005; L'Heureux et al., 2018), can be used.

2.3 Statistical models to describe spatial variability

2.3.1 Dutch practice

In Dutch practice for assessment and design of flood defences the characteristic lower bound value of soil properties which are related to slope instability analyses, such as friction angle or undrained shear strength, is calculated according to TAW (2002) and Calle (2007) with:

$$X_{loc\ gem.char} = \hat{\mu}_X - t_{N_{tot}-1}^{0.95} \hat{\sigma}_{X,reg} \sqrt{\frac{1}{N_{tot}} + \Gamma^2} \quad (2.1)$$

where:

$X_{loc\ gem, char}$	characteristic lower bound value of any parameter X.
$\hat{\mu}_X$	estimated mean value of any parameter X.
$t_{N_{tot}-1}^{0.95}$	student t factor for 5% lower bound value (95% probability of exceedance) (-).
$\hat{\sigma}_{X, reg}$	standard deviation of any parameter X of a regional dataset.
N_{tot}	number of observations (-).
Γ^2	variance reduction factor (-).

In equation (2.1) the term $\sqrt{\frac{1}{N_{tot}} + \Gamma^2}$ accounts for averaging of the spatial variability of the soil properties along a slip surface of a potential slope failure of a dike. The parameter Γ^2 is a dimensionless reduction factor that lies between 0 and 1. This parameter reduces the standard deviation the more the fluctuations of a parameter tend to cancel in the process of spatial averaging (Vanmarcke, 1977). According to Calle (2007 and 2008) the parameter Γ^2 can be determined from the variance ratio α between the local variance σ_{loc} and the regional variance σ_{reg} of a dataset, since the local variations tend to average out while the regional variations do not. This is because the local variations are mainly occurring vertically and tend to have much smaller correlation lengths than the size of the failure plain. The variance reduction factor is: $\Gamma^2 = 1 - \alpha$ with $\alpha = \sigma_{loc}^2 / \sigma_{reg}^2$.

In TAW (2002) the default variance ratio $\alpha = 0.75$ ($\Gamma^2 = 0.25$) for regional datasets. This value is based on analyses of regional data sets of shear strength parameters of different soil layers derived from Dutch cell tests. These analyses indicated a range of α between 0.5 and 1.0. A very accurate determination of α was not possible. So α is an uncertain parameter. The value of α is therefore a pragmatic choice. In TAW (2002) it is suggested that the vertical correlation length is some decimeters and the horizontal correlation length is about 50 to 100 m. The correlation length is the distance in which the correlation between soil properties decreases from 1 to 0. For local datasets where the dataset covers the scale of a potential slip surface the default variance ratio $\alpha = 1.0$ ($\Gamma^2 = 0$) (TAW, 2002) and all uncertainty (except the statistical uncertainty due to limited number of samples) averages.

The approach of TAW (2002) and Calle (2007) is based on a model for spatial distribution of soil parameters with the assumption that the local values of a soil parameter vary in horizontal and vertical direction around a regional average (Calle, 2007 and 2008). Furthermore it is assumed in this approach that the local variation of a certain parameter is smaller than the regional variation of that parameter. The correlation between soil properties from samples coming from one borehole is assumed to be much larger than the correlation between soil properties from samples coming from different boreholes at larger distances. The variability in vertical direction is thought to average nearly completely on the scale of a slope failure, as the vertical correlation length is only some decimeters. The variance reduction in horizontal direction however is thought to be limited (TAW, 2002).

Calle (2008) states that each site investigation should be performed in a way that it is possible to determine the ratio between the local variance and regional variance. To be able to calculate the local variance a number of 4 to 6 samples per soil layer and per borehole are required.

The relevance of the reduction factor Γ^2 for the characteristic lower bound is illustrated in Figure 2.5 using equation (2.1). The mean value is 1.0 and the characteristic lower bound value is presented relative to the mean value. The dashed blue line shows the default value of the reduction factor Γ^2 for regional datasets according to TAW (2002). The dashed red box marks the range of the expected values of Γ^2 . Depending on the number of observations and the value of the reduction factor the characteristic lower bound can be remarkable lower than the mean value. So, it might be an interesting option to optimize the reduction factor to get a more accurate characteristic lower bound value.

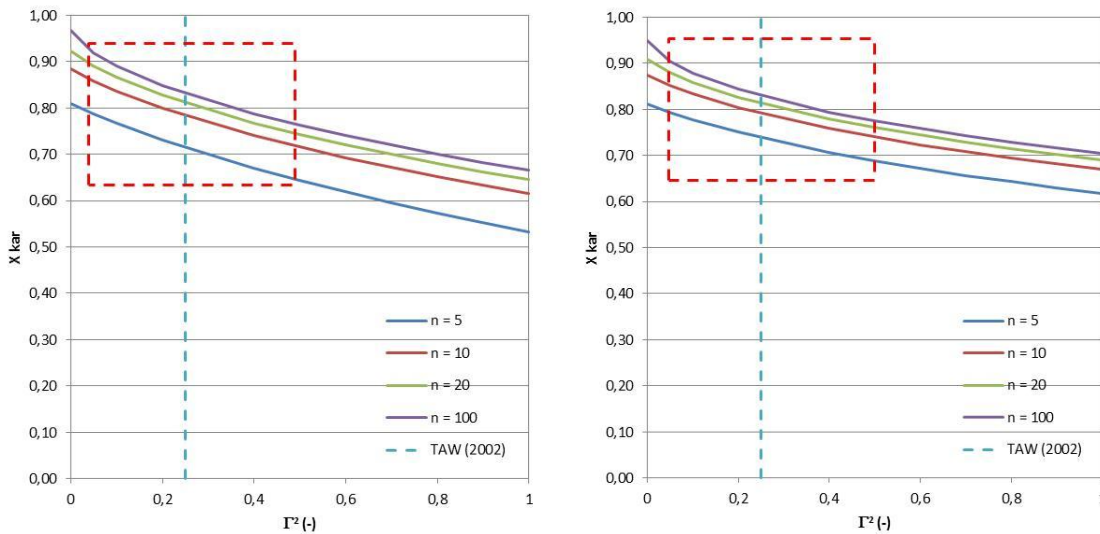


Figure 2.5 Relation between variance reduction factor, number of tests and characteristic lower bound value. Normal distribution (left) and log normal distribution (right) (CoV = 0.2). The area of interest is given by the red dashed box.

2.3.2 International literature

In geotechnical practice it is not very common to account for correlation between soil properties in horizontal direction (Cao et al., 2017). Usually the assumption is that a strong horizontal correlation results in a conservative design. Based on synthetic data, De Gast et al. (2018) performed a probabilistic analysis and showed that the factor of safety of a slope of a dike may increase by about 10% when the horizontal and vertical spatial scale of fluctuation is taken into account. From this study De Gast et al. (2018) suggest to perform site investigations where CPT's are located in groups. When using groups of CPT's the vertical and horizontal scale of fluctuation can be determined from the CPT data. This recommendation in essence is comparable with the recommendation of Calle (2008) who suggested to determine the reduction parameter Γ^2 from the ratio between the local variance and regional variance based on the results of site investigations.

According to Cao et al. (2017) two categories of models to describe spatial variability of soil properties are available: finite scale model (short-memory) and fractal model (statistically self-similar or long-memory; Fenton, 1999).

2.3.3 Spatial variability based on finite scale models

Correlation function

Using the finite scale model the correlation length of a soil parameter can be determined by fitting the theoretical correlation function on the empirical correlation function. Various theoretical correlation functions can be used (Cao et al., 2017), however the exponential function according to Markov is used very often. Spry et al. (1988) state that a physical base to prefer one of these theoretical correlation functions doesn't exist. The Markov model has an exponentially decaying correlation function (Fenton, 1999):

$$\rho(\tau) = \exp\left(-\frac{2|\tau|}{\theta}\right) \quad (2.2)$$

where:

- $\rho(\tau)$ correlation coefficient between two points separated by $\tau(-)$.
- τ lag distance (m).
- θ a distance called the 'scale of fluctuation' (m).

Following Fenton (1999) the ‘scale of fluctuation’ may be loosely interpreted as the separation distance beyond which soil properties are largely uncorrelated. This model is considered to be a finite-scale model because the correlation dies out very rapidly for separation distances $\tau > \theta$; the area under this function, in particular, is finite (Fenton, 1999).

The sample correlation $\hat{\rho}(\tau_j)$ is obtained by normalizing as given by Fenton (1999):

$$\hat{\rho}(\tau_j) = \frac{\hat{C}(\tau_j)}{\hat{C}(0)} \quad (2.3)$$

where:

$\hat{C}(\tau_j)$ estimator of the covariance function at discrete lag τ_j .

$\hat{C}(0)$ is the same as the estimated variance $\hat{\sigma}_X^2$.

The sample covariance function is obtained from the moment estimator (Fenton, 1999):

$$\hat{C}(\tau_j) = \frac{1}{n-j} \sum_{i=1}^{n-j} (x_i - \hat{\mu}_X)(x_{i+j} - \hat{\mu}_X) \quad \text{with } j = 0, 1, \dots, n-1 \quad (2.4)$$

where:

x_i observed value of X_Z .

$\hat{\mu}_X$ estimated mean of X_Z .

n number of observations in sample of X_Z .

j number of lag distances τ .

The data, $x_i, i = 1, 2, \dots, n$, are to be collected at a sequence of equispaced points along a line. Based on the calculated sample correlation at various lags ($\hat{\rho}(\tau_j)$), an autocorrelation function can be fitted. In Figure 2.6 an example of an empirical correlation function and a fitted theoretical correlation function is given.

One of the major difficulties with the sample correlation function resides in the fact that it is heavily dependent on the estimated mean (Fenton, 1999). When the soil shows significant long-scale dependence, characterized by long-scale fluctuations, then the estimated mean value is almost always a poor estimate of the true mean value.

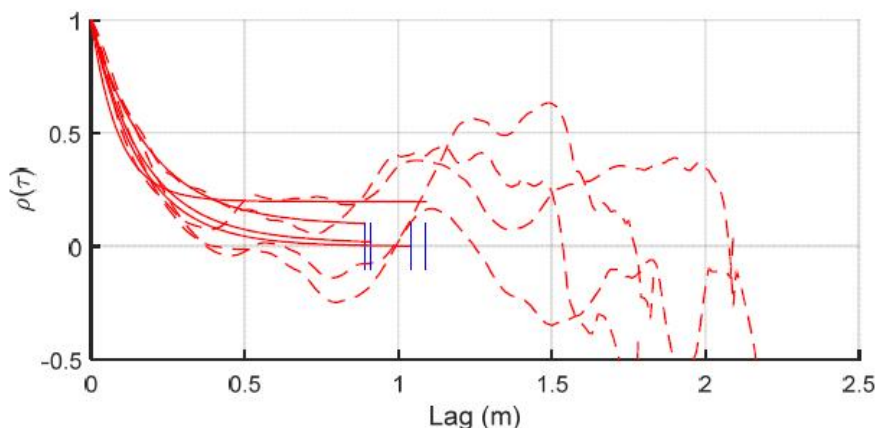


Figure 2.6 Example of empirical correlation function (dashed lines) and fitted theoretical correlation function (solid lines) showing vertical correlation of CPT data from De Gast et al. (2017). After the lag distance of 1 m the correlation becomes unreliable.

According to Fenton the estimator $\hat{\rho}(\tau)$ will typically dip below zero due to bias problems even when the field is actually highly positively correlated. However, the sample correlation function is a good estimator of short-scale processes as long as the correlation length is much shorter than the sampling domain. The sample correlation function fails to provide any useful information about large-scale processes. Furthermore, there needs to be sufficient data points with smaller lag distance than the correlation distance in order to compute the correlation distance. De Gast et al. (2017) point out that, while constructing the experimental correlation function, larger lag lengths are calculated with a decreasing amount of data and so the results can become increasingly erratic (see Figure 2.6). Therefore, a choice has to be made on how much of the correlation function should be taken into account when estimating the error. A correlation smaller than -1.0 is theoretically not possible.

Semivariogram

A semivariogram essentially gives the same information as a correlation function (Fenton, 1999). An advantage of the semivariogram is its independence of the estimation of the average value of the soil property (Fenton, 1999). This is a clear advantage because many of the problems of the correlation function relate to this dependence. The sample semivariogram $\hat{V}(\tau_j)$ is defined by:

$$\hat{V}(\tau_j) = \frac{1}{2(n-j)} \sum_{i=1}^{n-j} (x_{i+j} - x_i)^2 \quad \text{with } j = 0, 1, \dots, n-1 \quad (2.5)$$

where:

- x_i observed value of X_z .
- n number of observations in sample of X_z .
- j number of lag distances τ .

Figure 2.7 gives an example of a semivariogram. Range is the distance up till which spatial dependency exists. Sill is the variance around the mean of the observations. This is the maximum semivariance and at this distance no more spatial dependency exists. Another parameter, which is not drawn in the figure, is the nugget. The nugget is an offset of the semivariance which indicates that noise plays a role in the data.

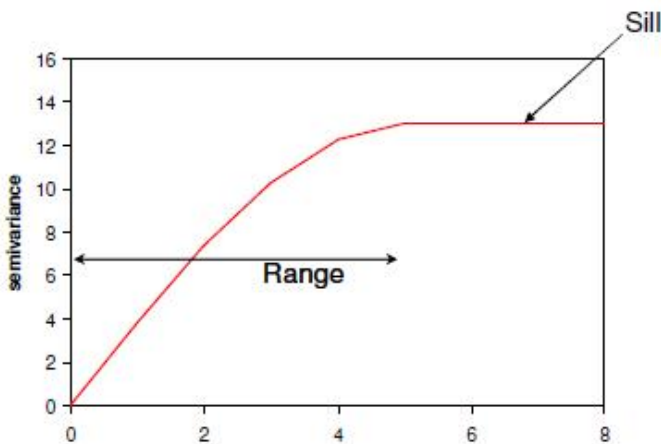


Figure 2.7 Semivariogram with lag distance on the x-axis, range and sill. The correlation length in this example is 5 lag distances.

The semivariance can be highly variable. This high variability in the semivariogram may hinder its use in discerning between model types unless sufficient averaging can be performed (Fenton, 1999).

Relation correlation length and variance reduction factor

Vanmarcke (1977) suggested that the variance reduction factor $\Gamma(b)$ can be related to the horizontal correlation length θ by:

$$\Gamma(b) = \left(\frac{\theta}{b}\right)^{1/2} \quad \text{with } b > \theta \quad (2.6)$$

In this equation the variance reduction factor $\Gamma(b)$ depends on the ratio of the horizontal correlation length θ and the length of a potential slope instability b . When applying this equation the horizontal correlation length θ can be easily related to the approach of TAW (2002) and Calle (2007). Note however that the meaning of the variance reduction factor $\Gamma(b)$ is not the same in the approaches of Vanmarcke (1977) and TAW (2002) and Calle (2007). In TAW (2002) and Calle (2007) it is assumed that the variance reduction in vertical direction is nearly complete, whereas the variance reduction in horizontal direction is limited. Vanmarcke (1977) assumes complete averaging of variability in vertical direction and the variance reduction factor decreases when the dimension of a slope failure in horizontal direction increases. When the dimension of a slope failure in horizontal direction is smaller than the correlation length no averaging of variability in horizontal direction occurs according to Vanmarcke (1977).

Vanmarcke (1977) considered that the precise pattern of decay of $\Gamma(b)$ may be rather complex, especially in situations where the spatial variation of strength along a line is attributable to two or more superimposed fluctuations with substantially different correlation length θ . These different types of spatial variation can be modelled as additional sources of uncertainty (Vanmarcke, 1977). In such a model the total variance is the sum of two independent random components, one slow varying and the other rapidly varying, with fractional contributions which add to one. De Gast et al. (2017) applied this idea to analyse the spatial variability in vertical direction using CPT data. They found reasonable results, which are in good agreement with the vertical correlation length as mentioned in TAW (2002).

2.3.4 Spatial variability based on fractal models

Fenton (1999) proposed the fractal model (Figure 2.8). A fractal model seems to fit very well to the character of the natural variability of soil properties. The fractal model implies that different correlation lengths exist on different scales; also on very long scales. This fractal model also follows naturally from the suggestion of Vanmarcke (1977) that the spatial variation of strength along a line may be attributable to two or more superimposed fluctuations with substantially different correlation length θ .

In trying to determine whether the soil property best follows a finite-scale model or a fractal type noise, the periodogram, wavelet variance, and semivariogram plots were found to be the most discriminating by Fenton (1999). In this sense, the periodogram is perhaps the most preferable due to the fact it has been extensively studied. The periodogram and wavelet variance are not investigated in this study.

According to Fenton (1999) there may be little difference between a properly selected finite scale model and the real fractal model over the finite domain.

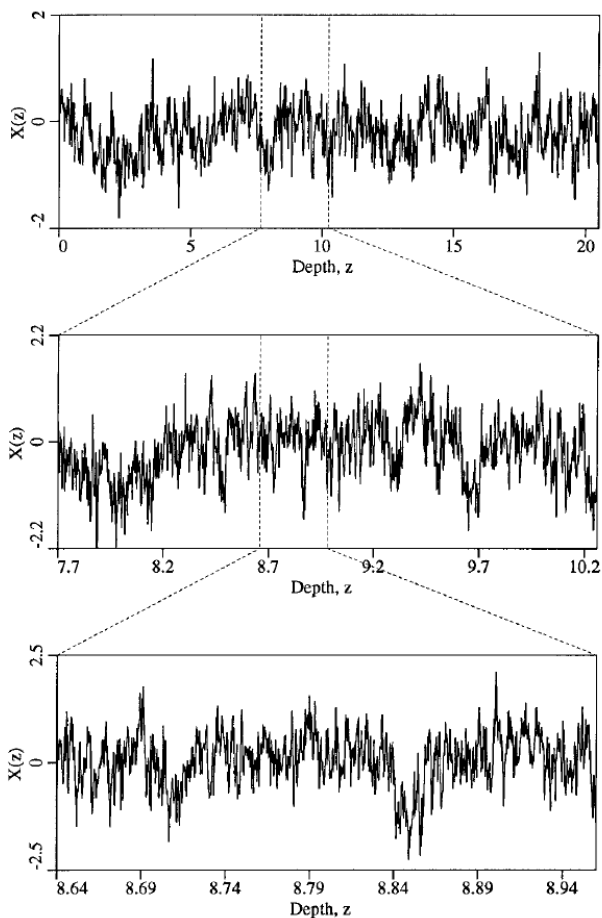


Figure 2.8 Fractal model with recurring pattern of variability according to Fenton (1999). Note that the variability increases when focussing on a smaller depth interval. So the small scale variability averages on the larger scale.

2.3.5 Summary

In summary there are two effects to be considered: 1) local variance and regional variance of a soil parameter and 2) averaging of local variance when the scale of the mechanism is larger than the correlation length.

2.4 Knowledge gaps

A number of uncertainties regarding the determination of the undrained shear strength and yield stress from CPTs and laboratory tests are discussed previously in this chapter. In this research the focus will be on spatial variability and sample disturbance.

Within the WBI 2017 approach it is currently not clear how to deal with several CPTs within a dike stretch. It is important to find out how the shear strength and yield stress vary along a dike stretch and how to calculate the characteristic lower bound of the shear strength or yield stress taking into account spatial variability of the subsoil.

Concerning sample disturbance in The Netherlands relatively simple sampling techniques are used, also for the assessment and design of very important infrastructure like water defences. In other countries much more advanced techniques are applied for important projects. It is discussed above that these advanced sampling techniques result in laboratory test results with higher peak strength and higher yield stress. It is therefore important to know for Dutch soil types whether sample disturbance affects the uncertainty of the empirical correlation factor N_{kt} , and especially have an influence on the systematic part of the uncertainty of N_{kt} .

3 Study areas

3.1 Measurement sites

The research involves site investigations at three locations:

- Lekdijk at S44_239_00 near Schalkwijk (south of Houten) in the dike trajectory Amerongen – Schoonhoven which is under the administration of Hoogheemraadschap De Stichtse Rijnlanden (HDSR). The tests are conducted in the inner toe of the dike.
- Waaldijk at TG198+015 in Waardenburg (south of Geldermalsen) in the dike trajectory Tiel – Gorinchem which is under the administration of Waterschap Rivierenland (WSRL). The tests are conducted at the crest, the berm and the inner toe of the dike.
- Achterwaterschap at AC 075, AC 090 and AC 251 near Alblasserdam which is under the administration of Waterschap Rivierenland (WSRL). The tests are performed in the inner toe of the dike.

The locations of the research sites are presented in Figure 3.1.

3.2 Geological setting

Figure 3.2 shows a longitudinal section through the coastal prism of the Rhine-Meuse delta (figure modified from Hijma & Cohen, 2011). The research sites Waaldijk (W) at Waardenburg, Lekdijk (L) near Schalkwijk and Achterwaterschap (A) near Alblasserdam are projected on the longitudinal section.

The Holocene wedge of the Rhine-Meuse delta shows an increasing thickness in western (downstream) direction, reaching more than 20 meters at the coastal barrier. The Holocene wedge consists of a succession of deposits, reflecting the changing boundary conditions of the delta. Extensive descriptions of the changing boundary conditions during the Holocene and the consequences for the depositional environment and the lithological built-up can be found in Berendsen & Stouthamer (2000), Cohen (2003), Hijma et al. (2009) and Hijma & Cohen (2011). In the alluvial plain clastic sediment is dominant. In the back-barrier basin also clastic sediment is present, both from fluvial and marine origin. Beside clastic sediments also a lot of peat has been formed in the back-barrier basin. The timelines in Figure 3.2 indicate a decrease of the gradient of the river both in western direction and in time, resulting in a more swampy (low energy) depositional environment in time.

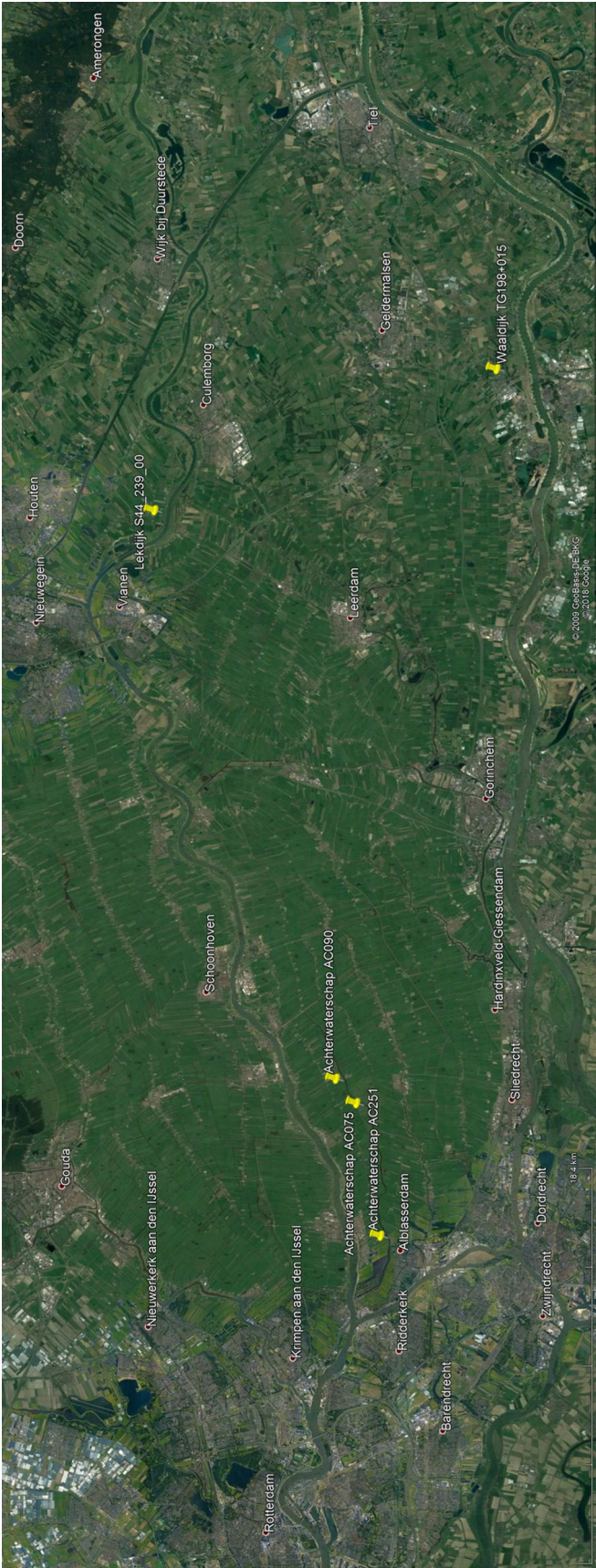


Figure 3.1 Locations of the research sites (Google Earth).

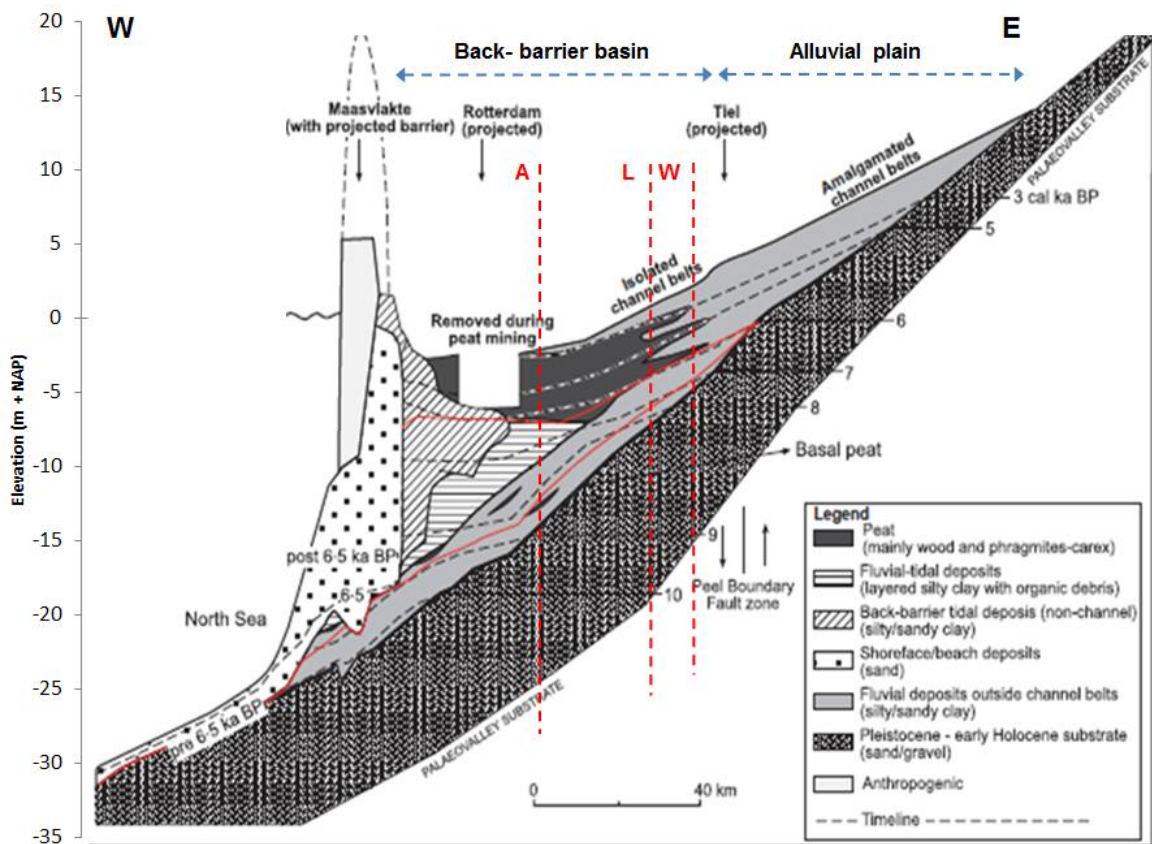


Figure 3.2 Longitudinal section through the Rhine-Meuse delta. The sites Waaldijk (W), Lekdijk (L) and Achterwaterschap (A) are projected on the longitudinal section. The three sites are located within the back-barrier basin. Figure modified from Hijma & Cohen (2011).

Waaldijk

The research sites are situated in the back-barrier basin of the delta. The Waaldijk site is the most eastern research location. The geological setting at the Waaldijk site is deduced from Gouw & Erkens (2007), who mapped the Holocene fluvio-deltaic system of the alluvial plain and the upper part of the back-barrier basin. The Holocene deposits at the Waaldijk site are about five to seven meters thick and are dominated by clastic sediment. This sediment can be assigned to the Echteld Formation. In the flood plain the Echteld Formation consists of silty clay, clay and humic clay. Peat (Nieuwkoop Formation) is relatively scarce in this upstream part of the basin, compared to the more downstream parts. At the top of the Pleistocene deposits sandy loam or loamy flood basin deposits (Wijchen Member of the Kreftenheye Formation) have been formed.

Achterwaterschap

The three Achterwaterschap sites are at the downstream end of the fluvially dominated part of the delta. At the Achterwaterschap sites the thickness of the Holocene deposits is in the order of ten to twelve meters. As illustrated in Figure 3.2 the deposits can be subdivided into several sequences. Generally the sequences show an increasing swampy depositional environment from bottom to the top of the deposits. At the top of the Pleistocene deposits again the sandy loam or loamy flood basin deposits of the Wijchen Member are present. Basal peat has been formed on top of the Wijchen Member. During the early Holocene rivers dominated the formation of the deposits. Outside the channel belts clayey flood basin deposits (silty/sandy clays) are formed. These clastic deposits belong to the Echteld Formation. Considering the time lines in Figure 3.2 and the palaeogeographic reconstruction by Berendsen & Stouthamer (2000) the clayey deposits might be formed by the Benschop

river system. This is the oldest known aggrading river system, which had its main branch to the North-West, but several smaller distributaries flowed to the South-West.

Above NAP -10 m also clayey sediment is deposited, but in this stage the depositional environment can be both fluvially and tidally influenced. These fluvial-tidal overbank deposits consist of layered silty clay with organic debris (see Figure 3.2 and Hijma & Cohen, 2011). In the area around the present city of Rotterdam this type of deposits is described as upper estuarine flood basin deposits and mentioned Terbregge Member of the Echteld Formation by Hijma et al. (2009). Characteristic for these deposits is the distinct layering due to the tidal influence and excellent preservation of the organic material. Hijma et al. (2009) encountered the Terbregge Member also around Ridderkerk (their cross-section A-A'), which is about 5 km westward from the location AC 251 of the Achterwaterschap. Following Hijma & Cohen (2011) the Terbregge Member has its most upstream occurrence along the main active channels. In the flood plains at larger distances from these main channels the tidal influence is more limited and therefore the upper estuarine flood basin deposits may be absent.

Above NAP -8 m thick peat layers occur (mainly wood and phragmites-carex, according to Hijma & Cohen, 2011), belonging to the Nieuwkoop Formation. These peat layers can be intercalated with clayey sediment. The large thickness of the peat layers can be related to the distal position of the main channel of the Utrecht river system (Berendsen & Stouthamer, 2000), which was close to the northern boundary of the river valley at the time of the formation of the peat layers at the Achterwaterschap research location.

At the top of the Holocene sequence a thin clayey layer has been formed in the Late Holocene (Echteld Formation). The formation of this clayey layer can be attributed to the fact that the present river Lek came into existence (Berendsen & Stouthamer, 2000) in the Late Holocene.

Lekdijk

The Lekdijk site is in between the other research sites. The geological setting of this area is also described by Gouw & Erkens (2007). At the Lekdijk site the Holocene deposits are about eight meters thick. At this location the deposits are fluvially dominated. Outside of the river channels the deposits consist of clayey flood plain sediment. As at the Achterwaterschap locations also at the Lekdijk location the clayey sediments are intercalated with peat. At the Lekdijk site these peat layers are relatively thin, indicating that the active river systems were most of the time in a proximal position during the Holocene. This seems to be in agreement with the reconstruction by Berendsen & Stouthamer (2000).

4 Methods

4.1 Introduction

The research regarding the natural spatial variability of the shear strength is performed at the locations AC 075, AC 090 and AC 251 along the drainage canal Achterwaterschap near Alblasserdam (see Figure 3.1). These locations are selected for this research because various soil layers from different sedimentary environments are available in this area. Therefore different patterns of spatial variability can be expected at these sites. For this research it was decided to conduct the research at different locations with the same sedimentary environments to be able to verify whether the spatial variability is equal for the locations. Furthermore data from CPTs and boreholes from the waterboard Waterschap Rivierenland (WSRL) was available for the Achterwaterschap. This data is used to select the exact locations of the research sites along the Achterwaterschap.

To analyse the natural heterogeneity of the cone penetration resistance three series of CPTs are performed along the drainage canal Achterwaterschap near Alblasserdam. These series of CPTs are performed at the three locations AC 075, AC 090 and AC 251. At each location 15 CPTs with measurement of cone resistance are performed within a row of 100 m length. So the distance between the CPTs is 7.0 m. These are class 1+ cones, the so called "dyke cone". These class 1+ cones only measure cone resistance, but they measure cone resistance with a measurement accuracy of 7.5 kPa, whereas the measurement accuracy of class 1 cone resistance is 35 kPa. The high measurement accuracy of the class 1+ cone is very important to measure the cone resistance in the soft soils at the Achterwaterschap very accurately. Especially because this location typically has very low effective stresses. Five additional CPTs with class 1 cones with measurement of cone resistance, sleeve friction and pore water pressure are performed at each location to be used for the interpretation of the stratigraphy of the subsoil. Because of this set-up a relatively large part of the heterogeneity of the subsoil on the scale of a potential slope failure can be investigated. The set-up of the site investigations at the three sites is given in Appendix A.

The research regarding sample disturbance is also carried out at three locations. For this research locations near the Waaldijk at Waardenburg, Lekdijk at Schalkwijk and at the drainage canal Achterwaterschap (AC 251) near Alblasserdam (see Figure 3.1) are selected. As for sample disturbance the soil conditions, such as strength, stiffness and in situ state may play a role research locations with different soil conditions were selected. For the three locations data from the waterboards Hoogheemraadschap De Stichtse Rijnlanden (HDSR) and Waterschap Rivierenland (WSRL) was available. This data is used to select the research locations. The set-up of the site investigations at the three locations is given in Appendix A.

To be able to carry out this research field and laboratory tests are conducted. The field and laboratory tests are CPTs class 1 and class 1+ (recently developed cone, which according to the specifications meets the highest accuracy class of the Deltares-protocol; Deltares, 2016a) and field vane testing and boreholes with sampling for triaxial tests and constant rate of strain tests on intact samples and reconstituted samples.

The effect of sample disturbance is verified by performing field vane tests (FVT), which measure intact peak shear strength and residual shear strength. The FVT is applied as it is thought that this apparatus causes minimal sample disturbance, because sampling and sample transport and handling are not needed. In the laboratory, also the peak shear strength on intact samples and remoulded shear strength on reconstituted samples are determined with triaxial compression tests. Constant rate of strain tests are also conducted on intact and reconstituted samples. In reconstituted samples, the contribution of soil forming processes, such as ripening, creep and cementation to the shear strength and compressibility is lacking. This contribution of ripening, creep and cementation to the strength and compressibility can be lost due to sample disturbance when sampling and treating natural intact soil samples in the laboratory. The ratio of the natural intact peak shear strength to the residual shear strength of the FVT will be compared with the ratio of the peak shear strength of natural intact

samples and the remoulded shear strength of reconstituted samples. The deviation of intact compression curves compared to compression curves of reconstituted samples will also be determined. The ratio of the intact peak shear strength to the residual shear strength from the FVT and the deviation of intact to reconstituted behaviour in laboratory tests is called sensitivity. When the sensitivity of the FVT is larger than the sensitivity of the laboratory tests on intact samples, this is a strong indication that sample disturbance is an issue. When the effect of sample disturbance can be determined, the contribution of sample disturbance to the uncertainty of the correlation factor N_{kt} can be quantified. The research is performed for clayey soils as for peat it will be very difficult to prepare reconstituted samples.

4.2 In situ tests

The site investigations are executed by Inpijn-Blokpoel by order and supervision of Deltares. The site investigations involve:

- CPTu class 1 according to NEN-EN-ISO 22476 with measurement of the cone penetration resistance q_c (measurement accuracy of cone resistance is 35 kPa), sleeve friction f_s and pore water pressure u_2 .
- CPTu class 1 according to NEN-EN-ISO 22476 with measurement of the cone penetration resistance q_c , sleeve friction f_s and pore water pressure u_2 , with dissipation tests each 0.5 m in the Holocene clay and peat layers.
- CPTs with the dykecone with measurement of the cone penetration resistance q_c (class 1+ cone with measurement accuracy of the cone resistance of 7.5 kPa according to the Protocol CPT testing for s_u determination; Deltares, 2016a). At the Waaldijk and Lekdijk sites the CPTs are carried out close to the boreholes and field vane tests. At the Achterwaterschap sites the CPTs are performed in three rows of 100 m length with 15 CPTs (distance interval 7 m).
- boreholes using the pushed or the hammered Ackermann sampling system with continuous sampling in the Holocene clay and peat layers.
- field vane tests with different combinations of rotation rate of the vane and vane diameter (6, 25, 60, 100, and 360 degrees per minute with vane diameters of 40, 65 and 75 mm). The waiting time between insertion of the vane and start of rotation of the vane is about 10 seconds or about 3 minutes. The tests are performed each 0.5 m in the Holocene clay and peat layers.

Table 4.1 gives an overview of the performed field tests. Table 4.2 gives the specifications of the Field vane tests. The set-up of the site investigations at the five sites is given in Appendix A.

Table 4.1 Overview of the performed field tests.

Field tests	Lekdijk, Schalkwijk	Waaldijk, Waarden- burg	Achterwaterschap, Alblasserdam		
			AC 075	AC 090	AC 251
CPTu class 1	1	4	5	5	6
CPTu class 1 with dissipation tests	1	2	-	-	1
CPT class 1+	3	3	15	15	18
Boreholes Ackermann pushed	-	3	-	-	1
Boreholes Ackermann hammered	2	-	-	-	
Field vane tests	5	2	-	-	3

Table 4.2 Specifications of the performed Field vane tests.

Location	Rotation rate (deg/min)	Vane diameter (mm)	Waiting time (s)
Lekdijk Schalkwijk	6	40	10
	6	65	10
	25	65	10
	100	65	10
	360	65	10
Waaldijk Waardenburg	6	65	10
	100	65	10
Achterwaterschap AC 251 Alblasserdam	6	75	180
	60	75	10
	360	75	10

The rotation rate, vane diameter and waiting time of the field vane tests are varied to verify when the test are performed at fully undrained conditions. This will be discussed further in Paragraph 4.8. The vane diameter also depends on the strength of the soil. For soft soils a larger vane diameter can be applied regarding to the maximum allowable torque of the apparatus. In soft soils the larger vane also allows to measure more accurately. The waiting time of 180 s meets the ISO 22476-9 standard.

The data received from the waterboard Hoogheemraadschap De Stichtse Rijnlanden (HDSR) at the location Lekdijk concerns CPTs with class 1 cones and class 2 cones and a borehole with hammered Ackermann sampling system. The measurement accuracy of a class 2 cone resistance is 100 kPa according to NEN-EN-ISO 22476.

The data received from the waterboard Waterschap Rivierenland (WSRL) at the Waaldijk location concerns CPTs with class 1 cones and class 2 cones and a borehole with Piston sampling system.

The data received from the waterboard Waterschap Rivierenland (WSRL) at location Achterwaterschap AC 251 concerns CPTs with class 1 cone and a borehole with Piston sampling system.

4.3 Laboratory tests

In the laboratory triaxial compression tests, constant rate of strain tests and classification tests are performed on intact and reconstituted samples. The triaxial tests and constant rate of strain tests are performed in order to determine the undrained shear strength s_u , strength

sensitivity S_t , and stress sensitivity S_σ . Tests on reconstituted samples are executed to determine the intrinsic strength and intrinsic compression behaviour of the soil without any contribution of natural structure of the soil due to soil forming processes and creep. Tests on intact samples are conducted to derive the undrained shear strength and compression behaviour with contribution of natural structure of the soil due to soil forming processes and creep. These triaxial tests on intact samples are consolidated by the estimated in situ effective stress conditions. For these stress conditions comparisons with field vane tests and cone penetration tests can be made. When the triaxial test results of the intact samples and the reconstituted samples are compared the sensitivity of the soil can be derived. The triaxial tests on intact samples are conducted by the laboratory of Inpijn-Blokpoel in Son. The triaxial tests on reconstituted samples and the constant rate of strain tests on intact and reconstituted samples are performed in the laboratory of Deltares in Delft. The classification tests are also performed by the laboratory of Inpijn-Blokpoel in Son. The classification tests involve the determination of the soil unit weight γ_{sat} and γ_{dry} , specific gravity G_s , liquid limit w_L , plastic limit w_P , plasticity index I_P , organic content OC and grain size distribution. The classification tests are meant to determine void ratio of the soil samples, to analyse the results of the laboratory tests and to be able to apply empirical corrections to the field vane test results. The laboratory tests are conducted according to the protocol (Deltares, 2016b).

During transport of a series of soil samples from the laboratory of Deltares in Delft to the laboratory of Inpijn-Blokpoel in Son some of the samples were damaged. Due to the damage it was expected that the sample quality would be poor and the samples could not be used to obtain the undrained shear strength of the natural intact soil. Therefore it was decided to trim the samples from the original 65 mm diameter to 50 mm in order to remove the outside of the samples, which might be most affected by the damage. After trimming, the samples were used for triaxial testing. Additional boreholes were executed at the inner toe of the Lekdijk near Schalkwijk and the Waaldijk in Waardenburg to obtain good quality 65 mm soil samples. This gave the opportunity to compare the undrained shear strength and sensitivity from intact 65 mm samples and damaged 50 mm samples.

The reconstituted samples are prepared from material from the boreholes using two methods:

- Slurry: water is added to the soil to get a slurry with water content w corresponding to approximately 1.25 times the liquid limit w_L . This is the classical way to obtain reconstituted samples (e.g. Burland, 1990). The sample is consolidated in a mould at 15 kPa.
- Dry compaction: the soil material is mixed intensively at the present water content.

Two different methods in preparing the reconstituted samples are used because of the sandy silty clay (transitional soils) which occurs at the three sites. For transitional soils the undrained shear strength depends on the initial density according to Nocilla et al. (2006) and Shipton & Coop (2015). By using different preparation techniques a range of initial densities can be obtained and the effect of the initial density on the intrinsic undrained shear strength can be derived.

To determine the strength gain due to thixotropic hardening four laboratory vane shear tests are performed on reconstituted samples, which are prepared by the slurry method. Thixotropic hardening is a time-dependent process whereby a material at rest stiffens under conditions of constant composition and volume (Mitchell & Soga, 2005). Upon remolding the material softens or liquefies. Five measurements are conducted in a period of eight to eleven days. Hardening of the reconstituted samples may occur during the consolidation phase. This hardening process induces some increase of the structure and strength of the soil.

An overview of the performed laboratory tests is given in Table 4.3.

Table 4.3 Overview of the performed laboratory tests.

Location	Triaxial tests			Constant rate of strain tests		
	Intact samples	Slurry	Dry compaction	Intact samples	Slurry	Dry compaction
Lekdijk, Schalkwijk	4 (50 mm) 11 (65 mm)	2	2	3	--	--
Waaldijk, Waardenburg	8 (50 mm) 6 (65 mm)	3	3	4	1	1
Achterwaterschap AC 251, Alblasserdam	9 (65 mm)	5	6	5	2	4

For each location triaxial tests, constant rate of strain tests (only Waaldijk and Achterwaterschap) and oedometer tests are received from the waterboards.

In order to calculate the initial specific volume v_i of the samples four different methods are used. As all parameters to calculate the specific volume have some degree of uncertainty the results of the four methods can be used to quantify the uncertainty of the specific volume and to choose the specific volume within the bandwidth of the specific volume. The four methods to calculate the initial specific volume are (Shipton & Coop, 2015):

$$v_i = \left(\frac{w_i G_s}{S_{ri}} \right) + 1 \quad (4.1)$$

$$v_i = \left(\frac{G_s \gamma_w}{\gamma_{di}} \right) \quad (4.2)$$

$$v_i = \frac{(G_s - S_{ri})}{\left(\frac{\gamma_i}{\gamma_w} - S_{ri} \right)} \quad (4.3)$$

$$v_i = \frac{(w_f G_s + 1)}{(1 - \varepsilon_v)} \quad (4.4)$$

Where:

- w_i initial water content (-).
- w_f final water content (-).
- γ_{di} initial dry unit weight (kN/m³).
- γ_i initial bulk unit weight (kN/m³).
- γ_w unit weight of water (kN/m³).
- G_s specific gravity of the soil grains (-).
- S_{ri} initial degree of saturation (-).
- ε_v overall volumetric strain reached during the test (-).

The relationship between strain as measured in the constant rate of strain tests and specific volume is (Den Haan, 1994):

$$\varepsilon^H = -\ln \left(\frac{v}{v_i} \right) \quad (4.5)$$

Where:

- v specific volume (-).
- v_i initial specific volume (-).
- ε^H natural strain (Hencky strain) (-).

4.4 Spatial variability

The spatial variability in horizontal direction is quantified based on the cone penetration resistance of successive CPTs. The semivariogram and correlation function as discussed in Paragraph 2.3.3 are used to calculate the horizontal correlation length of the cone penetration resistance. The three rows of 15 dykecone CPTs (class 1+) with distance interval of 7 m at the measurement sites at the Achterwaterschap AC 075, AC 090 and AC 251 (see Paragraph 4.2) are used to conduct this analysis. The measured cone penetration resistance and the normalized cone penetration resistance (see Paragraph 4.6) are used for the analysis. It is assumed that the spatial variability of the cone penetration resistance in each CPT in vertical direction of the layers averages out on the scale of a slope failure of a dike. With the horizontal correlation length and an assumption for the horizontal scale of a slope failure of 75 m of a dike (normally between 30 and 100 m) the variance reduction factor I is calculated as discussed in Paragraph 2.3.3. The variance reduction factor determines the reduction of the standard deviation in the calculation of the characteristic lower bound values of soil parameters as explained in Paragraph 2.3.1. This analysis of the spatial variability is performed for the layers where sufficient data was available in successive CPTs. To perform the analyses the stratigraphy is derived from the class 1+ (dykecone) CPTs and class 1 CPTs as discussed in Paragraph 4.6. The borehole descriptions are also used for the derivation of the stratigraphy.

4.5 Undrained shear strength behaviour

The operational shear strength of soils depends on the drainage conditions during failure, stress level, stress history and the failure mode due to anisotropy of the undrained shear strength.

In soft low permeable soils excess pore water pressures are generated during shear failure. When the excess pore water pressure can dissipate drained shear strength is mobilized. The soil behaves undrained when the time to failure is relatively short compared to the dissipation of excess pore water pressures. The undrained shear strength s_u is mobilized when the excess pore water pressure cannot dissipate. In case of undrained behaviour the excess pore water pressures influence the operational shear strength. The magnitude of the excess pore water pressures depends on the in situ state (or stress history), which can be expressed as the yield stress σ'_{vy} or overconsolidation ratio OCR .

In geotechnical engineering undrained shear failure is assumed to be relevant in soft clays and peat for the assessments of the stability of slopes. For the interpretation of CPTs and FVTs in soft soils also undrained shear failure is assumed.

Undrained shear strength can be modelled with the SHANSEP (Stress History And Normalized Soil Engineering Properties)-model (Ladd & Foot, 1974; Ladd, 1991):

$$s_u = \sigma'_v \cdot S \cdot OCR^m \quad \text{with} \quad \sigma'_{vy} = \sigma'_{vi} \cdot OCR \quad \text{and} \quad \sigma'_{vy} = \sigma'_{vi} + POP \quad (4.6)$$

where:

- s_u Undrained shear strength (kPa).
- σ'_v Effective vertical stress (kPa).
- S Normally consolidated undrained shear strength ratio (-).
- OCR Overconsolidation ratio (-).
- m Strength gain exponent (-).
- σ'_{vy} Yield stress (kPa).
- POP Pre overburden pressure (kPa).

Soft soils in The Netherlands are commonly overconsolidated (OCR around 2). The yield stress is about 10 or 20 kPa higher than the effective vertical stress. For variations of the

effective vertical stress below the yield stress the undrained shear strength is more or less constant, following the SHANSEP-model, because the strength gain exponent is around 0.8.

Clayey soils with high soil unit weight above 17 to 18 kN/m³ do not behave like the SHANSEP-model. These are soils with high silt and sand content. These soils are called Transitional soils, as they are in-between sand and clay. Due to their compact structure they behave dilative during undrained shear failure; negative excess pore water pressures give the soil a temporary additional strength. For transitional soils the operational undrained shear strength depends on the initial void ratio of the soil (Coop, 2015). The operational undrained shear strength can be much higher than what could be expected based on the SHANSEP-model.

4.6 Cone penetration tests

Cone penetration tests (CPT or CPTu when the pore water pressure u_2 is measured) are relatively simple in situ tests. They are good reproducible and economic. The CPT gives a more or less continuous measurement as during penetration of the cone the cone penetration resistance q_c , sleeve friction f_s and excess pore water pressure u_2 are measured every 2 cm. The surface area of the cone is mostly 10 cm² and sometimes 15 cm². The penetration rate is 2 cm per second. In soft low permeable soils this penetration rate induces undrained soil behaviour. CPTs are carried out according to ASTM D 5778 and NEN-EN-ISO 22476-1.

Derivation of the undrained shear strength s_u from the cone penetration resistance q_c is not straightforward due to the complex interaction between the soil and the cone. Commonly an empirical relationship between the undrained shear strength and cone penetration resistance is applied:

$$s_u = \frac{q_{net}}{N_{kt}} \quad (4.7)$$

with net cone resistance:

$$q_{net} = q_t - \sigma_{vi} \quad (4.8)$$

and corrected cone resistance:

$$q_t = q_c + u_2(1 - a) \quad (4.9)$$

where:

- N_{kt} empirical correlation factor (-)
- q_t corrected cone resistance for pore pressure effects (MPa).
- σ_{vi} in situ total vertical stress (MPa).
- σ'_{vi} in situ effective vertical stress (MPa).
- q_{net} net cone resistance corrected for pore pressure effects and in situ total vertical stress (MPa).
- q_c measured cone tip resistance (MPa).
- u_2 pore water pressure measured just behind the cone during penetration (MPa).
- a area ratio (that area affected by the pore water pressure) (-).

Based on finite element analyses Teh & Houlsby (1988) and Lu et al. (2004) pointed out that N_{kt} depends on the stiffness of the soil, horizontal stress and roughness of the cone and the shaft.

Typical values of N_{kt} are between 10 and 20 (Ladd & DeGroot, 2004; Schnaid, 2008). It is important to note that N_{kt} depends on the reference strength as the undrained shear strength is not a unique soil parameter but a measure of the strength which depends on several factors, as mentioned in Paragraph 4.5.

Determination of stratigraphy

To deduce the stratigraphy from the CPT data the Begemann (1965) classification system and the Been and Jefferies (1992) classification system are applied. In Dutch engineering practise the classification of Begemann (1965) is a very common method. Begemann defined values of the friction ratio and related soil types to these friction ratio values. The friction ratio R_f is the ratio of the sleeve friction resistance f_s to the cone tip resistance q_c in percentages ($R_f = f_s/q_c \times 100\%$).

Been and Jefferies (1992) modified the classification chart of Jefferies and Davies (1991) and uses the dimensionless parameter group $Q_t(1 - B_q) + 1$ versus the normalised friction ratio F_r . Q_t is the normalized dimensionless cone penetration resistance:

$$Q_t = \frac{(q_t - \sigma_{vi})}{\sigma'_{vi}} = q_{net}/\sigma'_{vi} \quad (4.10)$$

The corrections for measured pore water pressure and total vertical stress are applied as given in equations (4.8) and (4.9). These corrections are based on the work of Campanella et al. (1982), Robertson et al. (1990), Robertson et al. (1999), Zhang et al. (2002) and others. The correction for pore water pressure has to be applied because of the pore water pressure effects acting in the joints of the penetrometer.

The normalised friction ratio is:

$$F_r = (f_s/q_{net}) \times 100\% \quad (4.11)$$

with:

- F_r normalized friction ratio (%).
- f_s sleeve friction resistance (MPa).

In the Been and Jefferies (1992) approach the drainage conditions around the cone during penetration are incorporated with the normalised excess pore water pressure B_q :

$$B_q = (u_2 - u_0)/q_{net} \quad (4.12)$$

with u_0 the stationary pore water pressure (MPa).

The boundaries between the soil types following the Been and Jefferies (1992) approach are marked with the soil type behaviour index I_c :

$$I_c = \sqrt{\left(3 - \log(Q_t(1 - B_q) + 1)\right)^2 + \left(1.5 + 1.3\log(F_r)\right)^2} \quad (4.13)$$

The different soil types are given in Table 4.4.

Table 4.4 Boundaries of the soil types according to Been and Jefferies (1992).

Zone	I_c (-)	Soil classification
2	$I_c > 3.22$	Organic soils
3	$2.76 < I_c < 3.22$	Clays
4	$2.40 < I_c < 2.76$	Clayey silt to silty clay
5	$1.80 < I_c < 2.40$	Silty sand to sandy silt
6	$1.25 < I_c < 1.80$	Sands: clean to silty
7	$I_c < 1.25$	Gravelly sands

The results from the class 1 cones at each location are used in a first step to characterize the stratigraphy of the subsoil. This is because these cones measure cone penetration resistance, sleeve friction and pore water pressure. So, these cones give more information than the class 1+ cones (dykecone). After that the cone penetration resistances from the 15 class 1+ cones at each location are used to characterize the stratigraphy of the subsoil between the locations of the class 1 cones. Information from boreholes as performed by Waterboard Rivierenland is also used for the characterization of the subsoil.

After the interpretation of the stratigraphy and the corrections of the CPT data statistical analyses on the CPT data are performed. Therefore the theory to determine the horizontal correlation length as discussed in Paragraph 4.4 is applied.

4.7 Dissipation tests

From pore pressure dissipation tests with the CPTu the horizontal coefficient of consolidation is obtained. This coefficient of consolidation is used to assess the rotation speed of the FVT in order to verify whether the rotation speed is fast enough to initiate undrained shear behaviour of the soil.

A pore pressure dissipation test using the CPTu can be performed during a pause of the penetration process. When the penetration process stops, the excess pore water pressure which is generated due to penetration of the cone, will show a decay with time until equilibrium with the initial in situ pore water pressure will be reached. The rate of dissipation of the excess pore water pressure is determined by the coefficient of consolidation. As the time required to obtain equilibrium of the measured pore water pressure with the in situ pore water pressure the dissipation tests are usually continued to 50% dissipation.

Various researchers studied the dissipation process using different theories. A well-known method to derive the coefficient of consolidation from CPTu dissipation tests is the Housby & Teh (1988) method (see Figure 4.1). This solution is based on the strain path method (SPM).

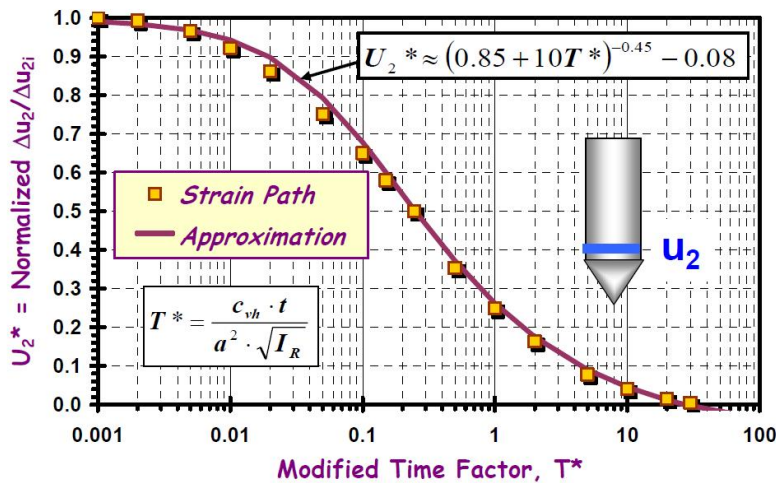


Figure 4.1 Derivation of the coefficient of consolidation from CPTu dissipation tests using the shoulder position (u_2) of the cone (Mayne, 2007). The strain path method of the Housby & Teh (1988) method is approximated by the algorithm of Mayne (2007).

Housby & Teh (1988) used a dimensionless time factor T^* to relate the consolidation coefficient to the time during dissipation:

$$T^* = \frac{c_h t}{R^2 \sqrt{I_r}} \quad (4.14)$$

where:

- c_h horizontal coefficient of consolidation (m^2/s).
- t time during dissipation (s).
- R probe radius (m).
- I_r rigidity index (-) ($= G/s_u$) and G the shear modulus.

The measured pore water pressure at the shoulder position (u_2) of the cone is normalized using:

$$U_2^* = (u_t - u_0)(u_i - u_0) \quad (4.15)$$

where:

- u_i initial value of the pore water pressure at the start of the dissipation test (MPa).
- u_t the measured pore pressure at time t (MPa).
- u_0 in situ equilibrium pore water pressure (MPa).

Houlsby & Teh (1988) give time factors for a range of degrees of consolidation based on their SPM solution. Using these time factors the coefficient of consolidation can be derived from the dissipation test results. Mayne (2007) proposed an approximate algorithm to relate the normalized pore water pressure U^* to the dimensionless time factor T^* (see Figure 4.1). The advantage of using this algorithm is that instead of matching just a single point (usually 50%) of the dissipation curve, the complete dissipation curve is used to obtain the best overall value of the horizontal coefficient of consolidation. Applying CPTu with pore pressure filter at the shoulder of the cone (u_2) the approximate algorithm is:

$$U_2^* \approx (0.85 + 10T^*)^{-0.45} - 0.08 \quad (4.16)$$

Burns & Mayne (1998) developed a model to evaluate the coefficient of consolidation in soft to hard clays based on a pore pressure filter at the shoulder of the cone (u_2). Based on their analyses it can be concluded that for soft clays with $\text{OCR} < 3$ a decrease of normalized pore water pressure can be expected (see Figure 4.2). For clays with $\text{OCR} > 3$ the dissipation process starts with an increase of pore water pressure followed by a decrease of pore water pressure. For heavily overconsolidated soils the initial increase of the measured pore water pressure is caused by the dilatatory response of these soils.

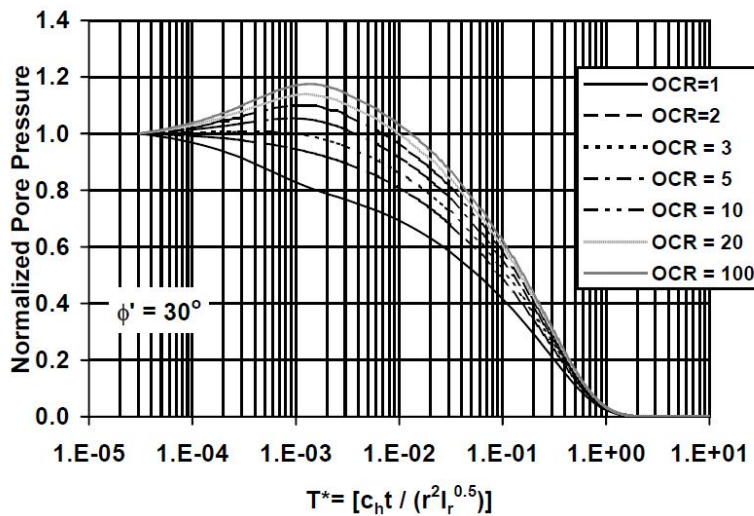


Figure 4.2 Relationship between normalised pore water pressure and dimensionless time factor T^* for a range of overconsolidation ratios OCR (Burns & Mayne, 1998). For soft clays with $OCR < 3$ a decrease of normalized pore water pressure from the start of the dissipation tests is to be expected.

4.8 Field vane tests

The field vane test (FVT) is applied to determine the in situ peak undrained shear strength, residual shear strength and sensitivity.

With a FVT a vane with four rectangular blades is rotated in the soil. It is assumed that a cylindrical shear plane is formed around the rotating vane. The shear stress on this cylindrical shear plane can be determined based on the torque which is applied to rotate the vane. The failure mode of the FVT is thought to compare with the failure mode of a direct shear test (Chandler, 1988).

For standard vane dimensions with the height of the vane two times the diameter of the vane the undrained shear strength $s_{u,FVT}$ of the soil can be determined with (ISO 22476-9):

$$s_{u,FVT} = 0.273 \frac{T}{D^3} \quad (4.17)$$

where:

T torque on the vane (kNm).

D diameter of the vane (m).

The sensitivity $S_{t,FVT}$ can be calculated from the FVT with:

$$S_{t,FVT} = s_{u,peak,FVT} / s_{u,res,FVT} \quad (4.18)$$

where:

$s_{u,peak,FVT}$ peak undrained shear strength (kPa).

$s_{u,res,FVT}$ residual undrained shear strength (kPa).

To convert the FVT measurements to an accurate estimation of the operational shear strength there are several issues to be considered, such as friction along the rods, shear stress distribution on the vane blades, anisotropy of the soil, rate effects, and partial consolidation (Chandler, 1988; Schnaid, 2008).

The friction along the rods plays no role in this project as a FVT device is applied with the motor just above the vane.

Stress distribution and anisotropy

The shear stress distribution on the vane blades is uncertain. Several studies are conducted to determine the stress distribution on the vane blades. Anisotropy of the undrained shear strength due to the soil fabric developed during deposition and consolidation effects enhance the complexity of the shear stress distribution on the vane. When considering stress distribution and anisotropy a number of variations on equation 4.17 are possible (Schnaid, 2008). Equation 4.17 as proposed by ISO 22476-9 assumes isotropic soil conditions and uniform stress distribution on the vanes. Applying other assumptions the calculated undrained shear strength may deviate substantially, at least when anisotropy is large. Bjerrum (1973) showed that the anisotropy of the undrained shear strength is low for soils with plasticity index above 40%. Assuming isotropic soil conditions and uniform stress distribution yields a low estimate of the undrained shear strength. As the stress distribution and anisotropy are very difficult to assess in practice equation 4.17 as proposed by ISO 22476-9 is commonly adopted (Schnaid, 2008). The resulting undrained shear strength is then corrected with empirical corrections which account for several aspects, such as strain rate, soil disturbance and anisotropy of the shear strength.

Becker et al (1988) proposed that the FVT interpretation could be refined when the in situ horizontal effective stress and horizontal yield stress would be considered. As the common practice uses the vertical effective stress and empirical correlations are also based on the vertical effective stress in the present research also the vertical effective stress will be used. For CPT interpretation the horizontal stress also plays a role (see Paragraph 4.6), but for CPT interpretation also the vertical stress is commonly applied.

Rate effects

Rate effects are important because the rotation of the vane is much faster than the rate of a slope failure. As the undrained shear strength exhibit rate dependency, correction for rate effects is required. This correction is generally incorporated in empirical corrections for the FVT. The empirical corrections are derived using a rotation rate of 6 degrees/minute. To correct the undrained shear strength obtained by other rotation rates the undrained shear strength can be normalized with:

$$s_u = s_{u.ref} \left(\frac{\dot{w}}{\dot{w}_{ref}} \right)^\beta \quad (4.19)$$

where:

$s_{u.ref}$ reference strength measured at an angular strain rate \dot{w}_{ref} (kPa).

\dot{w}_{ref} angular strain rate of 6 degrees/minute.

\dot{w} angular strain rate (degrees/minute).

β soil dependent material parameter (-).

The soil dependent parameter β ranges between 0.006 and 0.20 for various natural clays as summarized by Biscontin & Pestana (2001). There seems to be a tendency that β increases for increasing plasticity index I_p , however the scatter for higher values of I_p is large. Based on their experiments with artificial clay with I_p of 75% these authors proposed that the peak undrained shear strength should be corrected for strain rate effects and that the residual shear strength is independent of strain rate effects. For organic harbour mud with I_p of 92.6% and organic matter content of 12% Schlue et al. (2010), in contrast, found that the residual shear strength with β between 0.18 and 0.34 is much more sensitive for strain rate than the peak undrained shear strength with β is 0.11. The data from Biscontin & Pestana (2001) and Schlue et al. (2010) is presented in Figure 4.3.

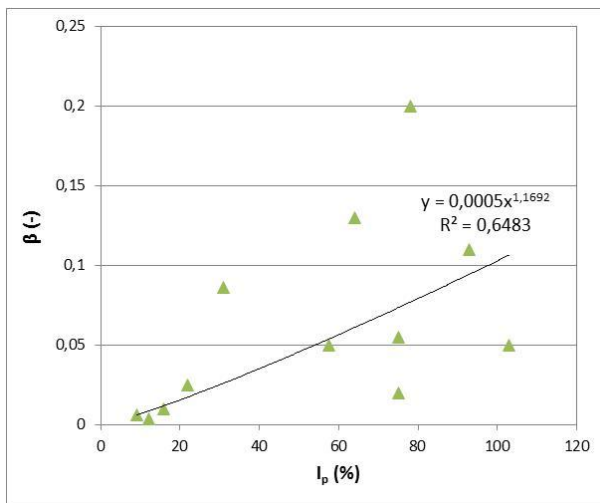


Figure 4.3 Relationship between β and plasticity index I_p based on the data of Biscontin & Pestana (2001) and Schlue et al. (2010). For clays with high plasticity the uncertainty of β is considerable.

The relationship $\beta = 0,0005 I_p^{1,1692}$ with a maximum of 0.15 is applied in this project to correct the peak undrained shear strength in this research. For peat an arbitrary value of β is 0.08 is used. The residual shear strength is not corrected for strain rate effects.

Partial consolidation

During FVT partial consolidation of excess pore water pressures can occur, resulting in changes of the effective stress and shear strength. According to ISO 22476-9 the FVT should be carried out such that that failure of the soil occurs in undrained conditions. So, changes in excess pore water pressures should be negligible. The time from the moment when the desired test depth has been reached to the start of the vane test (waiting time) shall be at least 2 minutes and not more than 5 minutes. Applying a rotation rate between 6°/min to 12°/min the maximum torque should be reached within 2 to 4 minutes to fulfill the criterion of undrained failure.

The normalized rotation rate V accounts for the rotation rate and consolidation rate of the soil:

$$V = \frac{v \cdot d}{c_v} \quad (4.20)$$

where:

- v rotation rate (m/s).
- d vane diameter (m).
- c_v coefficient of consolidation (m^2/s).

Drained shear conditions are obtained for $V < 0.1$, whereas undrained shear conditions occur around $V > 100$ (Schnaid, 2008). So for permeable soils the rotation rate has to be relatively high to reach undrained shear behaviour. Note that in this approach the waiting time plays no role on the consolidation process.

Morris & Williams (2000) suggested another approach to determine the effect of partial consolidation on FVT results. These authors proposed a normalized time T which accounts for the coefficient of consolidation and time to failure, where time to failure must be measured from the end of the vane insertion rather than from the start of vane rotation. This approach is based on the observations of Kimura & Saitoh (1983) and others who found that excess pore water pressures are generated due to vane insertion (Figure 4.4). These excess pore water pressures will decrease during the waiting time before the start of the vane rotation and during vane rotation.

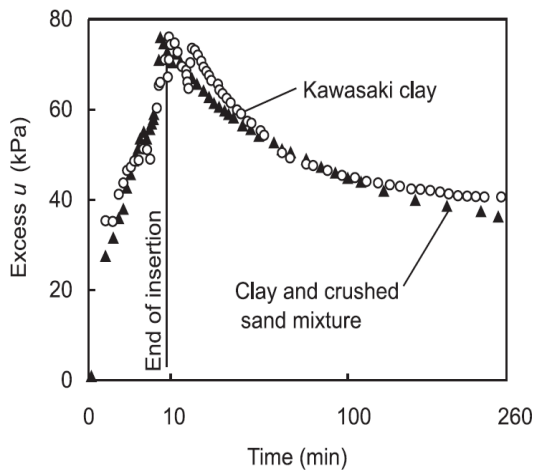


Figure 4.4 Observed excess pore water pressures during and following vane insertion as found by Kimura & Saitoh (1983). A remarkable high excess pore water pressure is generated by the insertion of the vane, and starts to dissipate directly after insertion.

The normalized time T is:

$$T = \frac{c_v \cdot t}{d^2} \quad (4.21)$$

where:

- c_v coefficient of consolidation (m^2/s).
- t time to failure measured from the start of vane insertion (s).
- d vane diameter (m).

When $T < 1$ the soil behaviour is undrained and when $T > 20$ the soil behaviour is drained (Morris & Williams, 2000).

Empirical corrections

Bjerrum (1972) derived an empirical correction factor μ to adjust the measured undrained shear strength from the FVT to the operational undrained shear strength in the field. This correction factor is related to the plasticity index I_p and accounts for effects of shear strength anisotropy and strain rate. Bjerrum obtained the correction factor from back calculated case histories. The correction factor decreases from 1.1 for I_p is 10% to 0.55 for I_p is 120%. The correction factor is applied as follows:

$$S_{u,field} = \mu S_{u,FVT} \quad (4.22)$$

Azzouz et al. (1983) also examined the required correction of the measured undrained shear strength from the FVT. These authors pointed out that Bjerrum (1972) ignored three-dimensional effects in the back-analyses of the case histories. Therefore the correction factor proposed by Bjerrum can be reduced by some 10% for field conditions with a plane strain mode of failure (see Figure 4.5).

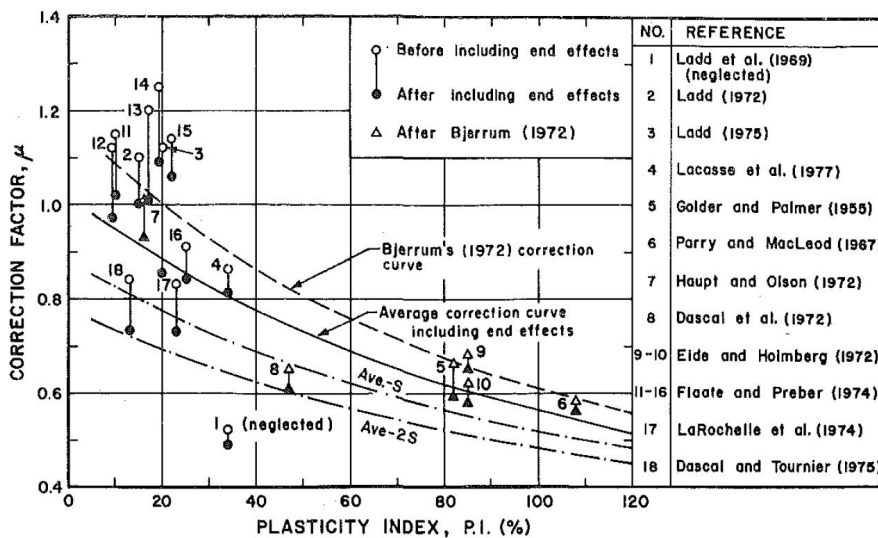


Figure 4.5 Correction factor to adjust FVT measurements (Azzouz et al., 1983). The correction factor is based on back-analyses of failures. Be aware of the considerable uncertainty of the correction factor.

A widely used correction for the FVT measurements is suggested by Chandler (1988). This correction is also based on the plasticity index. The Chandler correction depends on the time to failure for which the correction factor is required (not the time to failure in the FVT). The Chandler (1988) correction corresponds with the correction of Azzouz et al. (1983) for the time to failure of 10^4 minutes. The Chandler correction is:

$$\mu_R = 1.05 - b (I_p)^{1/2} \quad \text{with } b = 0.015 - 0.0075 \log t_f \quad (4.23)$$

where:

I_p plasticity index (%).
 t_f time to failure (min).

In Swedish practice the empirical correction for FVT as proposed by Larsson et al. (1987) and Larsson et al. (2005) is used. Instead of the plasticity index the liquid limit w_L is applied. The Larsson correction is largely based on high plastic soils, whereas the Bjerrum correction is mainly based on low- and medium plastic clays (Larsson et al., 1987). The lower limit of the Larsson correction is 0.5, which is based on Swedish experience with qualified laboratory investigations on organic soils with very high plasticity. For soils with overconsolidation ratio OCR larger than 1.3 an additional correction is applied. The correction from Larsson et al. is:

$$\mu = \left(\frac{0.43}{w_L} \right)^{0.45} \geq 0.5 \quad \text{and} \quad \mu_{OCR} = \left(\frac{OCR}{1.3} \right)^{-0.15} \quad (4.24)$$

where:

w_L liquid limit (%).

For peat a correction factor $\mu = 0.5$ is recommended by Edil (2001). When performing FVT in peat the correction factor has to adjust the measurements for fibre action and partial drainage. The recommendation from Edil is confirmed by Zwanenburg & Jardine (2015).

According to ASTM D 2573 sensitivity, S_t , is based on the ratio of measured peak shear strength and residual shear strengths and is not corrected.

4.9 Sensitivity framework

Sensitivity is used in this research to quantify the effect of soil fabric and structure on shear strength and compressibility in order to determine the effect of sample disturbance. Sensitivity is originally the ratio of the intact undisturbed peak strength to the fully remoulded strength at the same water content. Various phenomena may contribute to the sensitivity, such as metastable fabric (cardhouse arrangement of particles), cementation by carbonates or iron oxide or organic matter, weathering, leaching of salt (Mitchell & Soga, 2005). The various mechanisms cause different ranges of sensitivity. However, according to the definition of sensitivity and the various causes of sensitivity any soil has some amount of sensitivity (Mitchell & Soga, 2005; Cotecchia & Chandler, 2000). The FVT is often used to determine the sensitivity, but the unconfined compression test or the fall cone test can also be used (Mitchell & Soga, 2005).

A sensitivity framework is developed by Cotecchia & Chandler (2000) and Chandler (2000). This framework is based on earlier work of Skempton & Northey (1952), Skempton (1970), Burland (1990), and others. Skempton & Northey (1952) found that the laboratory compression curves for reconstituted clay samples from various sites were similar when the test results are normalized using the liquidity index I_L and plotted against effective stress. In their plot the in situ states of natural clay samples are above the curves of the reconstituted samples. Analyzing the data it became clear that the more sensitive clays were further from the reconstituted curves than the less sensitive clays. Skempton (1970) added more data from other sites to the database and confirmed the earlier findings. Quick clays, diatomaceous clays, clays with more than 5% organic matter, and clays with carbonate content above 25% were excluded from these studies (Burland, 1990).

Burland (1990) reanalyzed the data from Skempton & Northey (1952) and Skempton (1970) and normalized the data with the void index I_v instead of the liquidity index. The void index is:

$$I_v = \frac{e_0 - e_{100}^*}{e_{100}^* - e_{1000}^*} = \frac{e_0 - e_{100}^*}{C_c^*} \quad (4.25)$$

where:

- e_0 current void ratio (-).
- e_{100}^* void ratio for a normally consolidated reconstituted sample at 100 kPa (-).
- e_{1000}^* void ratio for a normally consolidated reconstituted sample at 1000 kPa (-).
- C_c^* compression index for a normally consolidated reconstituted sample (-).

The star notation refers to intrinsic parameters derived from reconstituted samples, so that the intrinsic parameters depend solely on the mineralogy and grading of the soil, whereas parameters obtained from intact undisturbed samples may additionally depend on soil forming processes. The reconstituted samples are composed from a slurry with a water content between the liquid limit w_L and 1.5 times the liquid limit and then consolidated (Burland, 1990).

Based on this normalization Burland (1990) was able to define the Intrinsic Compression Line (ICL), as all compression curves of reconstituted samples from various sites lie exactly on this line, at least between 100 and 1000 kPa, but generally also outside these points. The coordinates of the ICL in the void index effective stress space are:

$$I_v = 2.45 - 1.285x + 0.015x^3 \quad (4.26)$$

where $x = \log \sigma'_v$ in kPa.

Burland also gives relationships between the void ratio at the liquid limit e_L and the intrinsic compression index C_c^* and e_{100}^* :

$$C_c^* = 0.256 e_L - 0.04 \quad (4.27)$$

$$e_{100}^* = 0.109 + 0.679 e_L - 0.089 e_L^2 + 0.016 e_L^3 \quad (4.28)$$

The data of the intact samples from Skempton & Northey (1952) and Skempton (1970) plot above and parallel to the ICL. The distance between the data points of the intact samples and the ICL is caused by the natural structure of the soil. The trendline through the data points of the intact samples is called the Sedimentation Compression Line (SCL) by Burland.

A graph of the void index I_v and vertical effective stress with the position of the Intrinsic Compression Line (ICL) and the Sedimentation Compression Line (SCL) is given in Figure 4.6.

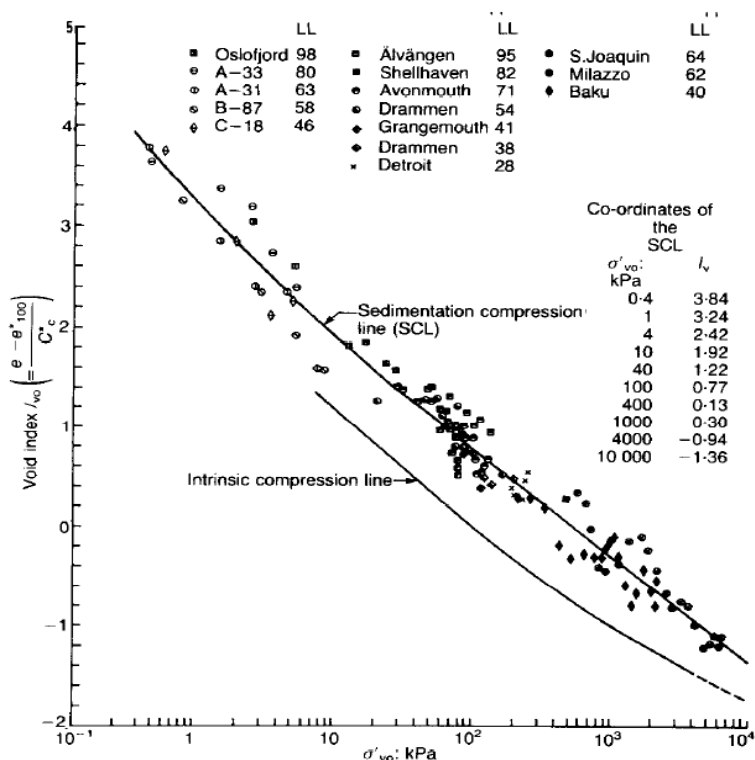


Figure 4.6 Graph of the void index I_v and vertical effective stress with the position of the Intrinsic Compression Line (ICL) and the Sedimentation Compression Line (SCL) according to Burland (1990). Using I_v compression curves of reconstituted samples of all clays fall over each other at the ICL. The position of natural clays is in a band around the SCL, when using I_v .

By conducting oedometer tests on high quality samples of three soft clays Smith (1992) confirmed the effect of structure of natural soils. Smith derived the sensitivity from the ratio of the yield stress σ'_{vy} on the compression curves to the vertical effective stress σ'_{v0} at the same void ratio on the ICL. Comparing these values of the sensitivity with the sensitivity obtained by the traditional definition of sensitivity based on shear strength Smith found similar values. The sensitivities found by Smith range from unity to 50, for clay in a high-energy estuarine environment at Queenborough, $S_t = 1$, shallow marine clay from Bothkennar, $S_t = 7$, and glacio-lacustrine clay at Berthierville, $S_t = 50$ (see Figure 4.7).

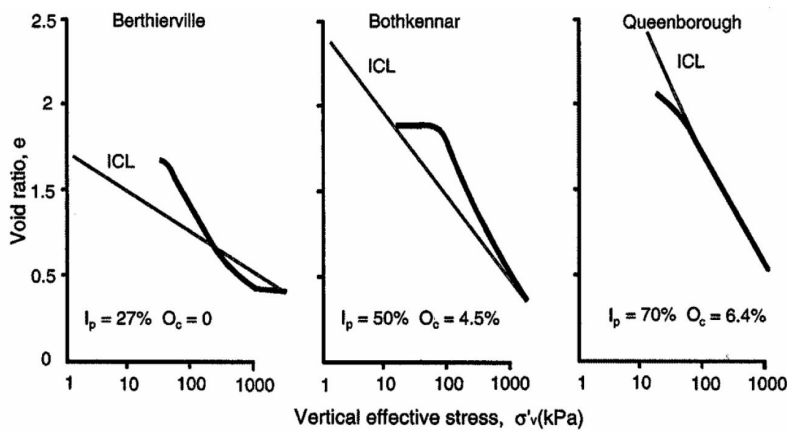


Figure 4.7 Compression lines from three sites plotted with the Intrinsic Compression Line (ICL) illustrating the different sensitivities of the soils (Smith, 1992) (I_p = plasticity index, OC = organic matter content). The figures show a clear relation between the depositional environment and sensitivity.

In the sensitivity framework of Cotecchia & Chandler (2000) and Chandler (2000) an infinite number of parallel sedimentation compression lines (SCL) as developed by Burland (1990) is defined. Each SCL (also called Sedimentation Compression Curves, SCC, by Cotecchia & Chandler (2000) and Chandler (2000)) belongs to a particular value of sensitivity. The ICL has sensitivity of unity. The SCL as defined by Burland is a SCL corresponding to a mean sensitivity of about 5, as all the clays used in the analysis of Burland had a sensitivity in the range 2-9, as pointed out by Cotecchia & Chandler (2000). This relatively small sensitivity range is caused by the fact that Skempton (1970) excluded various types of clays as mentioned before and Burland omitted clays of low sensitivity and clays with a clear cementation (Jardine et al., 2004).

For clays with structure each of the SCL of the sensitivity framework is a curve of yield stresses σ'_{vy} as measured in oedometer tests (Cotecchia & Chandler, 2000). The vertical effective stress σ'_{v0} on the ICL at the same void ratio as the yield stress σ'_{vy} is called the equivalent stress σ'_{ve} . The ratio of σ'_{vy} on one of the SCL to the equivalent stress σ'_{ve} is defined as the stress sensitivity S_σ . Smith (1992) also derived the sensitivity in this way, as discussed before. Based on their analysis Cotecchia & Chandler (2000) suggested that the stress sensitivity S_σ is numerically equal to the strength sensitivity S_t , i.e. the traditional definition of sensitivity. This also corresponds with the work of Smith as mentioned before. So, for intact undisturbed natural clays the stress sensitivity S_σ is a measure of the strength of the soil structure in excess of that exhibited by reconstituted soils (Chandler, 2000). Thus sensitivity is defined as:

$$S_t = s_u/s_u^* = S_\sigma = \sigma'_{vy}/\sigma'_{ve} \quad (4.29)$$

where:

- S_t strength sensitivity (-).
- S_σ stress sensitivity (-).
- s_u intact undisturbed peak undrained shear strength (kPa).
- s_u^* intrinsic undrained shear strength of reconstituted soil (kPa).
- σ'_{vy} yield stress intact undisturbed soil with structure (kPa).
- σ'_{ve} equivalent stress: vertical effective stress on the ICL at the same void ratio as the yield stress σ'_{vy} (kPa).

Chandler (2000) additionally defined an Intrinsic Strength Line, IS_uL , for the sensitivity framework (Figure 4.8). The meaning of this line is similar to the ICL as proposed by Burland (1990). The IS_uL defines the intrinsic undrained shear strength in the void index undrained

strength space and is a reference for the intact undisturbed strength of natural soils. Using the void index undrained strength space the intact undisturbed strength and the intrinsic strength are plotted against the same void index (or void ratio or water content) and the ratio between these two measures of strength is the strength sensitivity S_t . The slope of the ISuL is based on an undrained shear strength ratio $s_u/\sigma'_{vc} = 0.33$ for triaxial compression mode of failure. This value is based on a literature research performed by Chandler (2000), which resulted in a range between 0.226 and 0.460.

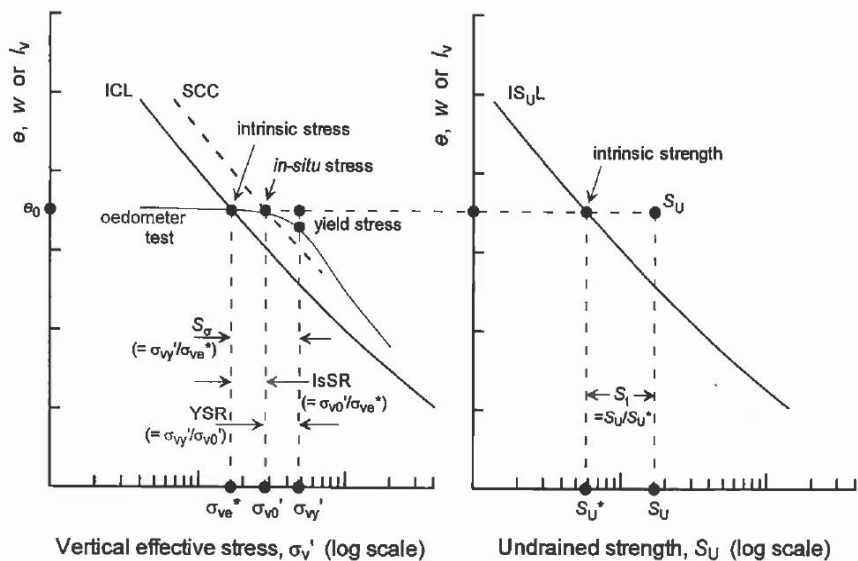


Figure 4.8 Sensitivity framework (Chandler, 2000). Strength sensitivity (figure right) and stress sensitivity (figure left) are numerically equal. The meaning of the IS_uL is similar to the ICL as proposed by Burland (1990).

Regarding the stress sensitivity S_σ in the void index effective stress space Chandler (2000) defined the in situ stress ratio, IsSR. This is the ratio of the in situ vertical effective stress σ'_{v0} and the equivalent stress σ_{ve}^* on the ICL at the same void ratio or void index. The yield stress ratio YSR (Burland, 1990) is the ratio between the yield stresses σ'_{vy} and the in situ vertical effective stress σ'_{v0} . Therefore the stress sensitivity S_σ is equal to the IsSR times the YSR (Chandler, 2000).

5 Results: Natural variability

5.1 Introduction

In this chapter the results regarding the natural spatial variability of the shear strength of the subsoil at the Achterwaterschap sites AC 075, AC 090 and AC 251 are presented. First the stratigraphy is deduced from the CPT data. The measured cone penetration resistance q_c is corrected for measured pore water pressure and total vertical stress to the net cone penetration resistance q_{net} and normalised with the effective vertical stress to the normalised dimensionless cone penetration resistance Q_t . The interpreted stratigraphy is used to estimate the total vertical stress and effective vertical stress profiles at the locations of the CPTs. The analysis of the natural spatial variability of the shear strength of the subsoil is based on the measured cone penetration resistance q_c , net cone penetration resistance q_{net} and normalised dimensionless cone penetration resistance Q_t .

5.2 Stratigraphy derived from CPT data

The measured cone penetration resistances q_c from the class 1 and class 1+ cones at the three investigated locations along the Achterwaterschap are given in Figure 5.1, Figure 5.2 and Figure 5.3.

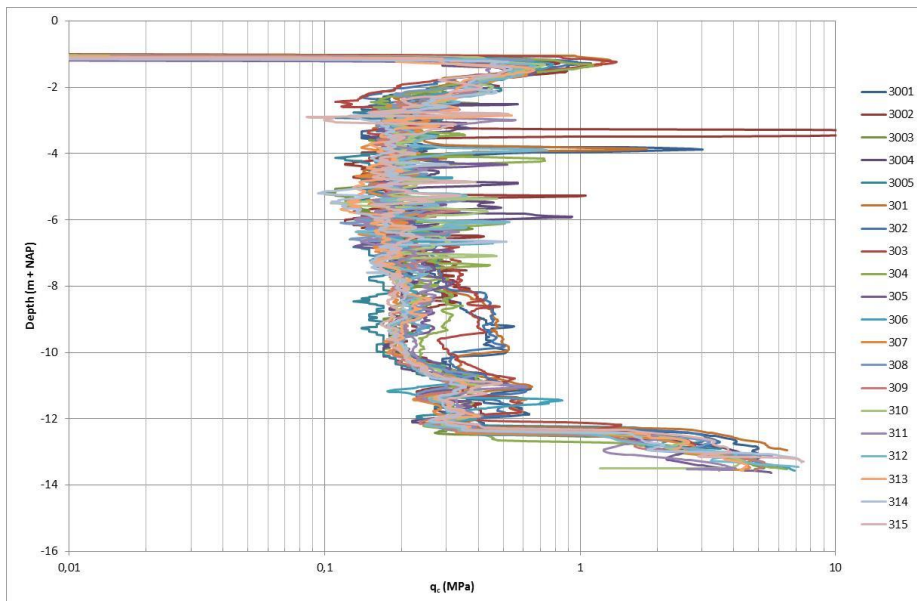


Figure 5.1 Measured cone penetration resistance q_c at location AC 075.

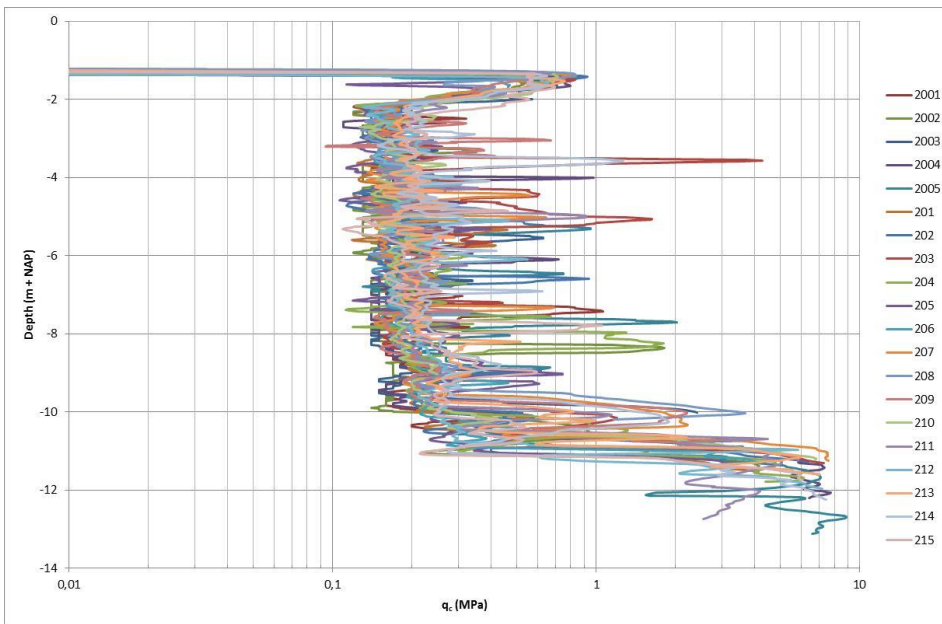


Figure 5.2 Measured cone penetration resistance q_c at location AC 090.

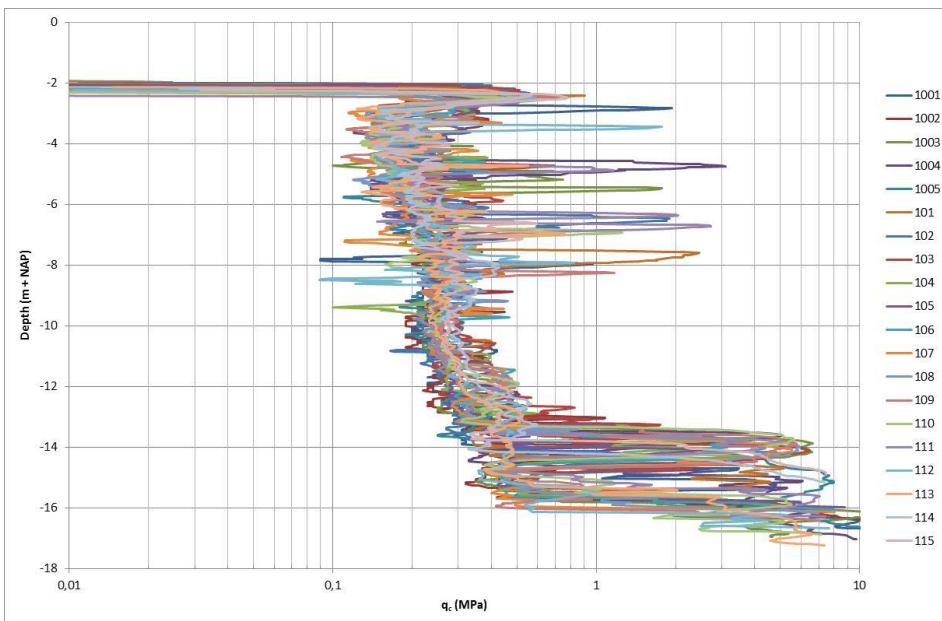


Figure 5.3 Measured cone penetration resistance q_c at location AC 251.

The figures show the variability of the measured cone penetration resistances q_c . In general, the q_c values show consistent results. The top of the firm Pleistocene sand layers can be found between NAP -11 m and NAP -16 m. The Holocene layers show a measured cone penetration resistance between 0.15 and 0.4 MPa. In the top layer near the surface higher cone resistances of about 0.8 MPa are measured. Roughly the cone penetration resistances at the three sites are in the same order of magnitude.

Figure 5.1, Figure 5.2 and Figure 5.3 show several spikes in the measured cone penetration resistances in the soft Holocene layers (between NAP -2 and -10 m), which can be attributed to fragments of wood in peat and humic clay. These fragments of wood can be recognized in the photo of the samples from borehole B-100 at location AC 251 (Figure 5.4). Spikes are ignored in the analysis of the variability of the cone penetration resistance, which

is a conservative choice given that the spikes are an increase in cone penetration resistance, but due to the limited scale of the fragments, this is not deemed sufficient to derive strength from.

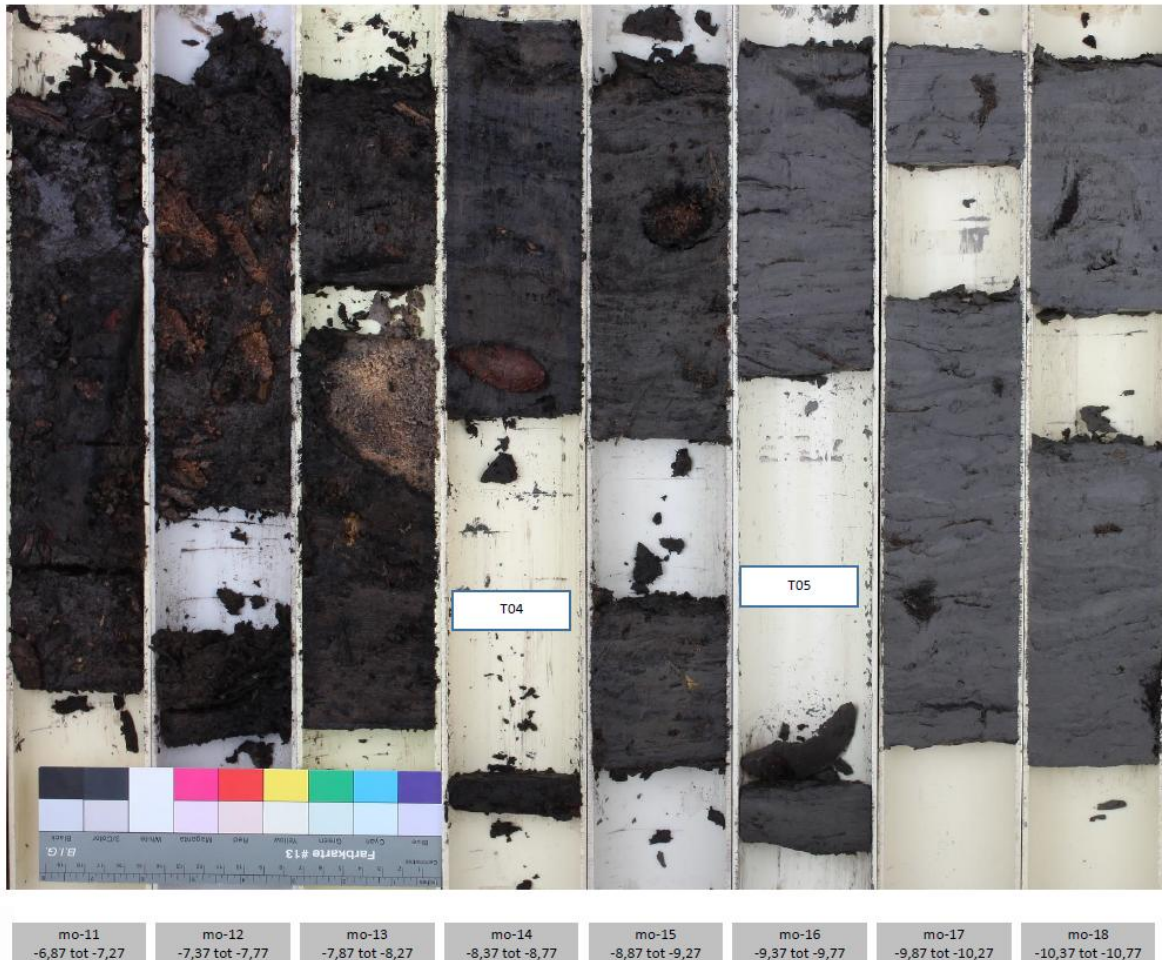


Figure 5.4 Photo of samples from borehole B-100 at location AC 251 with fragments of wood in peat and humic clay.

When applying the Begemann and Been and Jefferies (1992) classification systems it turns out that the Begemann classification system is more appropriate for Dutch humic soils than the Been and Jefferies classification. The Been and Jefferies classification classifies most of the soil layers in the same category ($I_c > 2.9$) as illustrated in Figure 5.6. The Begemann classification results in an increasing friction ratio R_f in upward direction. This trend fits well to the soil description as derived from borehole B-100 (Figure 5.5).

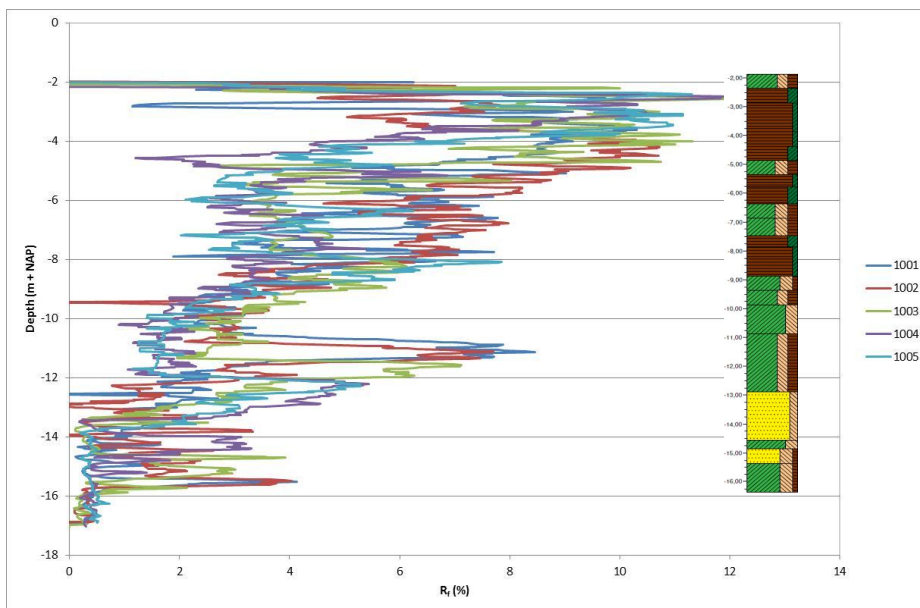


Figure 5.5 Begemann classification based on friction ratio R_f at location AC 251 and borehole B-100. R_f shows a remarkable decrease with increasing depth.

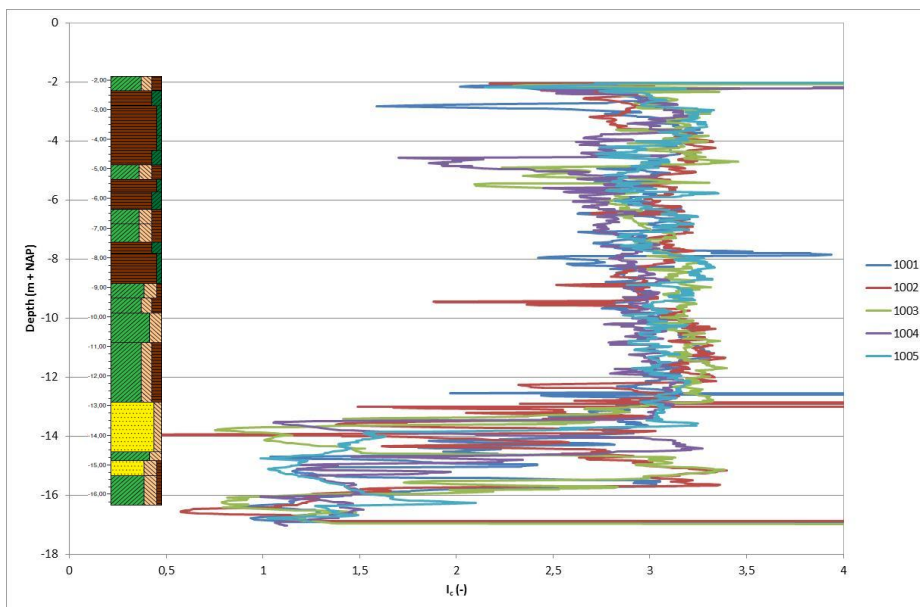


Figure 5.6 Been and Jefferies (1992) classification based on soil type behaviour index I_c at location AC 251 and borehole B-100. I_c shows a very constant course compared to R_f in Figure 5.5.

Figure 5.7, Figure 5.8 and Figure 5.9 show the interpreted stratigraphy of the three locations. As mentioned before the top of the Pleistocene sand layers can be found between NAP -11 m and NAP -16 m. The depth of the top of the Pleistocene sand layers increases from east to west. At location AC 251 the top of the Pleistocene sand layer shows a lot of relief of about 2.5 m. On top of the Pleistocene sand layer the flood basin deposits of the Wijchen Member can be recognized. The thickness of this layer ranges from some decimetres to about one meter. Basal peat has been formed on top of the Wijchen Member. Channel belt deposits (Echteld Formation) can be derived from the data below NAP -9.5 m. These channel belt deposits might be formed by the Benschop river system (see Paragraph 3.2 and Berendsen & Stouthamer, 2000). These channel belt deposits are very thin (≈ 0.5 m) with only one crevasse channel deposit at location AC 075. At both other locations the channel belt deposits are

much thicker; about 1 m at AC 090 and up to 3 m at AC 251. At AC 090 four channel belt sand bodies with varying dimensions can be derived from the CPT data. The former channels partly eroded the Basal peat and Wijchen Member. Above the channel belt deposits the subsoil is dominated by humic and peaty clay, which are flood basin deposits (Echteld Formation). Considering the layering and organic matter content of the clay around NAP -9.0 m to NAP -10 m in Figure 5.4 this clay may be part of the Terbregge Member (see Paragraph 3.2 and Hijma et al., 2009). On top of the Echteld deposits peat (Nieuwkoop Formation) has been formed. The peat layers can be divided in eutrophic peat and mesotrophic peat. The top of the eutrophic peat occurs around NAP -4 m to NAP -5 m. This stratigraphy is in good agreement with the stratigraphy as described by Gouw & Erkens (2007) and Hijma et al. (2009).

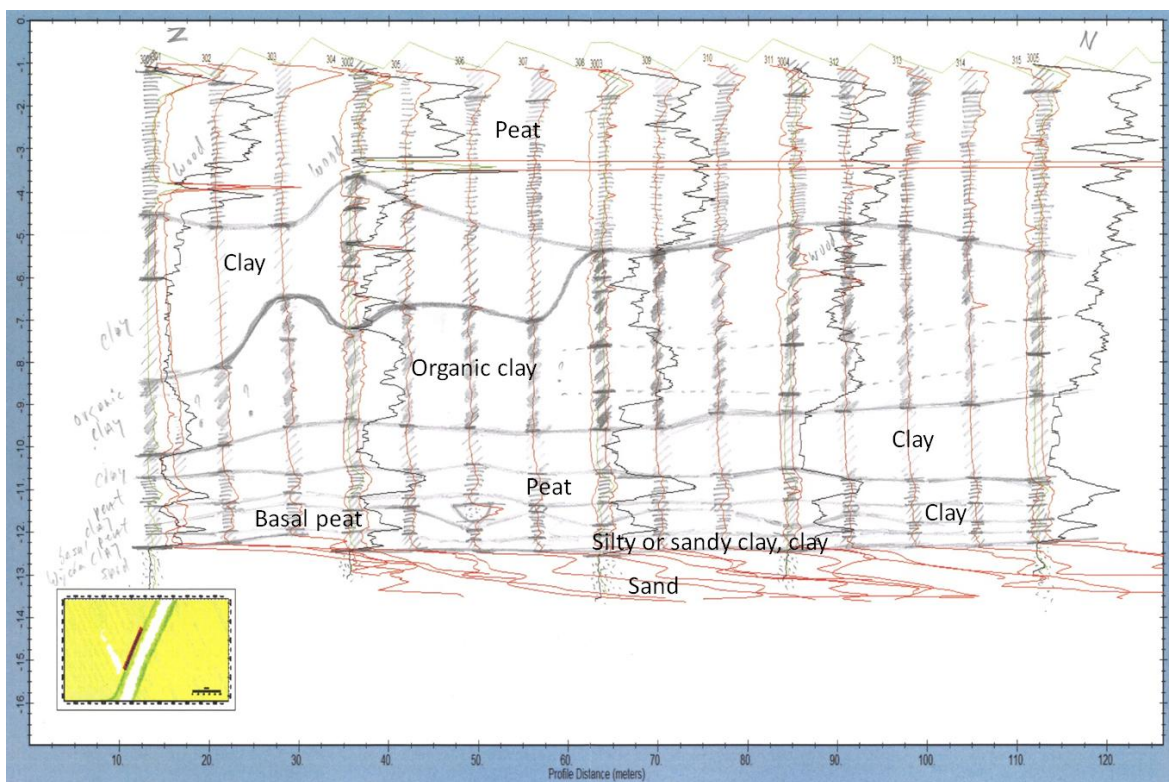


Figure 5.7 Interpreted stratigraphy at location AC 075.

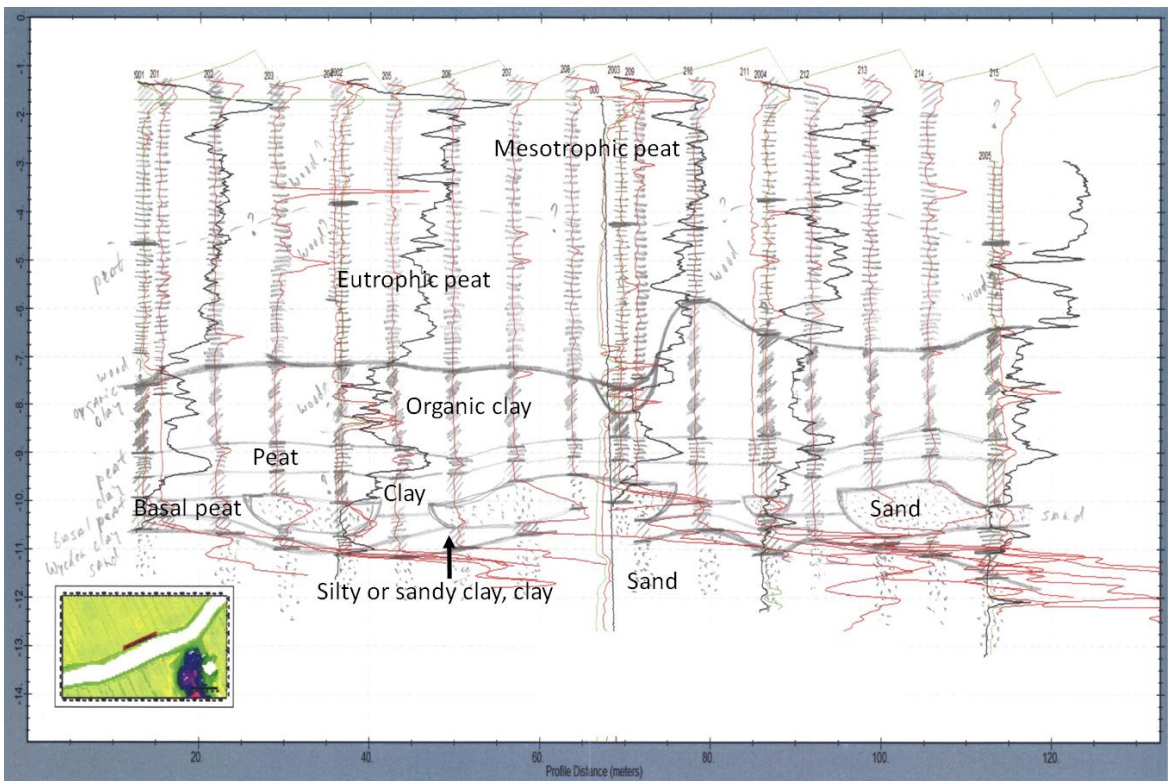


Figure 5.8 Interpreted stratigraphy at location AC 090.

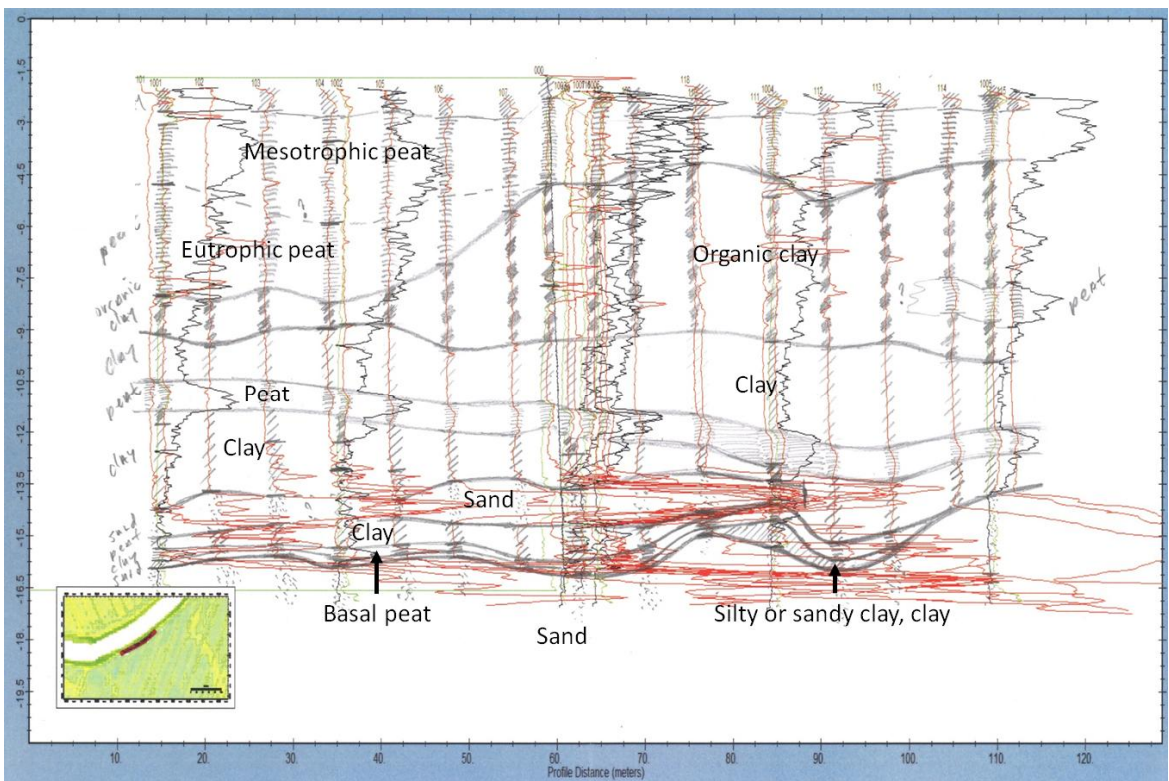


Figure 5.9 Interpreted stratigraphy at location AC 251.

Analysing the results of the class 1+ cones proves that the interpretation of these results is difficult because the pore water pressure u_2 and sleeve friction f_s were not measured. Only the cone penetration resistance is not sufficient to make accurate decisions on boundaries between soil layers. Pore water pressure and sleeve friction offer useful additional information for the soil classification. The measurements of the class 1 cones sometimes show an alternation of peaty and humic layers. Examples are location AC 075 at NAP -7 m to NAP -10 m and location AC 251 around NAP -8 m. The boundary between eutrophic peat and mesotrophic peat cannot be determined from the results of the class 1+ cones. It can be expected that these uncertainties will cause scatter in the analysis as discussed in the next paragraphs.

5.3 Correction and normalization of CPT data

When the stratigraphy has been determined, soil unit weights can be ascribed to the soil layers and stationary pore water pressures can be schematized. With this additional information the corrected cone penetration resistance q_{net} and normalized cone penetration resistance Q_t can be calculated according to equations 4.8, 4.9 and 4.10. It has to be noted that not much is known about the phreatic level during the measurement. The schematization of the stationary pore water distribution is based on the measurements of the pore water pressure during cone penetration (class 1 cone). The variation of the soil unit weight is also uncertain. So uncertainty is introduced in the analyses due to the corrections and normalization.

The corrected cone penetration resistance at location AC 251 is showed in Figure 5.10. The normalized cone penetration resistance is given in Figure 5.11. When comparing these figures with the measured cone penetration resistance as shown in Figure 5.3 the impact of the corrections and normalisation can be observed. The corrected cone penetration resistance is substantially lower (~40 - 50%) than the measured cone penetration resistance because of the corrections for measured pore water pressure and total vertical stress. This relatively large effect of the corrections is caused by the low measured cone penetration resistances. By normalising the corrected cone penetration resistance, the pattern of the CPT data changes. This normalisation is required because the stratigraphy as derived from the CPT's is not constant and some layers are not horizontal, as can be seen in Figure 5.7, Figure 5.8 and Figure 5.9; so the vertical effective stresses will be different at each CPT.

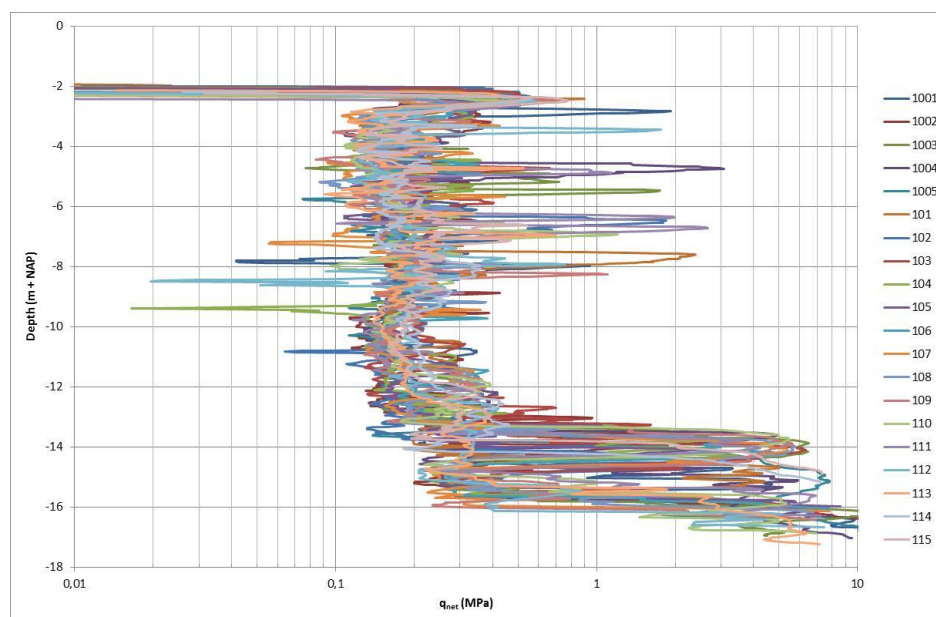


Figure 5.10 Corrected cone penetration resistance q_{net} at location AC 251.

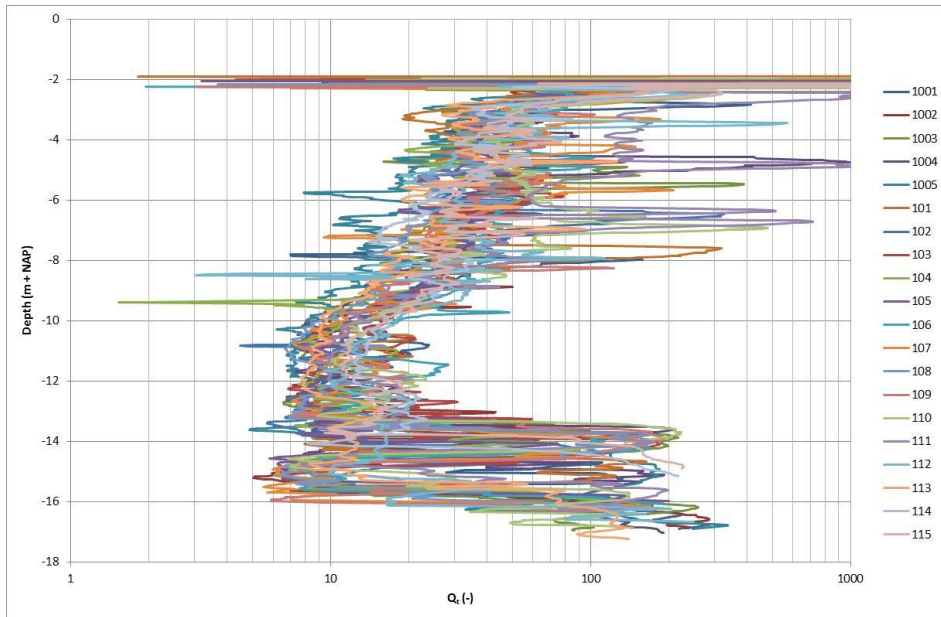


Figure 5.11 Normalized dimensionless cone penetration resistance Q_t at location AC 251.

Figure 5.12 and Figure 5.13 also illustrate the effect of the applied corrections and normalisation. For each CPT the cone penetration resistances are averaged over the thickness of the soil layers. The figures show the corrections and normalisation for the CPT data from location AC 075. At this location the stratigraphy varies because the thickness of the soil layers varies, as can be seen in Figure 5.7. Due to the corrections and normalisation the trends in Figure 5.13 differ from the trends in Figure 5.12, however, the magnitude of the variability is more or less the same. The normalized cone penetration resistance Q_t in Figure 5.13 shows some jumps, for example between CPT 303 and CPT 304 and between CPT 307 and CPT 308. When Figure 5.13 is compared with Figure 5.7 these jumps can be related to changes in the stratigraphy.

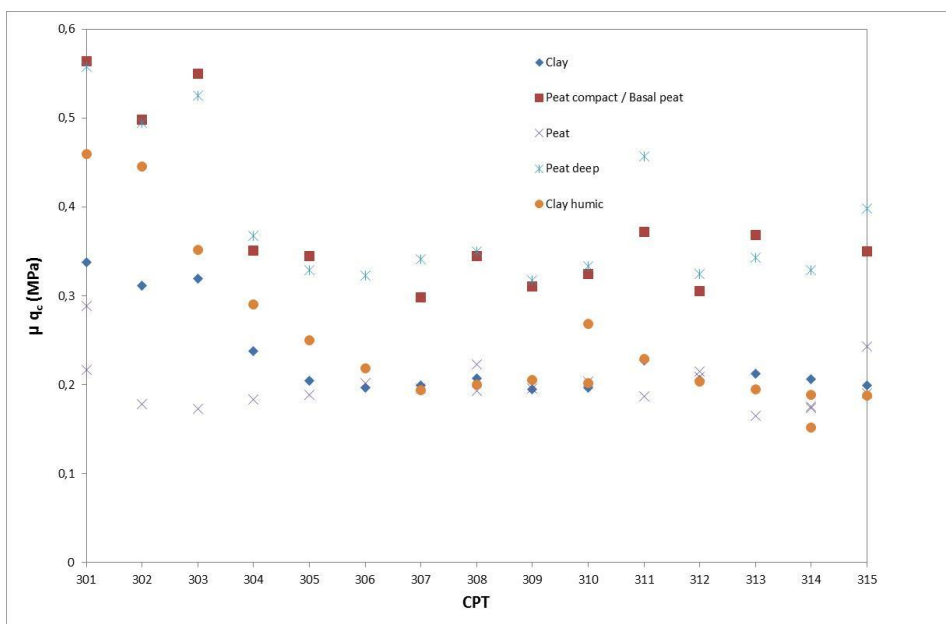


Figure 5.12 Measured cone penetration resistance q_c per soil layer at location AC 075.

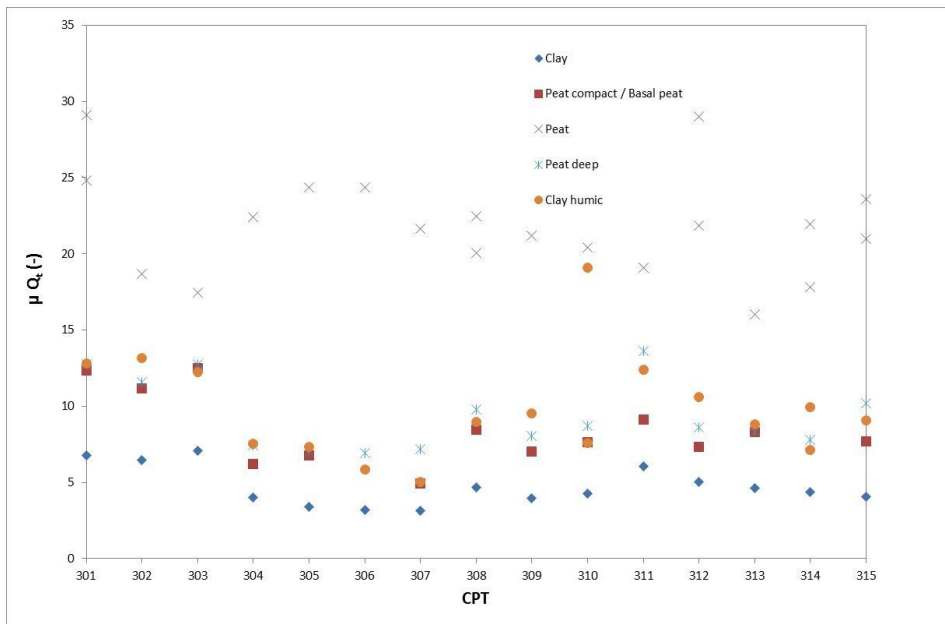


Figure 5.13 Normalized dimensionless cone penetration resistance Q_t per soil layer at location AC 075.

5.4 Variability cone penetration resistance

In order to quantify the variability of the cone penetration resistance mean values and standard deviations of the CPT data are calculated. Figure 5.14, Figure 5.15 and Figure 5.16 show the variability of the corrected cone resistance per location. For each location, the calculated mean values of the corrected cone resistances per soil layer and per CPT are presented at the depth of the middle of the concerning soil layer. First of all the stiff top layer can be recognized. Furthermore it can be seen that the middle of the soil layers varies enormously, meaning that the soil layers are not horizontal and vary in thickness. As can be seen in Figure 5.7 and Figure 5.9 this can for the deeper soil layers be attributed to shallower layers which also vary in thickness. These variations in thickness of soil layers cause variations in the vertical stress in the soil layers. For the magnitude of the vertical stress also variations in soil unit weight can play a role. The variability of the cone resistance is largest for the deep peat layers. This variability can be caused by variations in shear strength, variations in drainage conditions during cone penetration. Also the fact that these deep peat layers are relatively thin may play a role, because the mean values of the cone resistances of these peat layers are based on a limited number of measurement values. Overall the ratio between the high cone resistances and low cone resistances per soil layer is about 2 or 3.

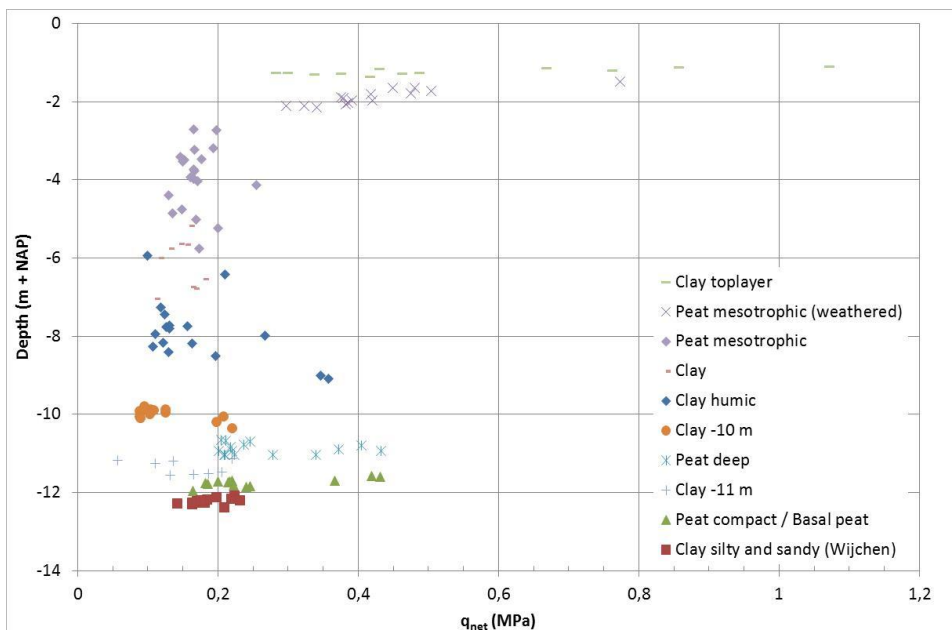


Figure 5.14 Variability of the corrected cone penetration resistance q_{net} at location AC 075.

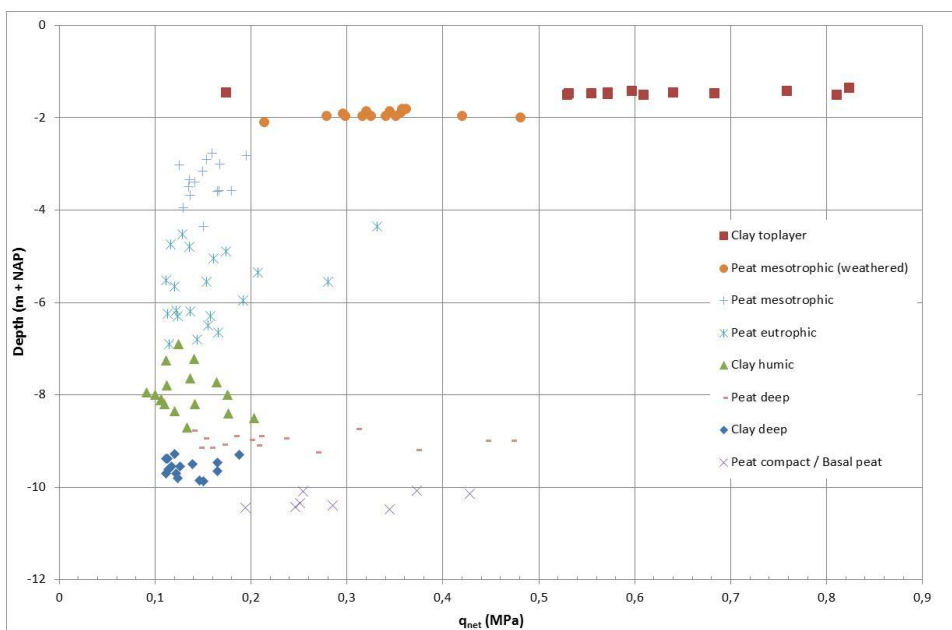


Figure 5.15 Variability of the corrected cone penetration resistance q_{net} at location AC 090.

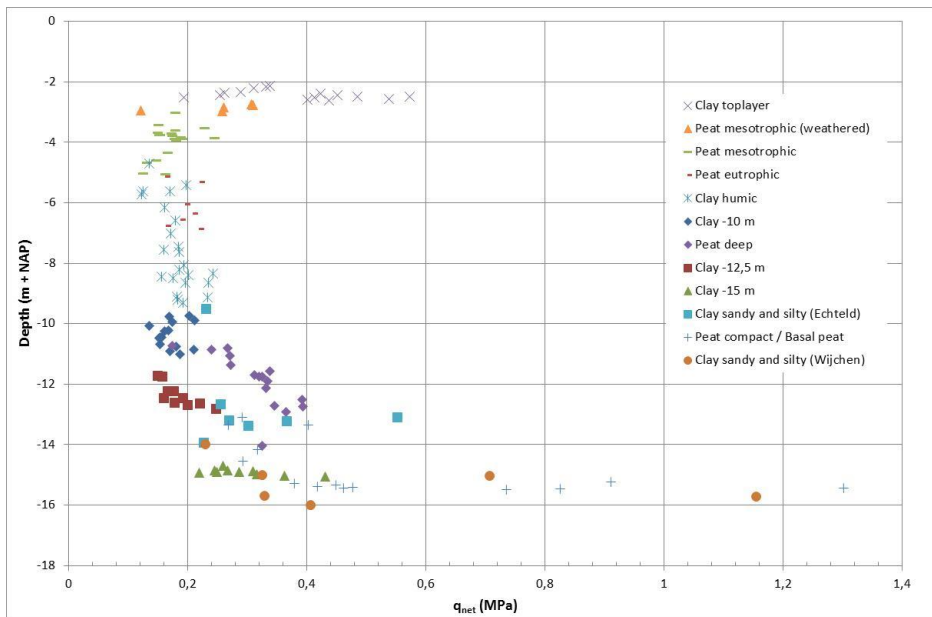


Figure 5.16 Variability of the corrected cone penetration resistance q_{net} at location AC 251.

Figure 5.17, Figure 5.18, Figure 5.19 and Figure 5.20 again show the variability of the cone resistance. In these figures the corrected cone resistance q_{net} versus the vertical effective stress σ'_{vi} is plotted per soil type. Each symbol represents the mean value of the corrected cone resistance of the concerning soil layer within one CPT. At each symbol the 90% confidence interval is given. The figures show a lot of differences. In all soil layers there is a lot of variability in mean values of the cone resistances, the 90% confidence interval and the effective stress level. A clear stress dependency of the cone penetration resistance cannot be identified.

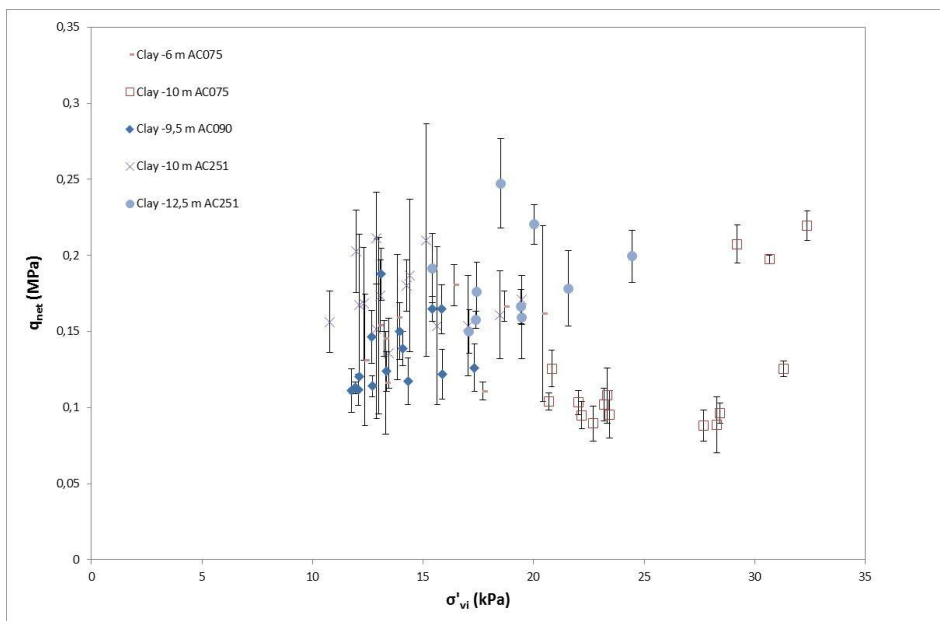


Figure 5.17 Variability of the corrected cone penetration resistance q_{net} of clays versus the vertical effective stress σ'_{vi} .

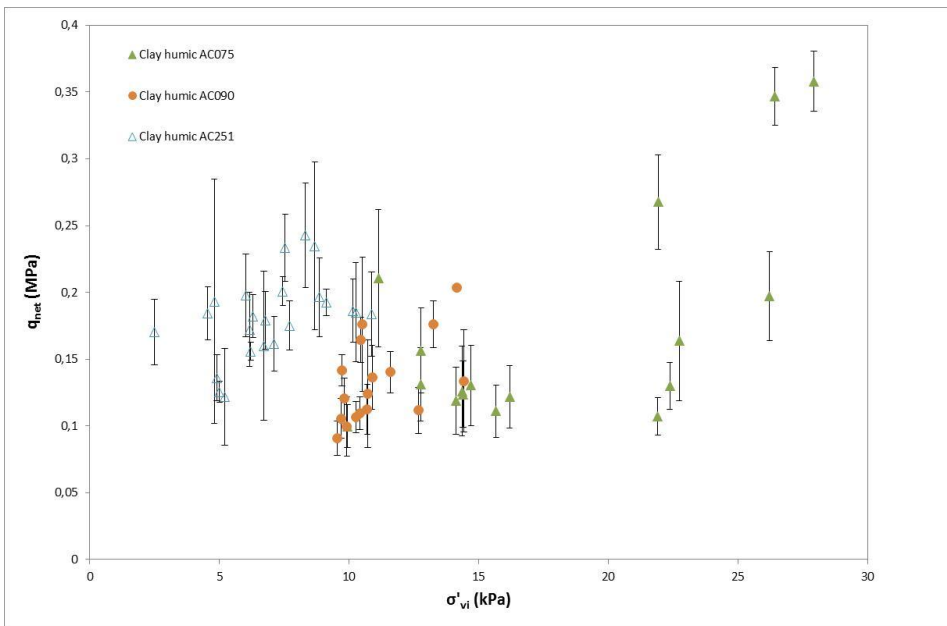


Figure 5.18 Variability of the corrected cone penetration resistance q_{net} of humic clays versus the vertical effective stress σ'_{vi} .

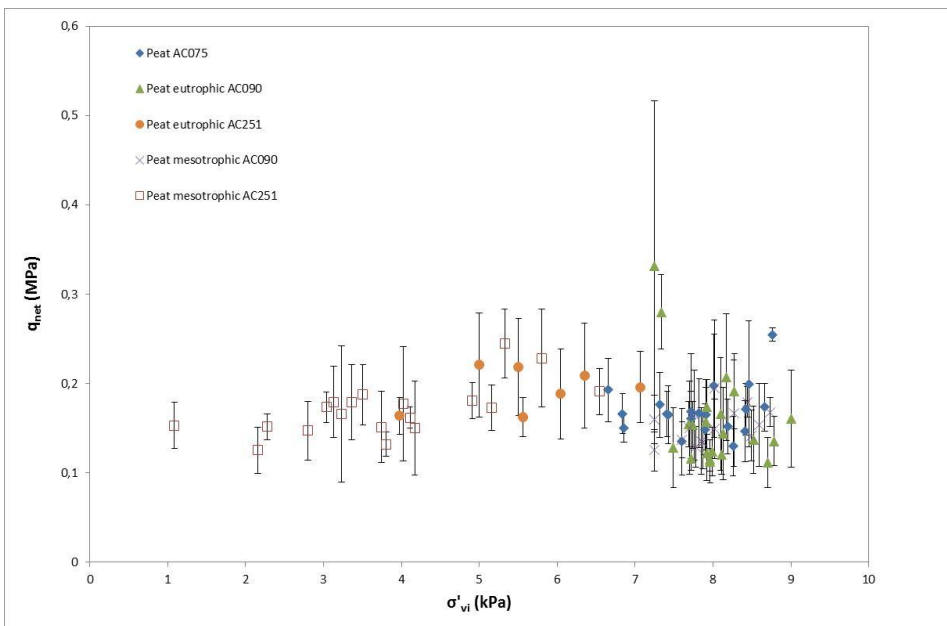


Figure 5.19 Variability of the corrected cone penetration resistance q_{net} of peat versus the vertical effective stress σ'_{vi} .

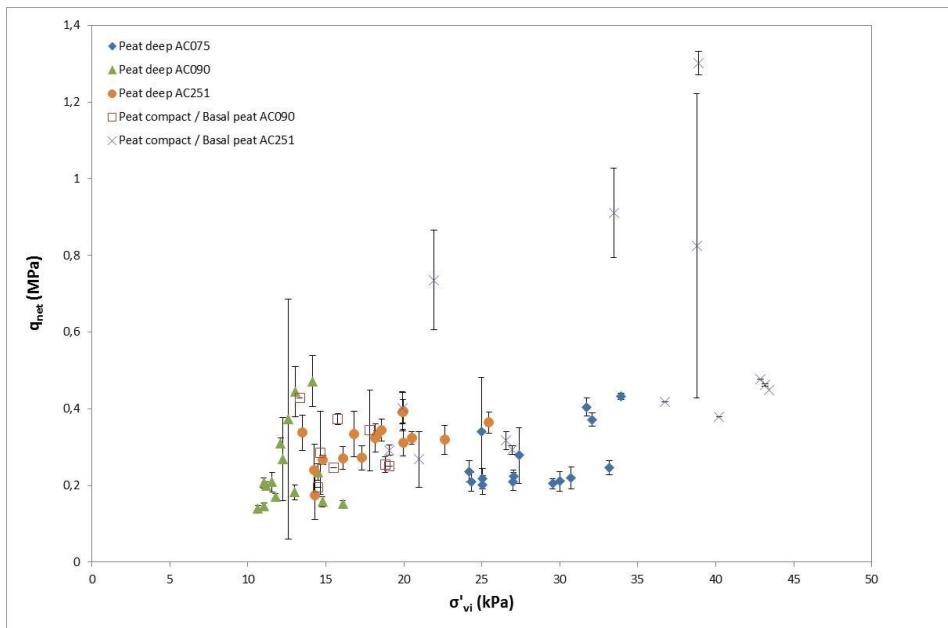


Figure 5.20 Variability of the corrected cone penetration resistance q_{net} of peat versus the vertical effective stress σ'_{vi} .

Table 5.1 gives an overview of the statistics of the cone penetration resistance data. It is interesting to note that for the various soil types the coefficient of variation (CoV) of the cone penetration resistance varies per location. So the variability of the cone penetration resistance of a certain soil type is not constant. This may imply that the conditions in a depositional environment also vary for different locations. Note that the reported CoVs are the result of various uncertainties: geological variability, measurement accuracy, uncertainties in soil unit weight and pore water pressure and errors in the interpretation of the CPT data. The contribution of each of these individual uncertainties to the reported CoVs is not investigated. Furthermore the coefficient of variation of some of the soil layers is larger for the class 1 cones compared to the class 1+ cone. The class 1 cone has the advantage of the information of the sleeve friction and pore water pressure which is very helpful for the interpretation of the CPT data. The measurement accuracy of the cone penetration resistance of the class 1+ cone is however about four times higher than the class 1 cone. So both effects will play a role in the resulting coefficient of variation. The more accurate 1+ cone not necessarily gives a lower uncertainty in q_{net} estimate.

The coefficient of variation of the corrected cone penetration resistance q_{net} and normalised cone penetration resistance Q_t is much larger than the coefficient of variation of the measured cone penetration resistance q_c . This can be attributed to the applied corrections and normalization as described in Paragraph 5.3. The coefficient of variation of the measured cone penetration resistance q_c and normalised cone penetration resistance Q_t are not in Table 5.1.

Table 5.1 Statistics of the cone penetration resistance per soil layer for class 1 cone and class 1+ cone.

Soil type	Location	CPT's with class 1+ cone					CPTu's with class 1 cone				
		n (-)	μq_{net} (MPa)	σq_{net} (MPa)	$\sigma^2 q_{net}$ (MPa)	CoV q_{net} (-)	n (-)	μq_{net} (MPa)	σq_{net} (MPa)	$\sigma^2 q_{net}$ (MPa)	CoV q_{net} (-)
Clay -10 m	AC075	15	0.123	0.046	0.0021	0.371	5	0.131	0.064	0.0041	0.490
Clay -10 m	AC251	15	0.172	0.022	0.0005	0.130	5	0.159	0.005	0.0000	0.034
Clay -11 m	AC075	8	0.152	0.054	0.0029	0.354	4	0.250	0.147	0.0216	0.588
Clay -12,5 m	AC251	10	0.185	0.031	0.0009	0.166	4	0.207	0.030	0.0009	0.146
Clay -15 m	AC251	10	0.295	0.063	0.0040	0.215					
Clay -6 m	AC075	9	0.147	0.024	0.0006	0.160					
Clay -9,5 m	AC090	15	0.134	0.024	0.0006	0.177	5	0.110	0.037	0.0014	0.335
Sandy silty clay (Echteld)	AC251	7	0.314	0.115	0.0133	0.366					
Sandy silty clay (Wijchen)	AC075	13	0.187	0.027	0.0007	0.146					
Sandy silty clay (Wijchen)	AC251	6	0.525	0.349	0.1218	0.664					
Humic clay	AC075	17	0.171	0.081	0.0066	0.475	9	0.184	0.084	0.0071	0.459
Humic clay	AC090	17	0.133	0.031	0.0010	0.237	7	0.127	0.041	0.0017	0.323
Humic clay	AC251	23	0.181	0.031	0.0010	0.170	7	0.183	0.025	0.0006	0.134
Eutrophic peat	AC090	21	0.159	0.056	0.0031	0.351	7	0.156	0.022	0.0005	0.138
Eutrophic peat	AC251	7	0.194	0.024	0.0006	0.124	6	0.226	0.069	0.0048	0.306
Mesotrophic peat	AC075	20	0.169	0.027	0.0007	0.161	5	0.184	0.041	0.0017	0.222
Mesotrophic peat	AC090	15	0.153	0.020	0.0004	0.129	6	0.149	0.018	0.0003	0.121
Mesotrophic peat	AC251	19	0.171	0.029	0.0009	0.172	7	0.235	0.105	0.0110	0.446
Peat deep	AC075	15	0.267	0.079	0.0063	0.297	5	0.304	0.094	0.0088	0.309
Peat deep	AC090	15	0.244	0.108	0.0117	0.443	5	0.181	0.074	0.0055	0.410
Peat deep	AC251	16	0.313	0.057	0.0032	0.181	5	0.310	0.038	0.0015	0.124
Peat compact / Basal peat	AC075	13	0.254	0.090	0.0081	0.355					
Peat compact / Basal peat	AC090	8	0.297	0.078	0.0061	0.262					
Peat compact / Basal peat	AC251	14	0.538	0.299	0.0893	0.556	4	0.351	0.092	0.0084	0.262

5.5 Correlation length

The horizontal correlation lengths of the measured cone penetration resistance q_c and the normalized cone penetration resistance Q_t for the various soil layers at the three locations are calculated with the semivariogram using equation 2.5 (Paragraph 2.3.3) and correlation function using equations 2.2, 2.3 and 2.4 (Paragraph 2.3.3). Note that the horizontal correlation length is calculated based on the mean values of the cone penetration resistances per soil layer and per CPT. So, the vertical variability within a soil layer in each CPT is thought to be averaged on the scale of a slip surface, as the vertical correlation length is assumed to be very short according to TAW (2002).

Semivariogram

Figure 5.21 and Figure 5.22 show the semivariogram of the measured cone penetration resistance q_c and the normalized cone penetration resistance Q_t of various clays.

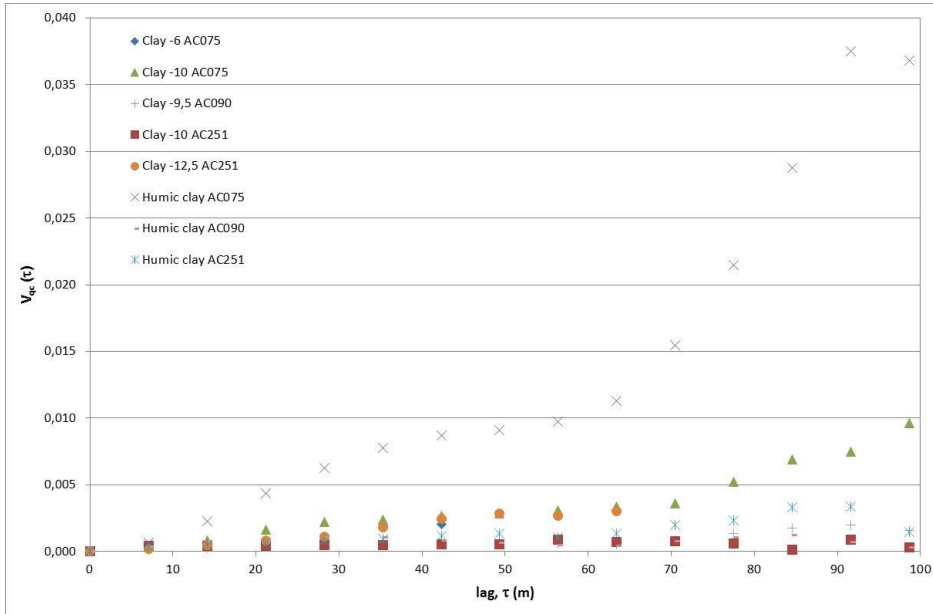


Figure 5.21 Semivariogram of the measured cone penetration resistance V_{q_c} versus lag distance τ of various clays.

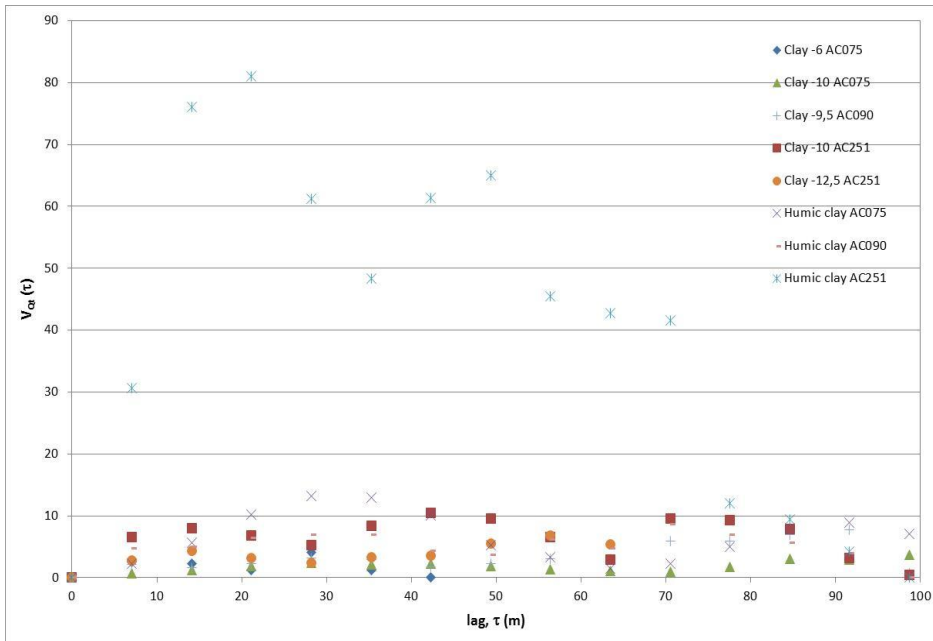


Figure 5.22 Semivariogram of the normalized cone penetration resistance V_{Q_t} versus lag distance τ of various clays.

Using the semivariogram no clear results could be found. Figure 5.21 and Figure 5.22 show the semivariogram of various clay layers at the three measurement locations. Figure 5.21 shows the semivariogram when applying the semivariogram to the measured cone resistance q_c . Figure 5.22 shows the semivariogram when applying the semivariogram to the normalized cone resistance Q_t . Both figures show poor results, however it seems that the correlation length is larger for the measured cone resistance q_c compared to the normalized cone resistance Q_t .

Correlation function

Figure 5.23, Figure 5.24 and Figure 5.25 show the correlation function of the measured cone penetration resistance q_c and the normalized cone penetration resistance Q_t of various clays and peat.

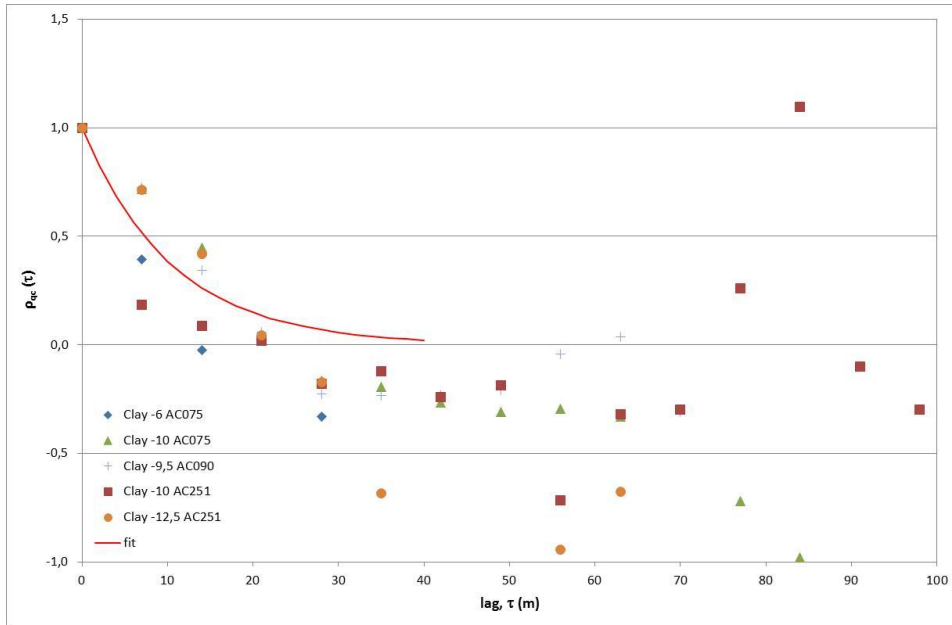


Figure 5.23 Correlation function of the measured cone penetration resistance ρ_{q_c} versus lag distance τ of various clays.

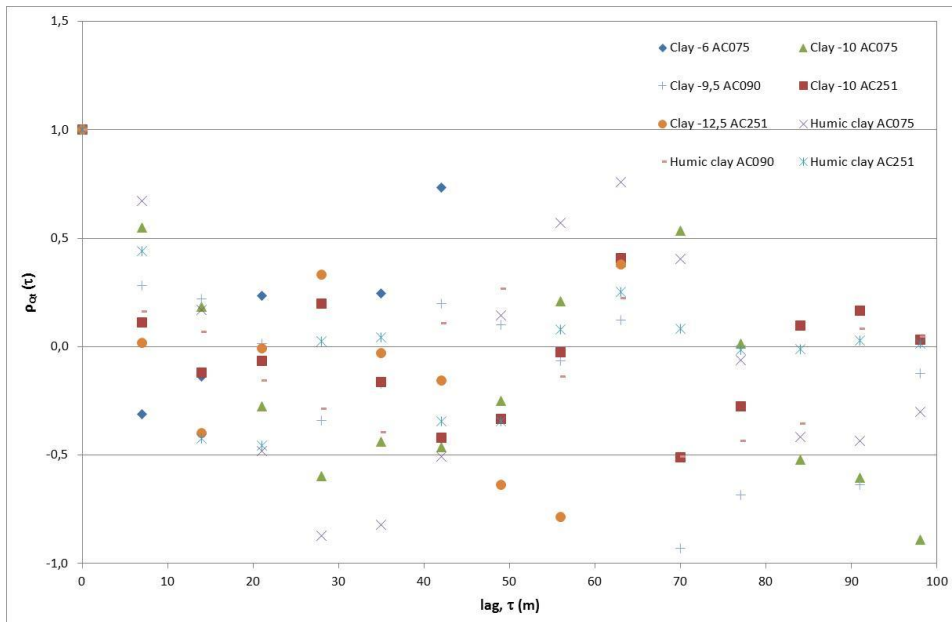


Figure 5.24 Correlation function of the normalized cone penetration resistance ρ_{Q_t} versus lag distance τ of various clays.

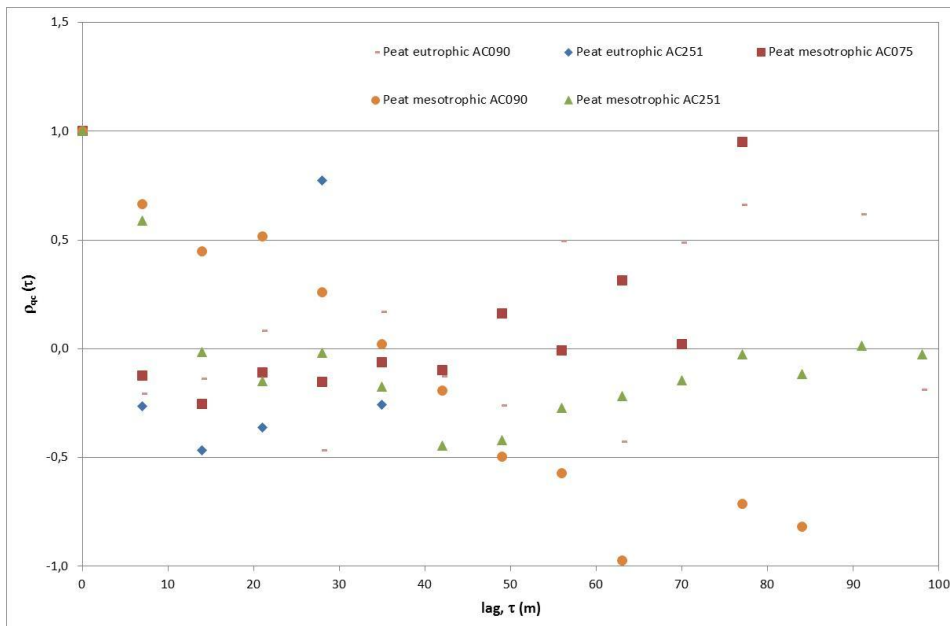


Figure 5.25 Correlation function of the measured cone penetration resistance ρ_{q_c} versus lag distance τ of various peat.

From Figure 5.23 and Figure 5.25 it can be seen that the correlation function gives more distinct results for the correlation length compared to the semivariogram. In these figures the correlation function is applied to the measured cone resistance q_c . Only in Figure 5.23, a consistent result is obtained and a correlation function is plotted. The correlation length seems not to be a constant for a depositional environment. From the derived results it can be seen that the correlation length differs for soil layers of the same soil type at different locations. The calculated horizontal correlation lengths for clay based on q_c (Figure 5.23) are generally much larger than the calculated correlation lengths for peat (Figure 5.25). It seems to be likely that the very different genesis of these soils is the cause of these different correlation lengths, as clay layers are a result of sedimentary processes in a certain depositional environment and peat layers are the remains of plants of different species. Sometimes the correlation of q_c shows a trend, for example clay at -12.5 m at location AC 251 (orange dots) in Figure 5.23. These trends disappear when calculating the correlation based on the normalized cone penetration resistance Q_t . So the normalization for effective stress level is important to remove trends in the data.

When applying the correlation function to the normalized cone penetration resistance Q_t , as presented in Figure 5.24, the derived correlation length is also unclear, similar to the semivariogram. For Q_t the correlation length is much shorter than for q_c . This seems to be in agreement with the results from the semivariogram. The poor results when applying the correlation function to Q_t can be caused by the corrections for measured pore water pressure and total vertical stress and normalisation with vertical effective stress as discussed in Paragraph 5.3 and Paragraph 5.4. Due to the uncertainties in these corrections and normalisation additional uncertainty is introduced in Q_t .

It can be seen in Figure 5.23 and Figure 5.25 that the determination of the correlation length becomes unreliable after a certain distance (see also Paragraph 2.3.2). In these figures much scatter is found at distances larger than 30 m. The correlation often dips below zero and sometimes also below 1.0, which is theoretically not possible. The low correlation can be caused by the uncertainty in the estimation of the average values of q_c and Q_t as pointed out in Paragraph 2.3.3. Hence, especially correlations at larger lag distance should not be considered for further analysis. When working with Q_t additional noise can be introduced because of the various uncertainties as mentioned before. Due to these uncertainties the calculated correlation lengths of Q_t are less reliable. The calculated

correlation lengths of q_c are probably more reliable, because there are less uncertainties, however in these correlation lengths the correction for trends is lacking.

Table 5.2 gives an overview of the horizontal correlation lengths θ of the measured cone penetration resistances q_c based on the class 1 cones and class 1+ cones as derived with the correlation function (see Paragraph 2.3.2).

Table 5.2 Derived horizontal correlation lengths of the measured cone penetration resistance q_c based on the class 1 cones and class 1+ cones. The related variance reduction factor is also given.

Soil type	Location	$\theta_{q_c, \text{class 1+}}$ (m)	$\theta_{q_c, \text{class 1}}$ (m)	I^2 ($\theta_{q_c, \text{class 1+}}$) (-)	I^2 ($\theta_{q_c, \text{class 1}}$) (-)
Clay -10 m	AC075	21	30	0.28	0.40
Clay -10 m	AC251	9	30	0.12	0.40
Clay -11 m	AC075				
Clay -12,5 m	AC251	21		0.28	
Clay -15 m	AC251				
Clay -6 m	AC075	9		0.12	
Clay -9,5 m	AC090	21	15	0.28	0.20
Sandy silty clay (Echteld)	AC251				
Sandy silty clay (Wijchen)	AC075				
Sandy silty clay (Wijchen)	AC251				
Humic clay	AC075	21	28	0.28	0.37
Humic clay	AC090	14	10	0.19	0.13
Humic clay	AC251	21	30	0.28	0.40
Eutrophic peat	AC090	3	10	0.04	0.13
Eutrophic peat	AC251	3		0.04	
Mesotrophic peat	AC075	3	10	0.04	0.13
Mesotrophic peat	AC090	33	20	0.44	0.27
Mesotrophic peat	AC251	12	30	0.16	0.40
Peat deep	AC075	15	30	0.20	0.40
Peat deep	AC090	3	30	0.04	0.40
Peat deep	AC251	30	30	0.40	0.40
Peat compact / Basal peat	AC075				
Peat compact / Basal peat	AC090				
Peat compact / Basal peat	AC251	5		0.07	

The variance reduction factor I^2 is also given in the table. This variance reduction factor is calculated according to Vanmarcke (1977) using equation 2.6 (see Paragraph 2.3.3). The variance reduction factor is related to the horizontal correlation length and the length of a potential slope instability, which is assumed here as 75 m. As proposed by Vanmarcke the variance reduction factor decreases when the dimension of a slip surface in horizontal direction increases.

The horizontal correlation lengths are calculated based on the mean values of the cone penetration resistances per soil layer and per CPT. The vertical variability within a soil layer in each CPT is thought to be averaged on the scale of a slope instability, because the vertical correlation length is assumed to be very short. Therefore the calculated variance reduction factor I^2 according to Vanmarcke accounts for the averaging of the horizontal fluctuation of the cone penetration resistance on the scale of a slip surface. Note that this definition of the

variance reduction factor differs from the definition used in TAW (2002) and Calle (2007) as discussed in Paragraph 2.3.1.

Table 5.2 shows a large variation in correlation lengths for the various soil types. The length over which the correlation dies out varies with a factor two to ten. Consequently also the variance reduction factor has a large variation. These findings seem to correspond very well with the results in the previous paragraph where the coefficient of variation was also not constant for a certain soil type. As the calculated horizontal correlation length varies considerably it may be that the spatial variability of the cone penetration resistance is very different at the three locations. It is also possible that the various uncertainties as discussed before play an important role on the results.

Furthermore the reliability of the correlation length based on the CPT's with class 1 cone is less than the correlation length based on the CPT's with class 1+ cones because of the limited number of CPT's with class 1 cone and the fact that the calculated correlation length is in the same order as the distance between the CPT's with class 1 cone.

Overall the horizontal correlation length ranges between 3 and 33 m resulting in a variance reduction factor between 0.04 and 0.44. The average value of the variance reduction factor is 0.19. The calculated horizontal correlation lengths are relatively short compared to the horizontal correlation length of 50 to 100 m as mentioned in TAW (2002). The calculated correlation lengths are also relatively short compared to the assumed dimensions of a slope failure of 75 m. As a consequence the calculated variance reduction for the horizontal direction is relevant, at least for the shortest correlation lengths. Although the approach of TAW (2002) and Calle (2007) differs from the approach of Vanmarcke (1977) the range of the calculated variance reduction factors compare very well with the recommended variance reduction factor Γ^2 is 0.25 in TAW (2002).

When working with the normalized cone penetration resistance Q_t the calculated horizontal correlation length is shorter (3 - 13 m) and consequently the variance reduction factor becomes smaller (0.04 - 0.17).

As each series of CPT's concern the scale of a slip surface of a potential slope failure the CPT data is deemed to be a local data set, for which TAW (2002) recommends a variance reduction factor Γ^2 is 0. So the calculated variance reduction factor based on the measured cone penetration resistances q_c is relatively high compared with the variance reduction factor in TAW (2002).

6 Results: Sample disturbance

6.1 Introduction

To investigate whether sampling affects the initial structure of the soil in this chapter the results of the field and laboratory tests of the research sites Waaldijk, Lekdijk and Achterwaterschap AC 251 are analyzed. The stress sensitivity S_σ and strength sensitivity S_t are derived from the constant rate of strain tests and triaxial tests respectively and compared with the strength sensitivity S_t from the field vane tests. In order to verify this comparison also the undrained shear strength s_u from the triaxial tests is compared with the undrained shear strength from the field vane tests.

The stress sensitivity S_σ is derived from the constant rate of strain tests on intact natural samples applying the sensitivity framework as discussed in Paragraph 4.9 and using the intrinsic compression parameters from the constant rate of strain tests on reconstituted samples as a reference. The strength sensitivity S_t from the triaxial tests is obtained by dividing s_u from the intact samples by s_u from the reconstituted samples. The strength sensitivity S_t from the field vane tests is calculated by dividing the peak strength by the residual strength.

As the field vane tests and the boreholes cannot be conducted at exactly the same point in the field spatial variability may play a role in the comparison between the laboratory test results on intact samples and the field vane test results. This aspect is verified by comparing the s_u derived from cone penetration tests which are performed around the boreholes and field vane tests within a distance of some meters.

To be able to interpret the field vane test results first the coefficient of consolidation c_h is derived from the dissipation tests. Based on c_h the field vane test results with different rotation rates can be assessed whether the soil behaviour was undrained. Only results reflecting undrained soil behaviour can be used in the analysis.

6.2 General soil properties

For the sites the bulk soil unit weight γ_{sat} , dry soil unit weight γ_{di} , unit weight of the particles γ_s , initial water content w_i , Atterberg limits (liquid limit w_L , plastic limit w_p and plasticity index I_p), organic content OC are determined. The results are presented in Figure 6.1, Figure 6.2 and Figure 6.3.

The figures show high soil unit weights, low plasticity index and low organic matter content at the Waaldijk. The profiles of the Waaldijk suggest a relatively high energy depositional environment, relatively close to the active river channel. On the other hand the Achterwaterschap site is dominated by very low soil unit weights, excepted for the Wijchen Member at NAP -15 m and the deepest deposits of the Echteld Formation at NAP -13 m, and increasing plasticity index and organic matter content in upward direction. The profiles of the Achterwaterschap show an increasing swampy sedimentary depositional environment. The Lekdijk site is more or less in between the other cases. Soil unit weights are somewhat higher than the Waaldijk site and plasticity index and organic matter content are somewhat lower.

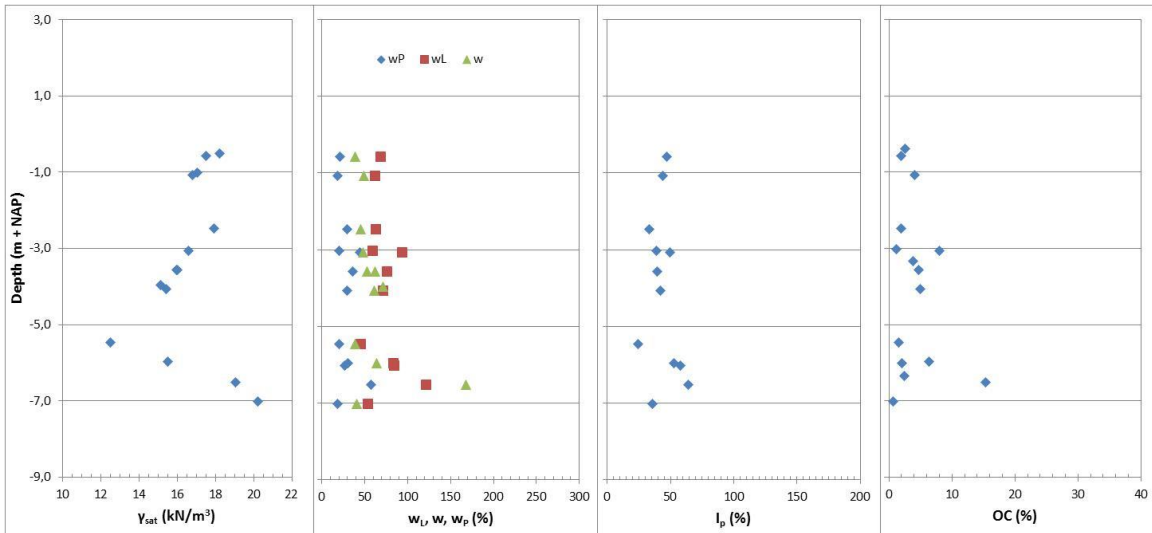


Figure 6.1 General soil properties of the Lekdijk site near Schalkwijk.

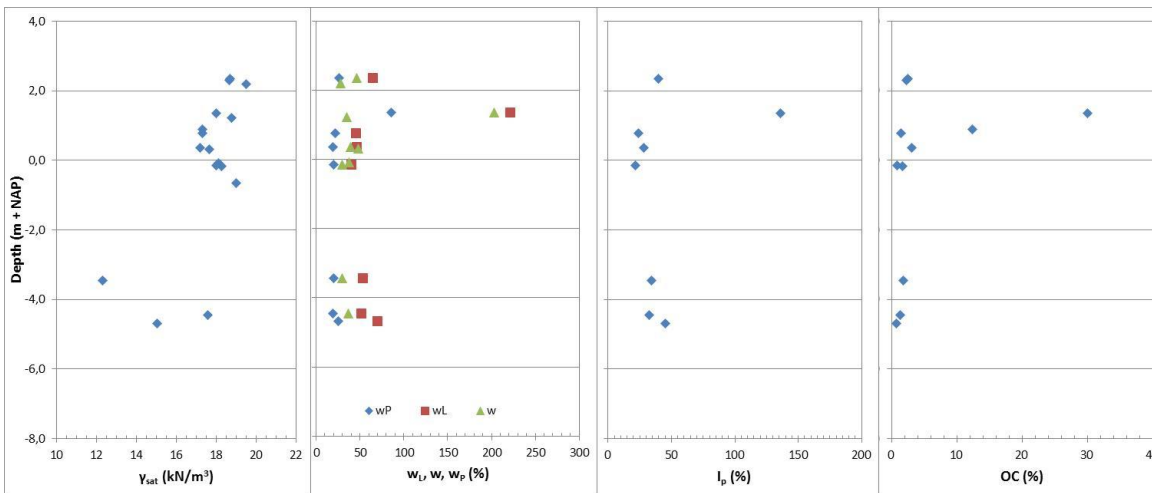


Figure 6.2 General soil properties of the Waaldijk site at Waardenburg.

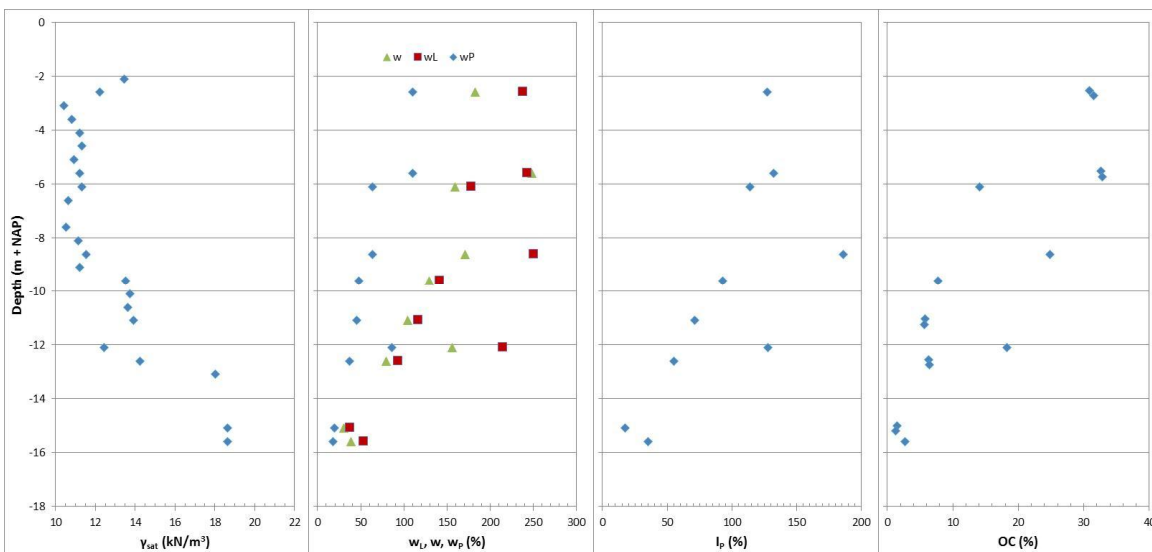


Figure 6.3 General soil properties of the Achterwaterschap AC 251 site near Alblasterdam.

6.3 Coefficient of consolidation from dissipation tests

The coefficient of consolidation is determined from dissipation tests and used to assess whether the FVT measurements with various rotation rates represent drained, undrained or intermediate behaviour. The interpretation of the dissipation test is performed as described in Paragraph 4.7.

Figure 6.4 shows two examples of the interpretation of the dissipation tests. In Figure 6.4a the normalized excess pore water pressure U starts at a very low level, increases considerably to U of about 0.65 and after that the dissipation process develops as expected. In Figure 6.4b U is substantially higher at the start of the dissipation test. Consequently the dissipation process starts at a relatively low value of the normalised time T^* .

The dissipation behaviour in Figure 6.4a is not expected. The overconsolidation ratio OCR can be estimated in the order of 2 or 3 based on the results of the FVT. For soils with relatively low OCR behaviour as in Figure 6.4b is to be expected according to Burns & Mayne (1998); see Figure 4.2. The dissipation behaviour as shown in Figure 6.4a occurs very often at Schalkwijk and sometimes at Waardenburg and Alblasserdam. In Figure 6.4a the increase of the excess pore water pressure at the start of the test takes about 2 minutes.

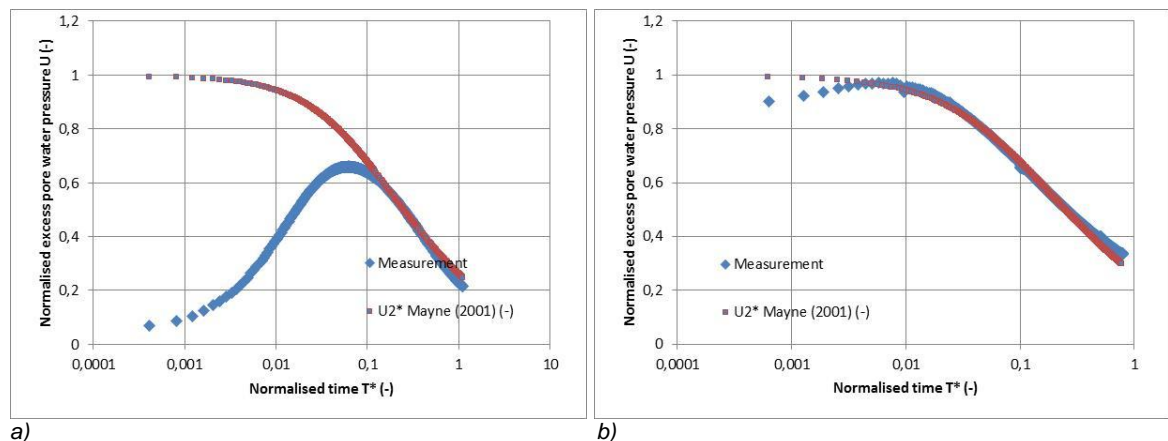


Figure 6.4 Measured dissipation behaviour and fit of the dissipation behaviour; (a) Lekdijk near Schalkwijk in clay at NAP -3.30 m and (b) Achterwaterschap near Alblasserdam in clay at NAP -12.05 m. The normalised excess pore water pressure at the left side shows an unexpected pattern.

According to the interpretation as suggested by Houlsby & Teh (1988) and Mayne (2007) the normalized measured excess pore water pressure U should start at 1.0. As this is not always the case for the obtained measurement results for each test an arbitrary initial excess pore water pressure u_i is chosen to be able to fit the approximate algorithm of Mayne (2007) to the measurements. This offset is taken as $U = 1$. This approach is also followed by Colreavy et al. (2016) and Carroll et al. (2018), who also found an increase of the excess pore water pressure at the start of their dissipation tests. In these studies the increase of the excess pore water pressures occurred in the first 20 seconds of the tests. Colreavy et al. (2016) performed dissipation tests in soft clay with OCR between 1.0 and 2.0 and deduced coefficients of consolidation c_h of about 7.0×10^{-8} to 5.3×10^{-6} m²/s. Carroll et al. (2018) conducted their dissipation tests in natural silty soil and found c_h around 4.0×10^{-6} m²/s. These authors attribute the increase of the excess pore water pressure to pore pressure redistribution around the cone tip and shoulder. In these studies the increase occurred much faster than in the present project, although c_h values as found by Colreavy et al. (2016) are relatively low compared to the results of the present project as presented in Figure 6.5 and Figure 6.6.

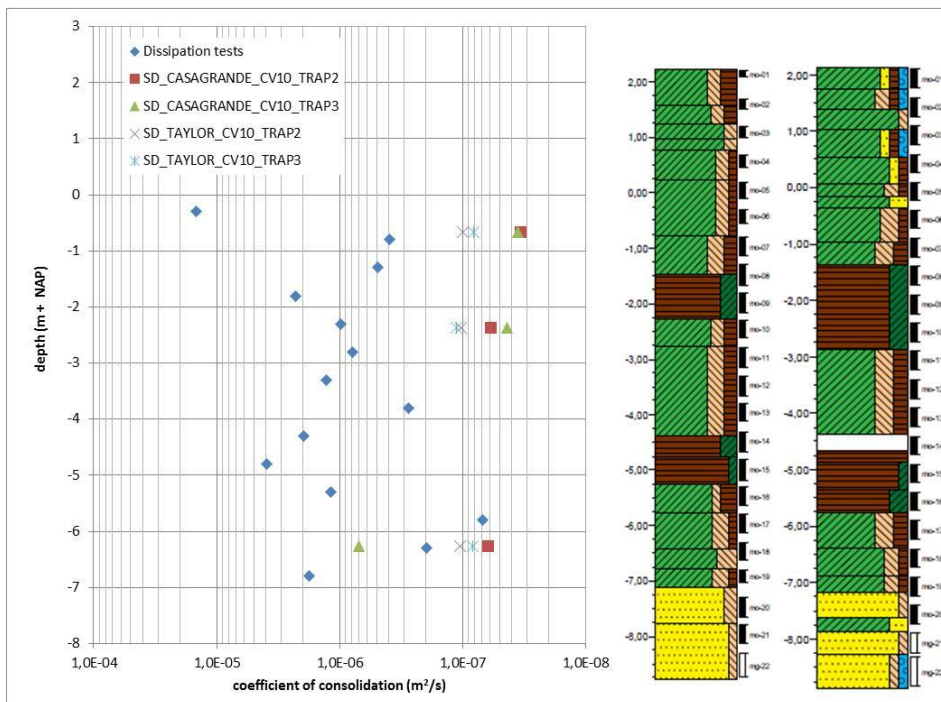


Figure 6.5 Coefficient of consolidation c_h from dissipation tests compared with coefficient of consolidation from oedometer tests for the Lekdijk near Schalkwijk. c_h from the dissipation tests is on average ten times higher than c_h from the laboratory tests. c_h from the dissipation tests shows a likely pattern compared to the borehole description. For legend of the borehole descriptions see Appendix B.

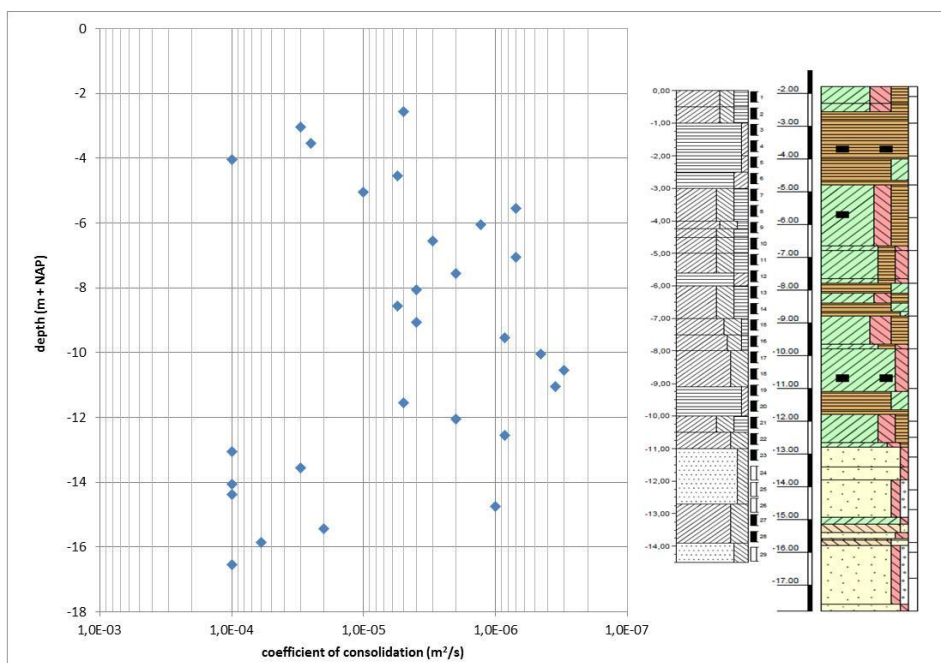


Figure 6.6 Coefficient of consolidation c_h from dissipation tests for the Achterwaterschap near Alblasterdam. Also in this case c_h from the dissipation tests shows a likely pattern compared to the borehole description. For legend of the borehole descriptions see Appendix B.

The coefficient of consolidation c_h as derived from the dissipation tests for the Lekdijk near Schalkwijk and the Achterwaterschap near Alblasterdam are presented in Figure 6.5 and Figure 6.6. In Figure 6.5 a comparison with the coefficient of consolidation c_v from oedometer

tests is made. The results from the dissipation tests are deemed to be reliable as the values in the low permeable layers at both sites are in the same order of magnitude, and the values at the surface and in the sandy layers at Alblasterdam have higher values than the soft clay and peat layers as can be expected. Within the low permeable layers at Schalkwijk it can be recognized that the peat layers have a higher coefficient of consolidation than the clay layers. Furthermore the comparison with the results from the oedometer tests at Schalkwijk also show that the results from the dissipation tests can be trusted as it can be expected that the horizontal coefficient of consolidation c_h will be higher than the vertical coefficient of consolidation c_v due to anisotropy and that the in situ tests will give higher coefficient of consolidation than laboratory tests, due to boundary conditions. For the site at the Waaldijk in Waardenburg similar results are obtained.

6.4 Undrained shear strength from field vane tests

The FVT results are interpreted following the discussion in Paragraph 4.8. Using the coefficient of consolidation from the dissipation tests (see Paragraph 6.3) the FVT results are analyzed to check if the measurements give drained, undrained or partly drained shear behaviour. To assess the drainage conditions of the FVT results for the various rotation rates the approaches with the normalized velocity V and normalised time to failure T are used.

Figure 6.7 to Figure 6.10 show that the approach using normalized time to failure indicates that all rotation rates are sufficiently fast to assure undrained shear behaviour, except some measurements with 6 degrees per minute and waiting time of about 180 seconds near the surface at Alblasterdam. Using the approach with normalized velocity, only the rotation rate of 360 degrees per minute results in undrained shear behaviour. As illustrated in Figure 6.7 and Figure 6.9 the normalized velocity of the FVT with rotation rate of 360 degrees per minute is comparable with the normalized velocity of the CPT. So the FVT results with the high rotation rate of 360 degrees per minute certainly have undrained behaviour and can therefore be used to derive the undrained shear strength.

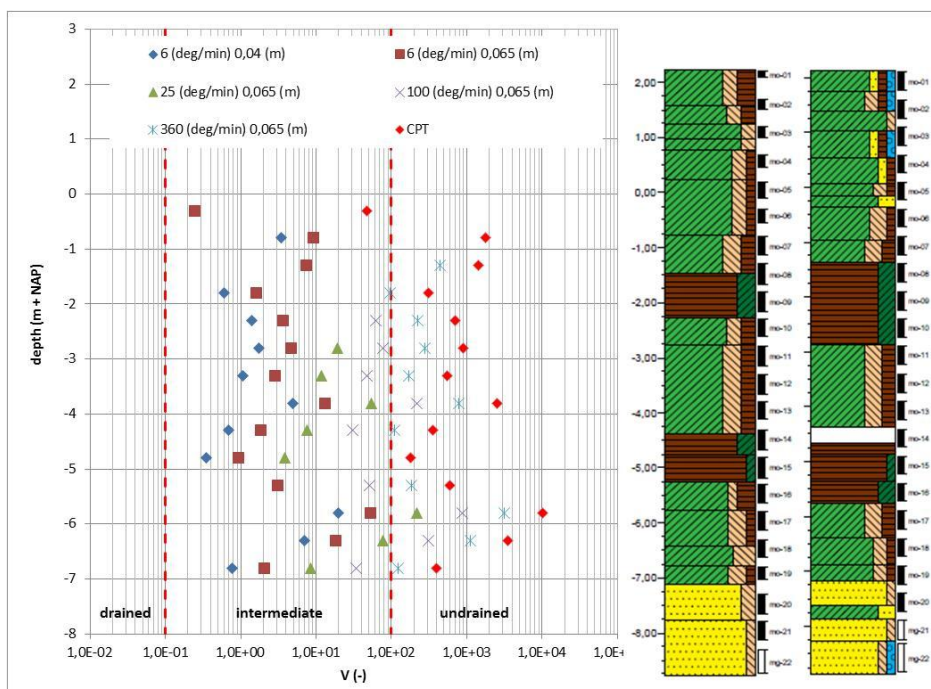


Figure 6.7 Normalised velocity V of the FVT compared with the normalised velocity of the CPT for the Lekdijk near Schalkwijk. The FVT with rotation rate of 360 degrees per minute results in undrained shear behaviour. For legend of the borehole descriptions see Appendix B.

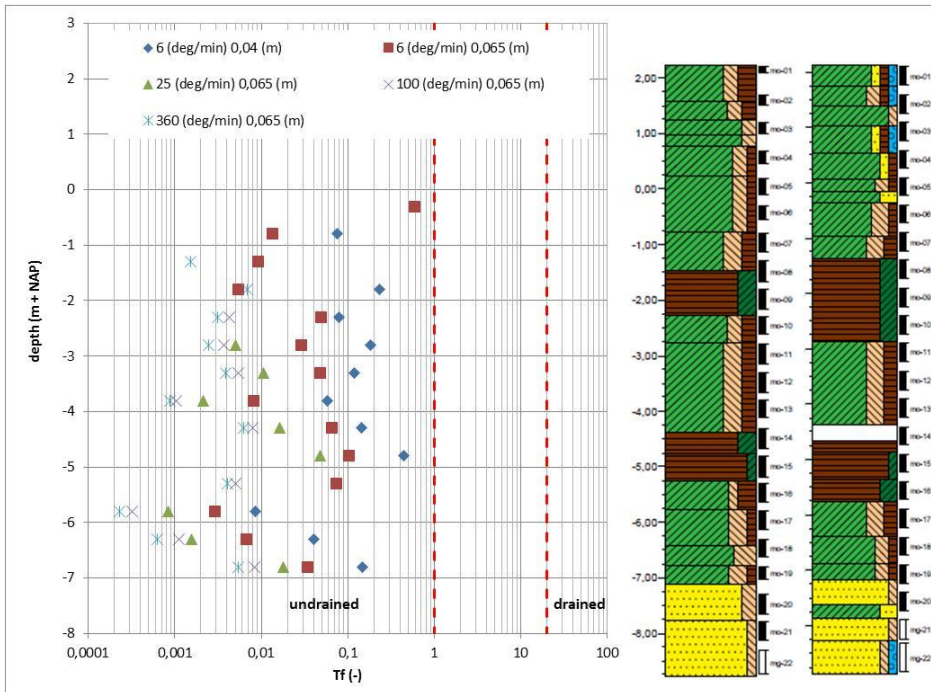


Figure 6.8 Normalised time to failure T_f of the FVT for the Lekdijk near Schalkwijk. All five rotation rates and waiting times result in undrained shear behaviour. For legend of the borehole descriptions see Appendix B.

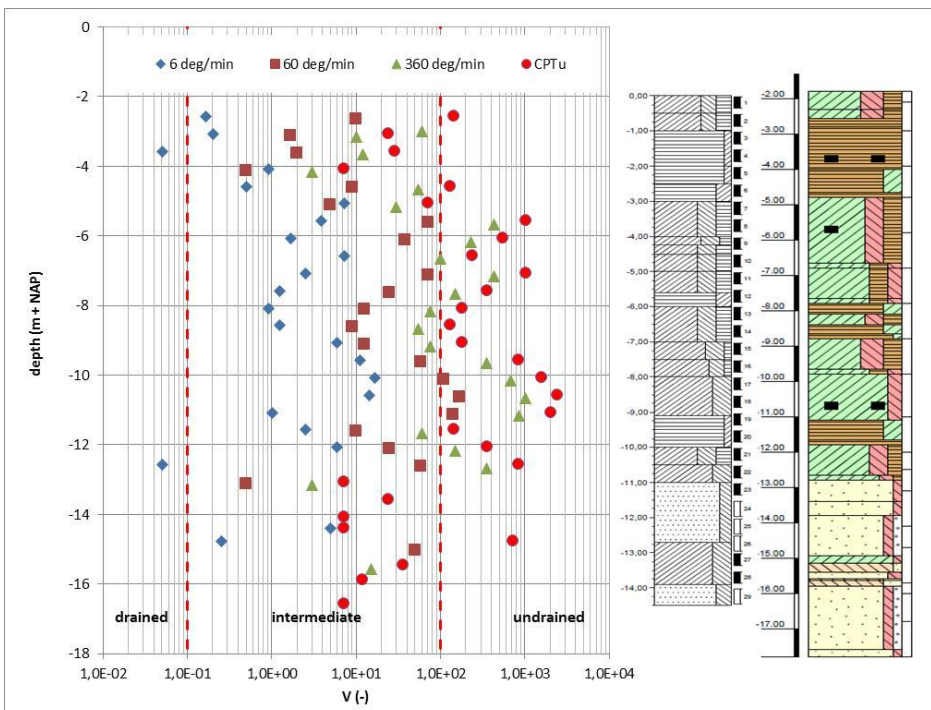


Figure 6.9 Normalised velocity V of the FVT compared with the normalised velocity of the CPT for the Achterwaterschap near Alblasterdam. The FVT with rotation rate of 360 degrees per minute results for most of the measurements in undrained shear behaviour. For legend of the borehole descriptions see Appendix B.

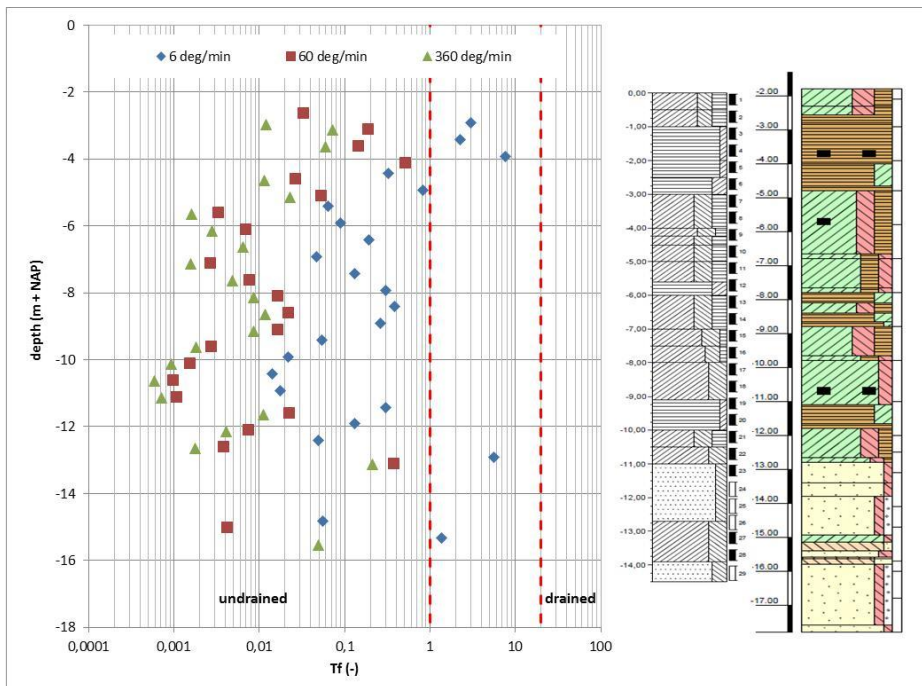


Figure 6.10 Normalised time to failure T_f of the FVT for the Achterwaterschap near Alblasterdam. All three rotation rates and waiting times result in undrained shear behaviour. For legend of the borehole descriptions see Appendix B.

In Figure 6.11 and Figure 6.12 the measured undrained shear strength (without corrections) is presented. It can be seen in these figures that the relation between the measured undrained shear strength and rotation rate is not straightforward. The highest rotation rate not always results in the highest undrained shear strength and the lowest rotation rate not always results in the lowest undrained shear strength.

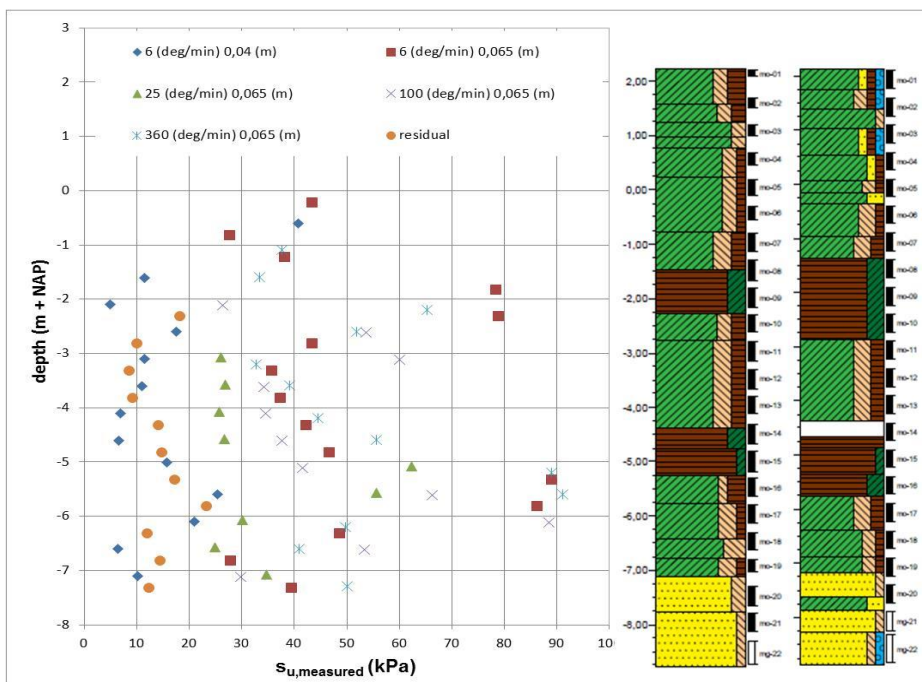


Figure 6.11 $s_{u,measured}$ of the FVT for the Lekdijk near Schalkwijk. The relation between the measured undrained shear strength and rotation rate is not straightforward. For legend of the borehole descriptions see Appendix B.

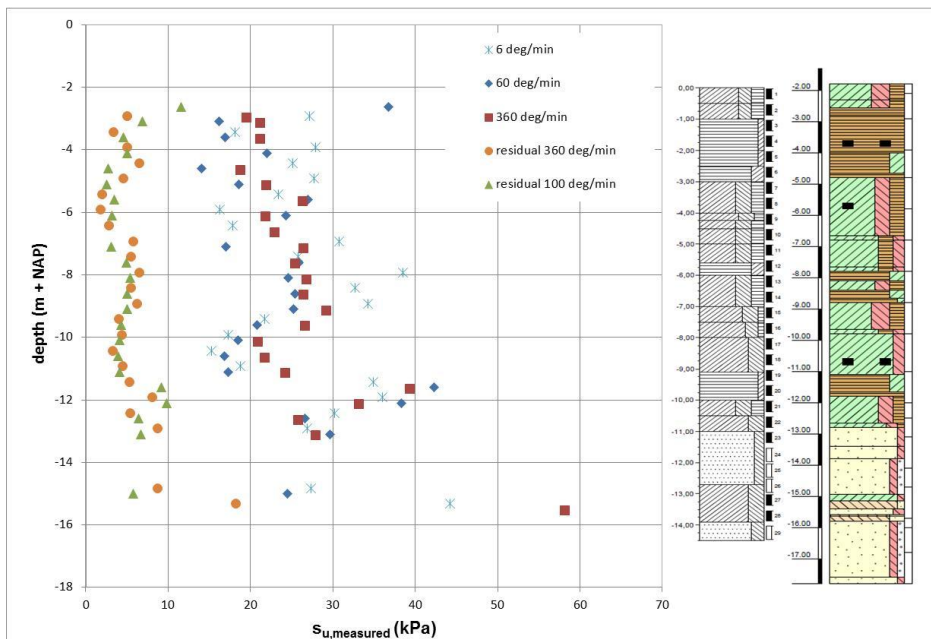


Figure 6.12 $s_{u,measured}$ of the FVT for the Achterwaterschap near Alblasterdam. The relation between the measured undrained shear strength and rotation rate is not straightforward. For legend of the borehole descriptions see Appendix B.

The residual shear strength with two different rotation rates at Alblasterdam in Figure 6.12 gives practically the same results. Therefore no correction for the strain rate effects for the residual strength is applied. This agrees with Biscontin & Pestana (2001).

Figure 6.13 shows $s_{u,corrected}$ of the FVT for the Achterwaterschap near Alblasterdam. The correction for strain rate effects is applied to obtain shear strength values which are comparable with values from the standard rotation rate of 6 degrees per minute. The $s_{u,corrected}$ of the FVT with rotation rate of 360 degrees per minute gives the lowest values. Therefore the FVT results derived from these fast tests are deemed to reflect truly undrained conditions. For the Waaldijk and Lekdijk sites the corrections for strain rate effects are much smaller than for the Achterwaterschap, because the plasticity index is on average much higher for the Achterwaterschap. So for the Waaldijk and Lekdijk sites the relation between the corrected undrained shear strength and rotation rate is not straightforward.

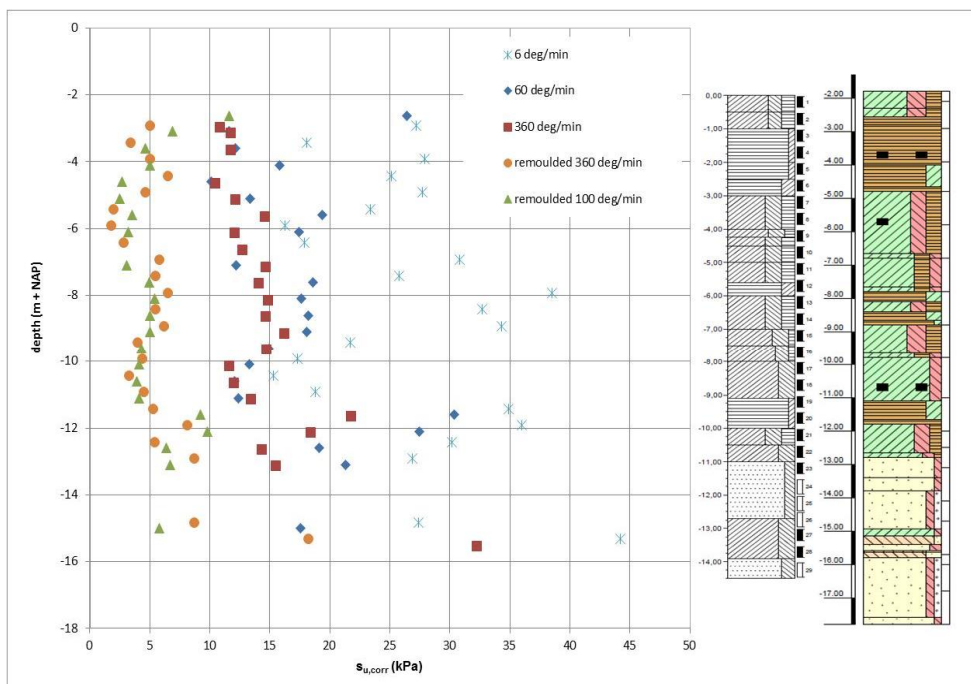


Figure 6.13 $s_{u,corrected}$ of the FVT for the Achterwaterschap near Alblasterdam. After correction for strain rate effect $s_{u,corrected}$ of the FVT with rotation rate of 360 degrees per minute gives the lowest values. For legend of the borehole descriptions see Appendix B.

6.5 Sample length and determination of soil unit weight

The sample length and the soil unit weight provide information on sample disturbance. This section describes the assessment of sample length and unit weight.

Figure 6.14 shows the sample length in the field and in the laboratory before and after extrusion of the samples at the Lekdijk near Schalkwijk. At this site the hammered Ackermann sampling system is applied, to be comparable with the data of the HDSR project.

The first six samples counted from the top are relatively short compared to the length of the sampler of 440 mm. For these samples many beats were required to hammer the sampler into the soil. In the deeper layers about 40 beats were required to hammer the complete sampler into the soil, but for the first six samples up to 200 beats were required to take 250 mm sample. For these samples also the force which was needed for the extrusion of the samples in the laboratory was high; about two times the force which was required for the deeper samples.

It is not clear why the first six samples are relatively short compared to the length of the sampler. It is possible that the soil is compacted due to the large number of beats which was applied to hammer the samplers into the soil (low recovery ratio). Another explanation is that the samples are broken during pulling the samplers upwards. As the first six samples are above the phreatic surface the soil is aggregated and the samples can be broken along existing cracks in the soil.

The deeper samples below the phreatic surface also show often a shorter length in the field compared to the sampler length. This can be attributed to compaction of the soil due to sampling. The recovery ratio is on average 0.94, with the lowest value 0.85, indicating that sample disturbance occurs.

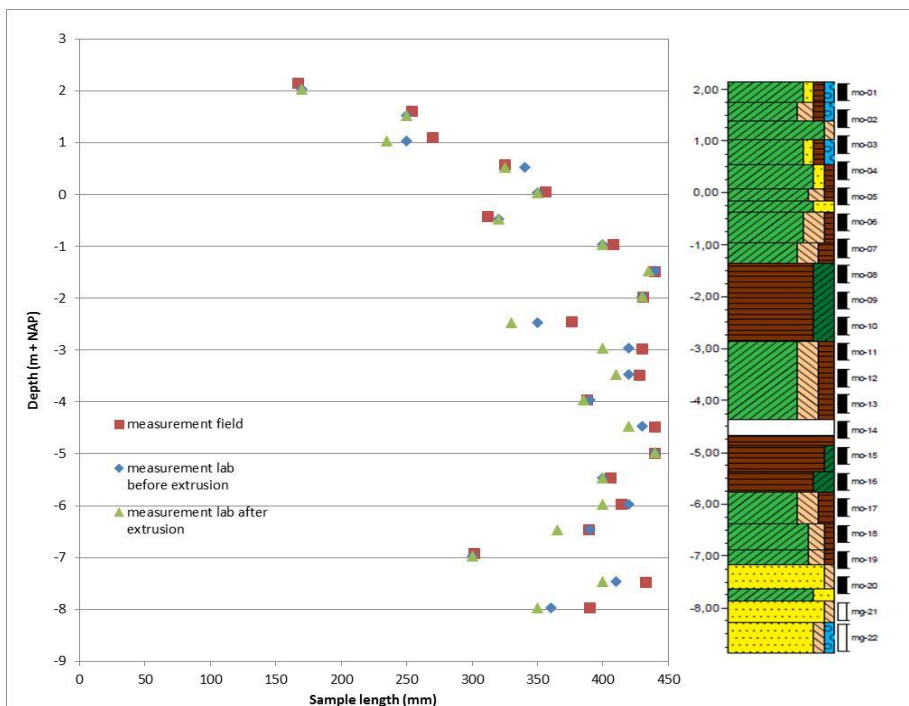


Figure 6.14 Sample length in the field and in the laboratory before and after extrusion of the samples at the Lekdijk near Schalkwijk. The length of the sampler is 440 mm. Most of the samples show an important decrease of the sample length, particularly the samples from the top of the subsoil. For legend of the borehole descriptions see Appendix B.

In the laboratory before extrusion of the samples the samples are often somewhat shorter than the length as measured in the field; differences were found up to 7%. Possibly this can be caused by measurement errors. Another explanation could be shrinkage of the samples during transportation and storage. After extrusion of the samples some samples again became shorter. This is in the same order of about 7%. Other samples however have the same length in the field and in the laboratory and before and after extrusion.

The FVT, dissipation tests and triaxial tests are performed from NAP -0.5 m and deeper. This is because positive pore water pressures are measured with the CPTu from about NAP +0.20 m, indicating the phreatic surface. As all tests are performed below the phreatic surface, no triaxial tests are conducted in the zone where much energy was required to take the samples and to extrude the samples.

Regarding the soil unit weight at the Lekdijk near Schalkwijk the variability is substantially. In Figure 6.15 the soil unit weight is presented. The soil unit weight is derived from two boreholes from the present project and also some data from waterboard HDSR is used. The bandwidth of the soil unit weight is about 2.0 kN/m^3 . For a large part this variability can be attributed to natural variability, although the boreholes are conducted within a mutual distance of about 3.0 m. However, the variability in soil unit weight due to sample disturbance is also relevant, as the changes in sample height as discussed before result in changes of soil unit weight in the order of magnitude of 0.8 kN/m^3 , with extreme values around 1.5 kN/m^3 .

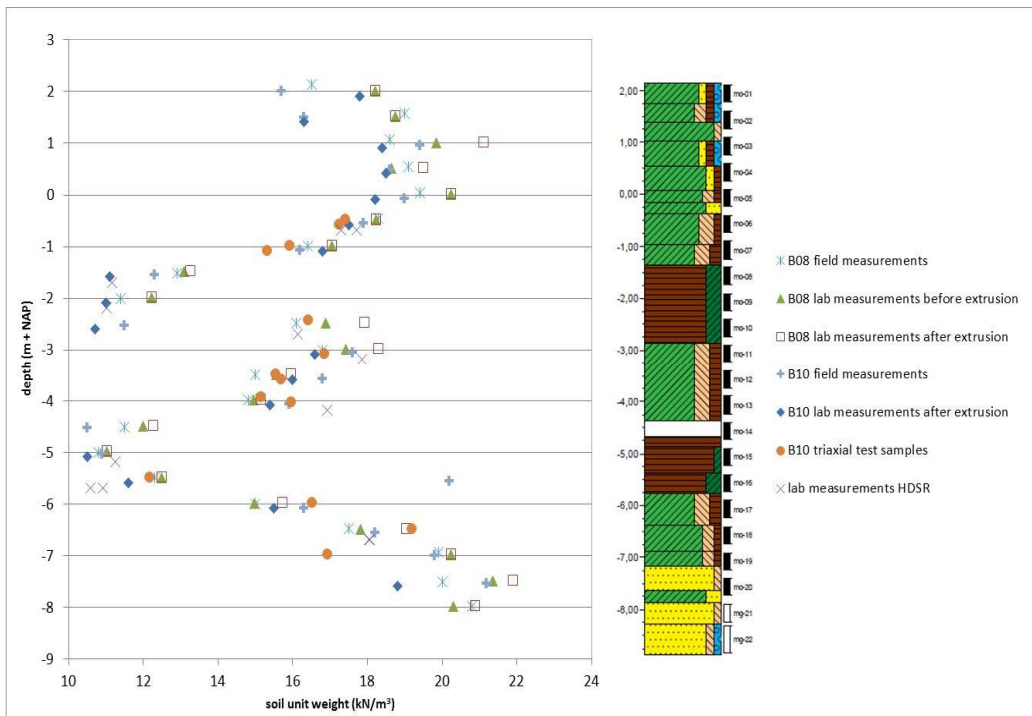


Figure 6.15 Variability of soil unit weight for the Lekdijk near Schalkwijk. The soil unit weight has a large range, which reflects the natural variability and the induced uncertainty due to sample disturbance. For legend of the borehole descriptions see Appendix B.

Results from the Achterwaterschap near Alblasterdam are presented in Figure 6.16.

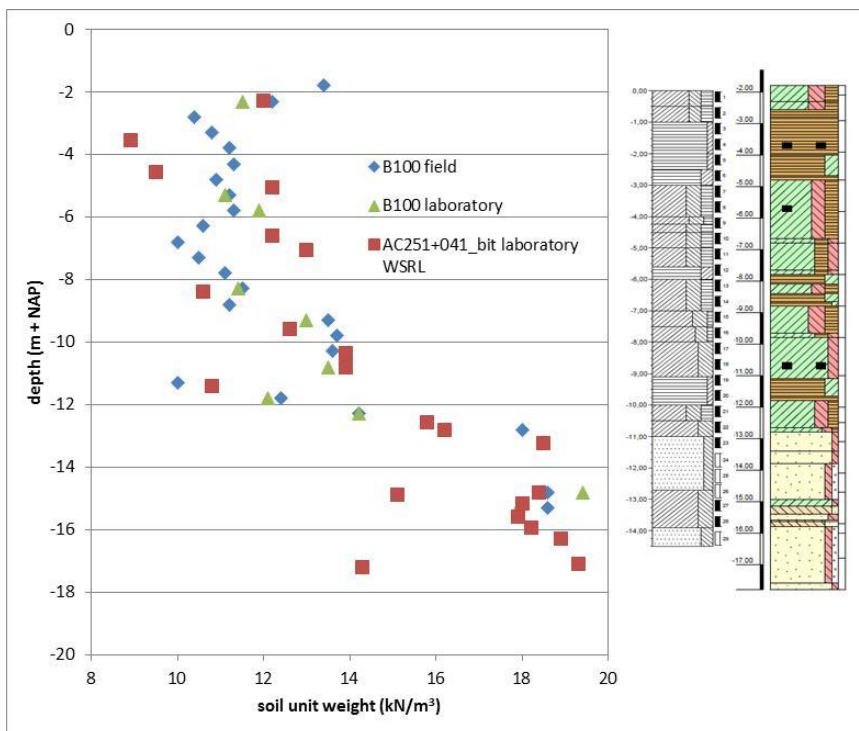


Figure 6.16 Variability of soil unit weight for the Achterwaterschap near Alblasterdam. The differences between borehole B100 and borehole AC251+041 can be attributed to natural variability and to differences in sampling system. Borehole B100 is performed with pushed Ackermann sampling system and borehole AC251+041 is performed with Piston sampling system. For legend of the borehole descriptions see Appendix B.

For the Achterwaterschap near Alblasterdam the pushed Ackermann sampling system is applied in the present research. As the subsoil is relatively soft at this site a high recovery ratio of 1.0 of the sample tubes was found. The differences in soil unit weight determined in the field and the soil unit weight determined in the laboratory can be attributed to the fact that the unit weights from the laboratory concern the specimen for the triaxial tests and constant rate of strain tests. Since samples are split into specimen, differences in unit weight might be found due to heterogeneity.

By order of waterboard WSRL also a borehole was drilled, applying the Piston sampling system, which uses samplers of 1000 mm length. As shown in Figure 6.16, by the red markers, the deviations of the soil unit weights from the Ackermann sampling system and Piston sampling system is remarkable. This type of differences may lead to different estimations of total stress and effective stress profiles. These estimations have consequences for all further analyses.

At the Waaldijk in Waardenburg where the pushed Ackermann sampling system is used the results regarding changes in sample length and changes in soil unit weight are very similar to the Lekdijk site. The recovery ratio is on average 0.85 with the highest value 0.91 for the samples in saturated soil. For the unsaturated top layer recovery ratios of 0.5 to 0.6 are found. The resulting variability of soil unit weight is somewhat smaller; about 1.5 kN/m^3 , which is partly caused by natural variability and partly by sample disturbance. At this location the field and laboratory tests are performed from NAP +1.80 m, as from this level positive pore water pressures are measured with the CPTu, indicating the level of the phreatic surface. For all samples however sample disturbance may play a role as can be concluded from the recovery ratios.

6.6 Intrinsic undrained shear strength ratios from reconstituted samples

Intrinsic undrained shear strength ratios are derived from the triaxial compression tests on reconstituted samples. The results are presented in Figure 6.17 and Figure 6.18.

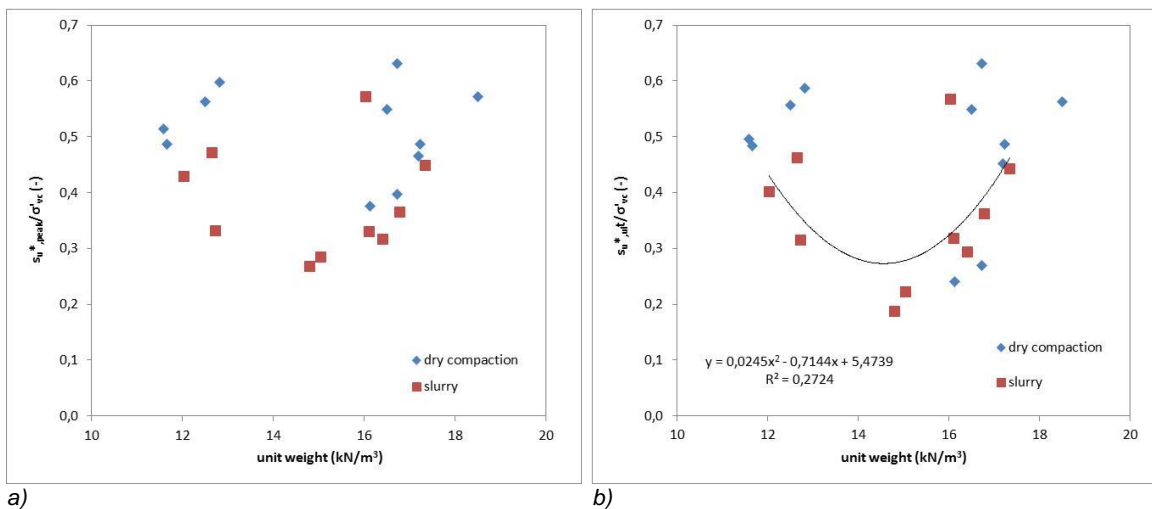


Figure 6.17 $s_{u,peak}^*/\sigma'_{vc}$ and $s_{u,ultimate}^*/\sigma'_{vc}$ versus soil unit weight from triaxial compression tests on reconstituted samples. The variability in the intrinsic undrained shear strength ratios is enormous.

In Figure 6.17 $s_{u,peak}^*/\sigma'_{vc}$ and $s_{u,ultimate}^*/\sigma'_{vc}$ are plotted versus soil unit weight. In both figures the variability is enormous. The variability is somewhat larger than found by Chandler (2000). For the ultimate strength (25% axial strain) the mean value is smaller than for the peak strength. The scatter is larger for the ultimate strength than for the peak strength.

In Figure 6.18 $s_{u,peak}^*/\sigma'_{vc}$ is plotted versus plasticity index I_p and organic matter content OC . In literature usually the relation between undrained shear strength ratio and plasticity

index is shown. In Figure 6.18a however, no clear trend can be observed. As Dutch soils are commonly more organic than soils in literature, the relationship with organic matter content is given in Figure 6.18b. The intrinsic undrained shear strength ratio however shows no clear trend with soil unit weight, plasticity index I_p and nor the organic matter content OC .

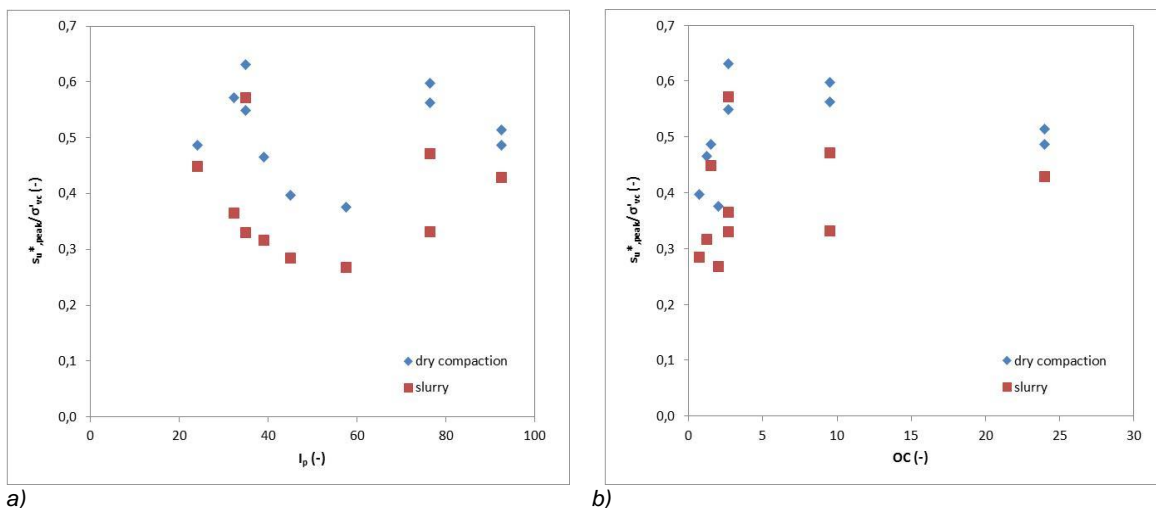


Figure 6.18 $s_{u,peak}^*/\sigma'_{vc}$ versus plasticity index I_p and organic matter content OC from triaxial compression tests on reconstituted samples. The intrinsic undrained shear strength ratios have no clear relation with plasticity index I_p and organic matter content OC .

Table 6.1 Mean values of the intrinsic undrained shear strength ratios from triaxial compression tests on reconstituted samples.

Preparation method	$s_{u,peak}^*/\sigma'_{vc}$ (-)	$s_{u,ultimate}^*/\sigma'_{vc}$ (-)
Dry compaction	0.51	0.48
Slurry	0.38	0.36

The mean values of the intrinsic undrained shear strength ratios from triaxial compression tests on reconstituted samples are summarized in Table 6.1. The values for the dry compaction method are higher than for the slurry method. As it is expected that the sedimentation and consolidation processes for the slurry method are closer to the natural processes and the lower values of the slurry method fit better to literature results the values of the slurry method will be used in the further analyses in the present study. However it may be clear that the different preparation methods result in uncertainty about the intrinsic undrained shear strength ratios, also within one method the variability of the intrinsic undrained shear strength ratios is large as shown in Figure 6.17 and Figure 6.18.

Thixotropic hardening

Laboratory vane tests conducted at four reconstituted samples with measurements over a period of 8 to 11 days show an increase in undrained shear strength with a factor 1.45 to 2.24; see Figure 6.19. This strength gain can be attributed to thixotropic hardening.

As the consolidation of the reconstituted samples in the triaxial tests took 1 to 3 days a strength gain with a factor 1.1 to 1.6 during the consolidation phase can be expected. This process of thixotropic hardening might be the explanation of the small peak strength which occurred in the triaxial compression tests. As the triaxial tests are performed on reconstituted samples without any structure, the peak shear strength and the ultimate shear strength are equal in theory. As some softening is observed in the triaxial tests, it can be supposed that the samples had some structure due to thixotropic hardening. To account for this effect $s_{u,ultimate}^*/\sigma'_{vc}$ of the slurry method is taken as the intrinsic undrained shear strength ratio in the analyses in the next paragraphs. The intrinsic undrained shear strength ratio is for all clay

samples approximated by the relation: $y = 0.0245x^2 - 0.7144x + 5.4739$ with x is the soil unit weight and y is the intrinsic undrained shear strength ratio, with $y \leq 0.4$ (see Figure 6.17). On average this approximation agrees reasonably with Chandler (2000), who mentions a value of 0.33.

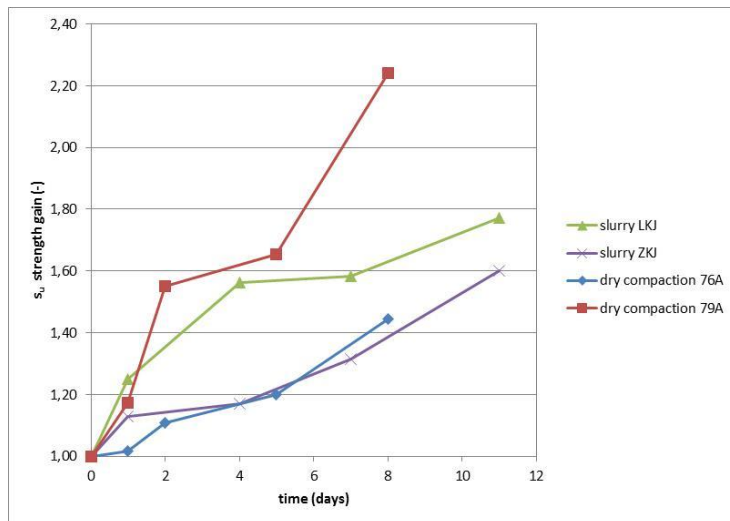


Figure 6.19 Strength gain of reconstituted samples measured by laboratory vane tests on reconstituted samples. This strength increase might have affected the strength which is measured in the triaxial compression tests.

6.7 Undrained shear strength ratios from intact natural samples

The effect of structure of intact natural soils can be determined from the triaxial tests on intact samples. As in the previous paragraph the undrained shear strength is normalized for the effective stress level. To normalize the undrained shear strength of the intact samples for the effective stress level the estimated in situ effective stress is used instead of the consolidation stress. This is because the triaxial tests on natural samples in the present research are from various projects with different estimates of the in situ effective stress, resulting in different estimates for the consolidation stress. As the undrained shear strength of overconsolidated samples is determined mainly by the yield stress, it is assumed that small variations in the effective stress below the yield stress will not affect the undrained shear strength (see Paragraph 4.5). Therefore it is thought to be allowed to use the estimations of the in situ effective stress profiles from the present project for the stress normalization of the triaxial test results obtained from other projects at the same sites.

Figure 6.20 and Figure 6.21 gives the undrained shear strength ratio s_u/σ'_{vi} versus soil unit weight from triaxial compression tests on reconstituted samples and intact samples. In Figure 6.20 $s_{u,peak}/\sigma'_{vi}$ of the intact samples is compared with $s_{u,ultimate}/\sigma'_{vi}$ of the reconstituted samples. In Figure 6.21 $s_{u,ultimate}/\sigma'_{vi}$ of the intact samples is compared with $s_{u,ultimate}/\sigma'_{vi}$ of the reconstituted samples. Both figures show more or less the same pattern, although the values differ.

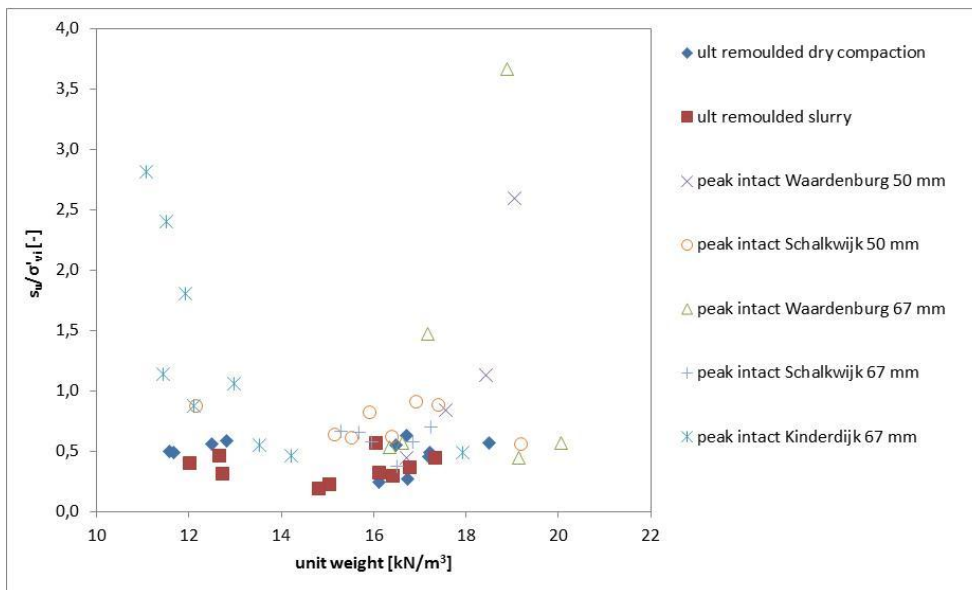


Figure 6.20 s_u/σ'_{vi} versus soil unit weight from triaxial compression tests on reconstituted and intact samples; $s_{u,peak}/\sigma'_{vi}$ of the intact samples compared with $s_{u,ult}/\sigma'_{vi}$ of the reconstituted samples. $s_{u,ult}/\sigma'_{vi}$ of the reconstituted samples forms the lower bound strength of $s_{u,peak}/\sigma'_{vi}$ of the intact samples.

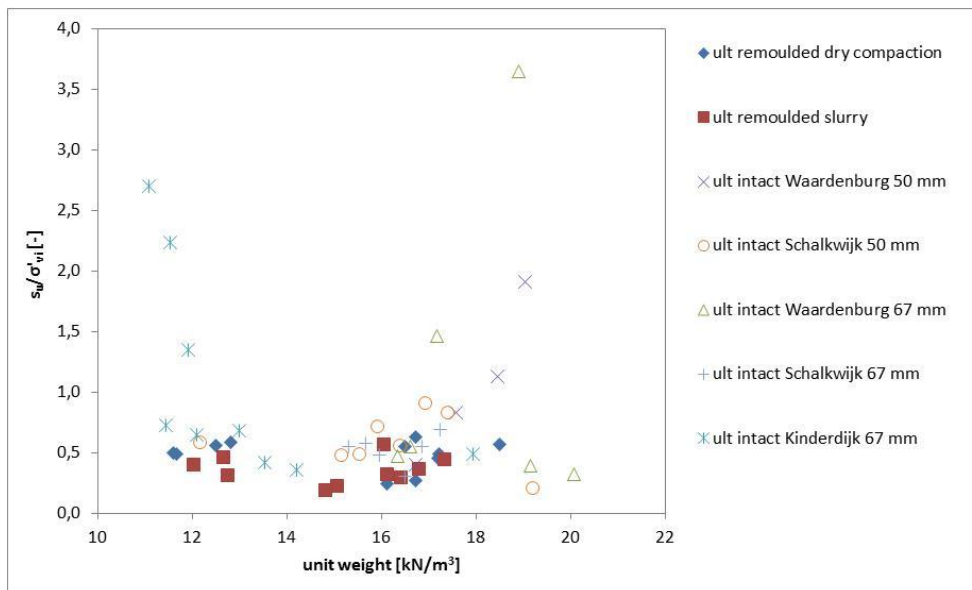


Figure 6.21 s_u/σ'_{vi} versus soil unit weight from triaxial compression tests on reconstituted and intact samples; $s_{u,ult}/\sigma'_{vi}$ of the intact samples compared with $s_{u,ult}/\sigma'_{vi}$ of the reconstituted samples. When using $s_{u,ult}/\sigma'_{vi}$ instead of $s_{u,peak}/\sigma'_{vi}$ of the intact sample $s_{u,ult}/\sigma'_{vi}$ of the reconstituted samples also forms the lower bound strength.

High undrained shear strength ratios are obtained from triaxial tests on intact samples for the soft organic clay at the Achterwaterschap near Alblasterdam and for firm sandy silty clays at the Waaldijk in Waardenburg. At the Lekdijk near Schalkwijk relatively low undrained shear strength ratios are derived. Generally for all sites the undrained shear strength ratios are very low for the soil unit weights between 13 and 16 kN/m³, compared to the intrinsic strength of the reconstituted samples and the intact strength of soils with soil unit weights below 13 kN/m³ and above 16 kN/m³.

Furthermore it can be noticed that no substantial difference in shear strength ratios is found between the 50 mm samples from the Lekdijk near Schalkwijk and the Waaldijk at

Waardenburg, which were damaged during transport and the 65 mm samples, which were not damaged.

6.8 Comparison of undrained shear strength ratios from reconstituted and natural samples

At the research locations of the present study also other data from the concerning waterboards HDSR and WSRL is available. This data is collected and added to the analyses of the present research. In Figure 6.22 and Figure 6.23 the undrained shear strength ratio s_u/σ'_{vi} versus soil unit weight from triaxial compression tests on reconstituted and intact samples from the present project and other projects are plotted. In Figure 6.22 $s_{u,peak}/\sigma'_{vi}$ of the intact samples is compared with $s_{u,ultimate}/\sigma'_{vi}$ of the reconstituted samples. In Figure 6.23 $s_{u,ultimate}/\sigma'_{vi}$ of the intact samples is compared with $s_{u,ultimate}/\sigma'_{vi}$ of the reconstituted samples. The estimated in situ effective stress is used to normalise the shear strength as discussed in Paragraph 6.7.

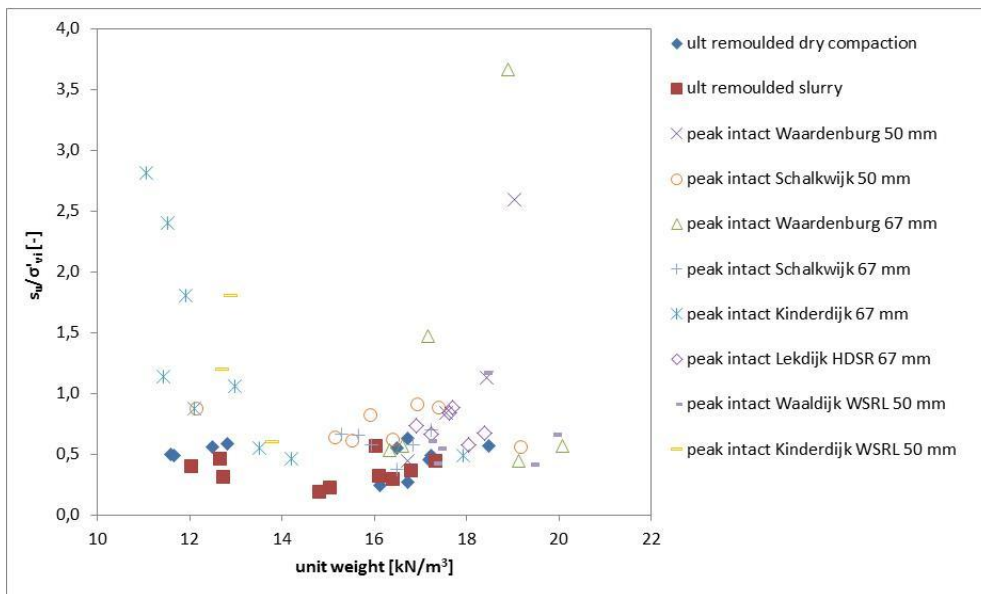


Figure 6.22 s_u/σ'_{vi} versus soil unit weight from triaxial compression tests on reconstituted and intact samples; $s_{u,peak}/\sigma'_{vi}$ of the intact samples compared with $s_{u,ult}/\sigma'_{vi}$ of the reconstituted samples. Due to structure of intact soils $s_{u,peak}/\sigma'_{vi}$ of the intact samples is higher than $s_{u,ult}/\sigma'_{vi}$ of the reconstituted samples.

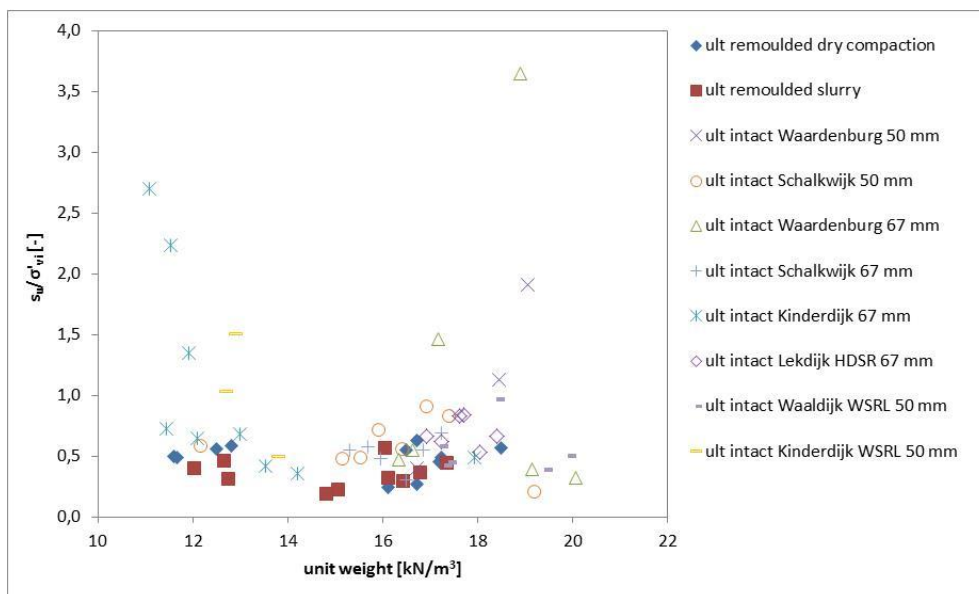


Figure 6.23 s_u/σ'_{vi} versus soil unit weight from triaxial compression tests on reconstituted and intact samples; $s_{u,ult}/\sigma'_{vi}$ of the intact samples compared with $s_{u,ult}/\sigma'_{vi}$ of the reconstituted samples.

Figure 6.22 and Figure 6.23 have the same general pattern as Figure 6.20 and Figure 6.21. For the Achterwaterschap at Alblasserdam the undrained shear strength ratios of the 50 mm samples from the WSRL project are relatively low compared to the undrained shear strength ratios of the 67 mm samples from present project. The samples from the WSRL research are obtained from Piston samplers with 100 mm samples which were trimmed to 50 mm samples for the triaxial tests. As described in Paragraph 4.2 in the present project the pushed Ackermann sampler system is used.

As already discussed in the previous paragraph in the range of soil unit weights above 13.5 kN/m^3 most of the intact samples have relatively low strength compared to the intrinsic strength as measured on the reconstituted samples. At the Lekdijk near Schalkwijk the strength derived from the project of waterboard HDSR is in the same order as the strength determined in the present project. In the HDSR project the hammered Ackermann sampling system is used. This is for the Lekdijk near Schalkwijk also the case in the present project. For the borehole of waterboard WSRL at the Waaldijk at Waardenburg the Piston sampler is used, whereas in the present project the Ackermann system with pushed samplers is used. The obtained undrained shear strength ratios are comparable, with exception of some samples with very high undrained shear strength ratios, which are relatively close to the surface.

When using the applied consolidation stresses of the triaxial tests the undrained shear strength ratios become smaller, as illustrated in Figure 6.24. Especially for the Achterwaterschap near Alblasserdam where the in situ stresses are low the effect of the stress level on the undrained shear strength ratio is large. In the range of the soil unit weight between 14 and 17 kN/m^3 the results of the triaxial tests on the intact samples coincide much more with the results of the triaxial tests on the reconstituted samples compared with Figure 6.22, where the estimation of the in situ effective stress is used.

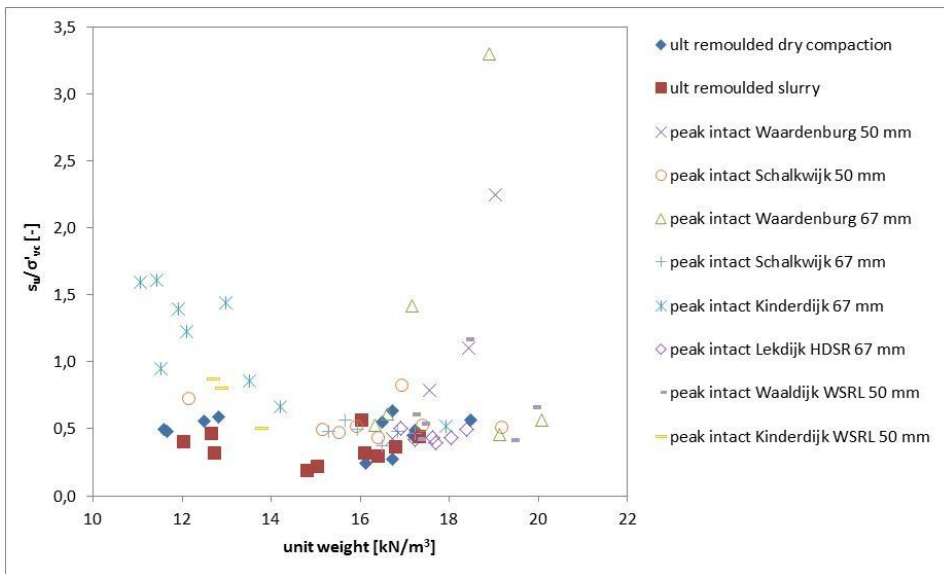


Figure 6.24 s_u/σ'_{vc} versus soil unit weight from triaxial compression tests on reconstituted and intact samples; $s_{u,peak}/\sigma'_{vc}$ of the intact samples compared with $s_{u,ult}/\sigma'_{vc}$ of the reconstituted samples. Note that the consolidation stress is used here instead of the estimated in situ effective stress.

Figure 6.25 and Figure 6.26 give the undrained shear strength ratio $s_{u,peak}/\sigma'_{vi}$ of the intact samples versus plasticity index I_p and organic matter content OC respectively. As the information on I_p and OC is not available from the projects of the waterboards these results are missing in the figures.

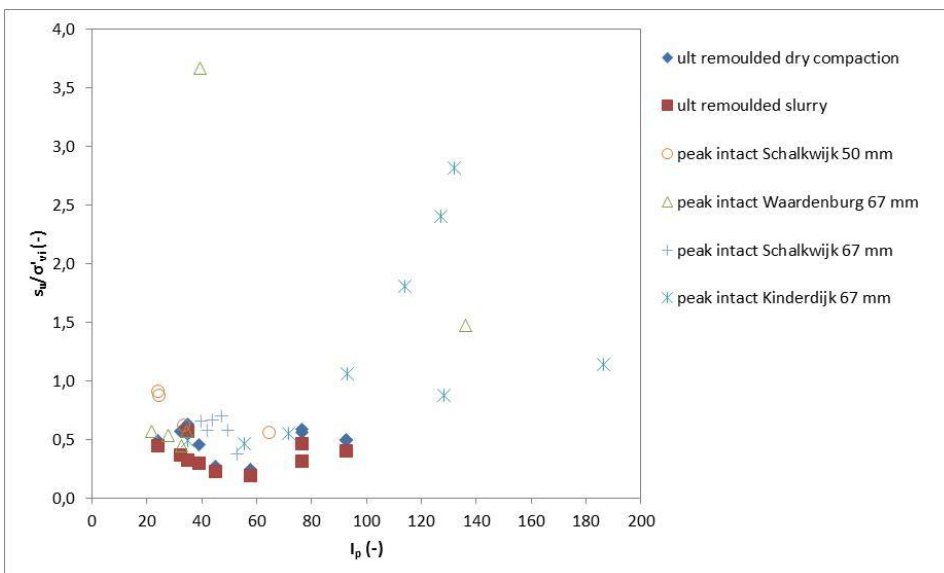


Figure 6.25 s_u/σ'_{vi} versus plasticity index I_p from triaxial compression tests on reconstituted and intact samples; $s_{u,peak}/\sigma'_{vi}$ of the intact samples compared with $s_{u,ult}/\sigma'_{vi}$ of the reconstituted samples.

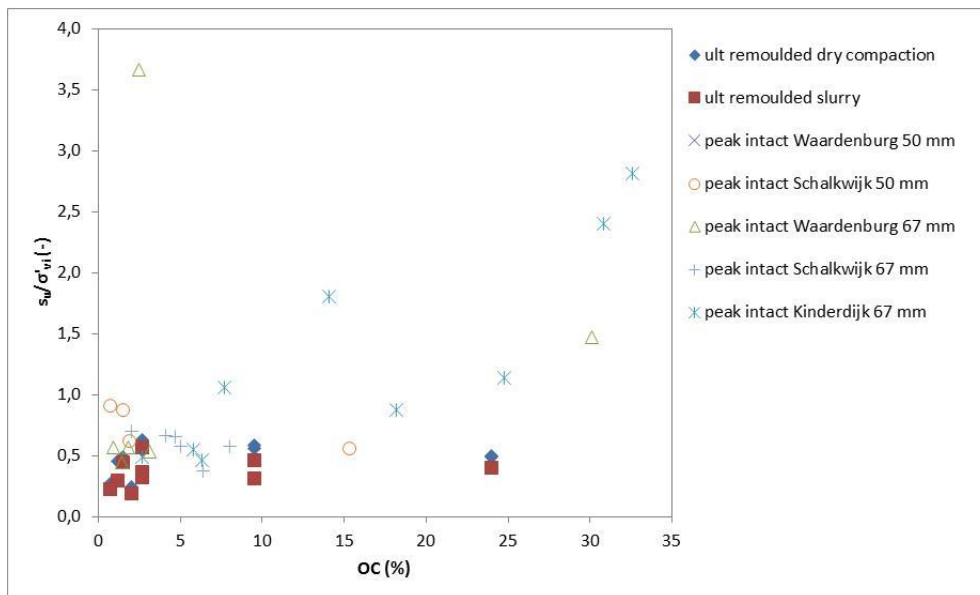


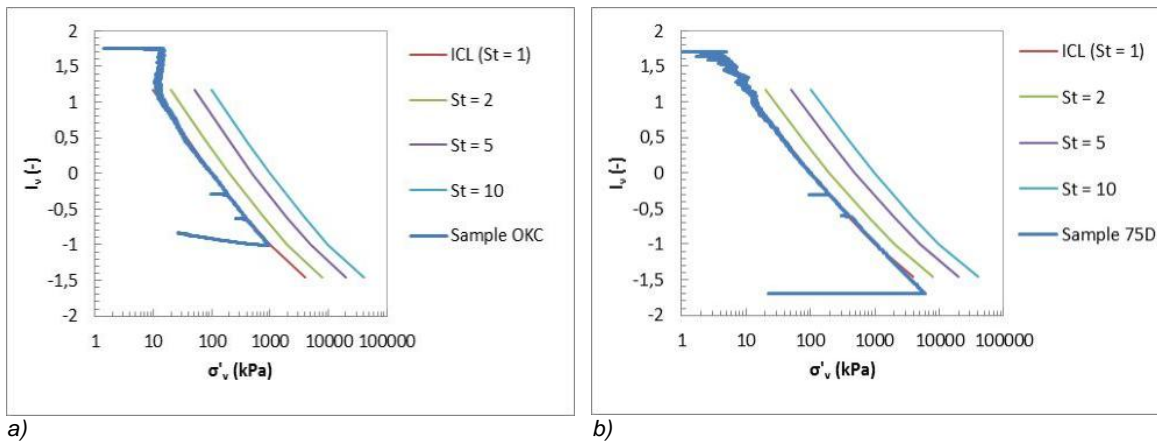
Figure 6.26 s_u / σ'_{vi} versus organic matter content OC from triaxial compression tests on reconstituted and intact samples; $s_{u,peak} / \sigma'_{vi}$ of the intact samples compared with $s_{u,ult} / \sigma'_{vi}$ of the reconstituted samples.

High undrained shear strength ratios can be observed for the soft organic clay at the Achterwaterschap near Alblasterdam and for some samples from the Waaldijk at Waardenburg. The high undrained shear strength ratios can be attributed to the high plasticity index and the high organic matter content. For soils with low plasticity index and low organic matter content the undrained shear strength is relatively low, except for one sample at the Waaldijk in Waardenburg, which is close to the surface, as mentioned before.

6.9 Intrinsic compression parameters from reconstituted samples

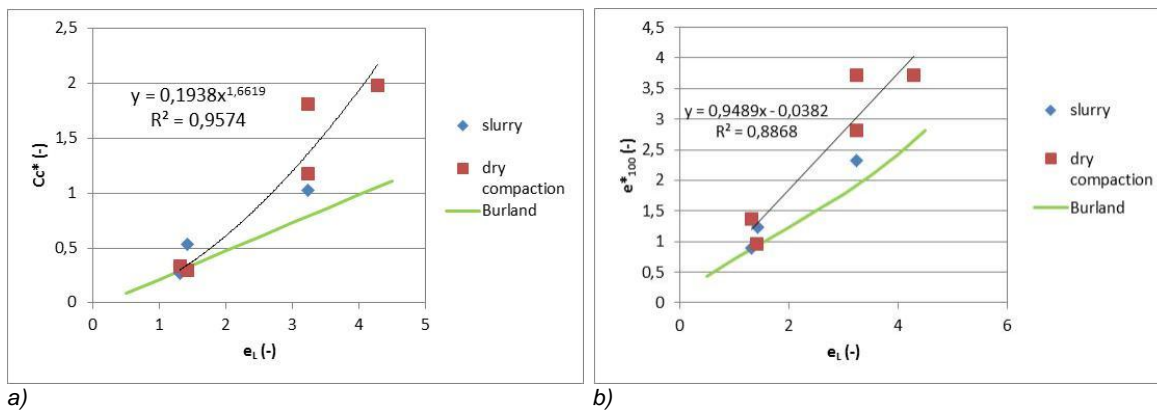
The eight CRS tests on reconstituted samples are analyzed using the normalization parameter void index I_v and the ICL as defined by Burland (1990) and discussed in Paragraph 4.9. The measured strains from the CRS tests are recalculated to the void index, using water content and specific gravity as described in Paragraph 4.3.

Two examples of compression curves from CRS tests on reconstituted samples are presented in Figure 6.27. Figure 6.27b show a compression curve of a clay with organic content of 1.7%. This specimen is prepared as slurry. So, this clay compares very well to the data used by Burland (1990). Figure 6.27a shows a compression curve of clay with 22.7% organic matter. This specimen is prepared with dry compaction. The organic matter content of the latter specimen is far outside the range of the data used by Burland. The examples show that the compression curves of both CRS tests fit to the ICL. At low stresses at the start of the tests the compression curves show a strange pattern and scatter due to connection problems of the specimen with the ring of the apparatus.



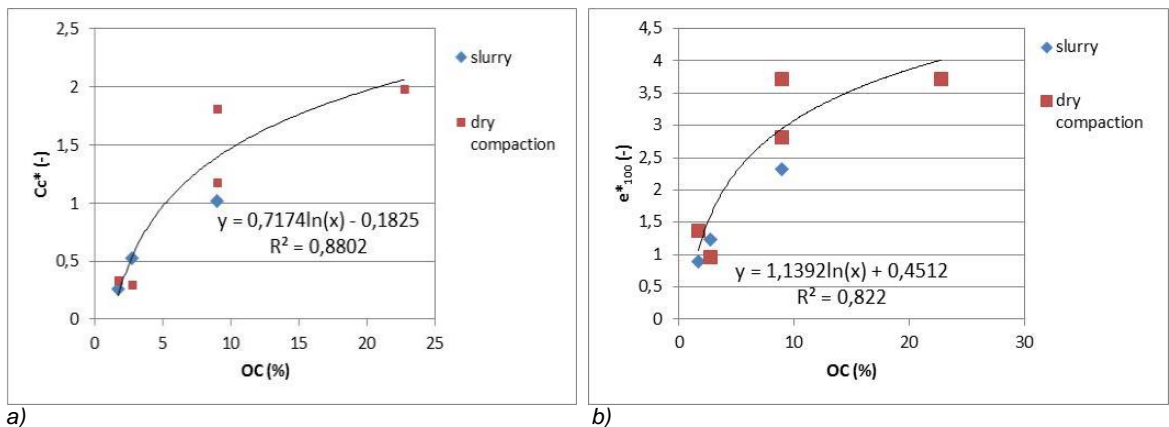
a) b)
 Figure 6.27 Constant rate of strain tests on reconstituted samples interpreted within the sensitivity framework. Due to the procedure the measured compression curves of reconstituted samples overlap the ICL.

The values of the intrinsic compression index C_c^* and e_{100}^* as obtained from the eight CRS tests on reconstituted samples are plotted against the liquid limit e_L in Figure 6.28. The values are compared with the relationships as given by Burland (1990), see Paragraph 4.9. It can be seen that the intrinsic compression index C_c^* and e_{100}^* for low values of the liquid limit e_L compare well with the relationships of Burland. For higher values of e_L the agreement decreases rapidly.



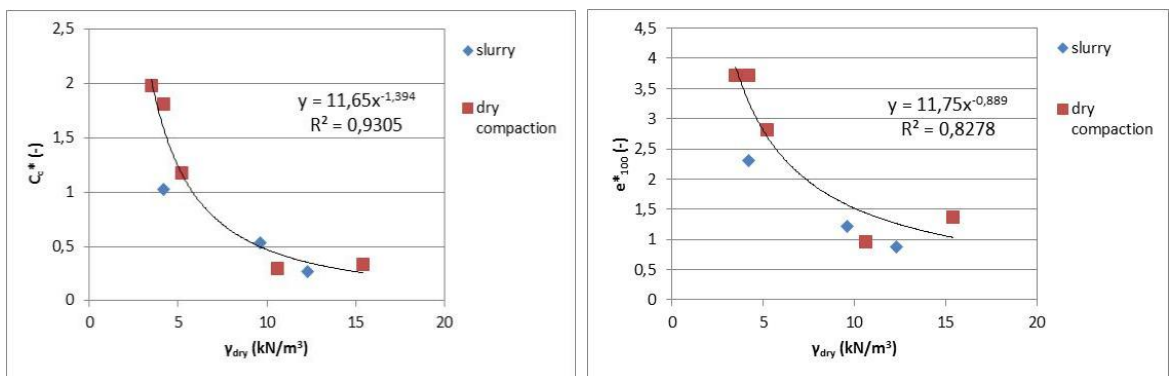
a) b)
 Figure 6.28 Values of the intrinsic compression index C_c^* and e_{100}^* derived from the CRS tests on reconstituted samples compared with the relationships as given by Burland (1990). For higher values of e_L the derived values deviate from the relationships as given by Burland (1990).

As the organic content of some of the tested soils is outside the range of the data used by Burland (1990) the influence of the organic content on the intrinsic compression index C_c^* and e_{100}^* is examined. The results are presented in Figure 6.29. It is clear that the intrinsic compression index C_c^* as well as e_{100}^* increase rapidly when organic matter content increases. However, the results show a relationship with a smaller accuracy compared to the relationships based on e_L (Figure 6.28).



a) b)
 Figure 6.29 Values of the intrinsic compression index C_c^* and e_{100}^* derived from the CRS tests on reconstituted samples plotted against organic matter content OC. The intrinsic compression index C_c^* as well as e_{100}^* increase rapidly when organic matter content increases.

The relationship between dry unit weight and intrinsic compression index C_c^* and e_{100}^* is also investigated (see Figure 6.30). The results show again a relationship with a smaller accuracy compared to the relationships based on e_L (Figure 6.28).



a) b)
 Figure 6.30 Values of the intrinsic compression index C_c^* and e_{100}^* derived from the CRS tests on reconstituted samples plotted against dry unit weight.

The relationships as presented in Figure 6.28, Figure 6.29 and Figure 6.30 are used to analyze the results of the CRS tests on natural samples with structure in order to determine the stress sensitivity S_σ .

6.10 Compression parameters and stress sensitivity from intact natural samples

CRS tests on intact natural samples are interpreted with the correlations for the intrinsic compression index C_c^* and e_{100}^* as discussed in the previous paragraph. The interpretation is performed within the sensitivity framework as described in Paragraph 4.9. From this interpretation the stress sensitivity S_σ is determined relative to the behaviour of the CRS tests on the reconstituted samples as represented by the ICL. At the interpretation of the CRS tests the tail of the compression curves can be fitted to the ICL, since at high stresses the soil structure disappears and the compression curve therefore converges to the ICL. This is helpful by the interpretation of the CRS tests. Figure 6.31 and Figure 6.32 give examples of the interpretation of CRS tests on intact samples.

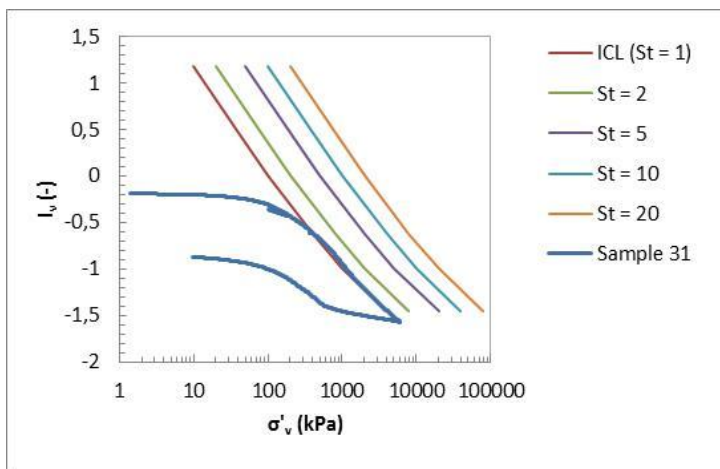


Figure 6.31 Constant rate of strain tests on intact sample 31 at NAP +0.92 m from the Waaldijk at Waardenburg interpreted within the sensitivity framework, resulting in $S_\sigma = 1.1$.

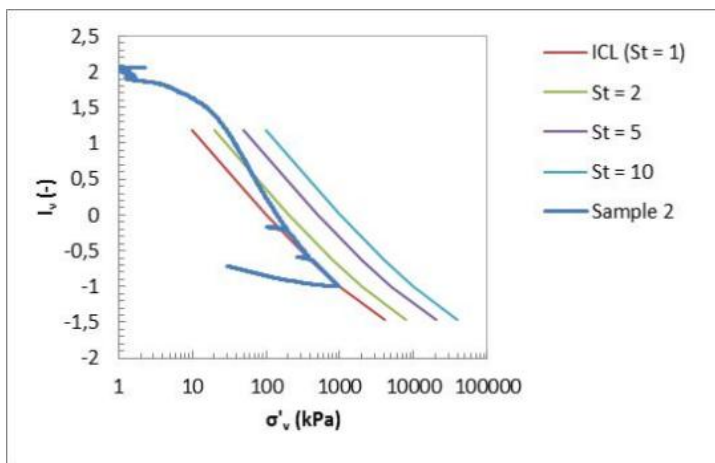


Figure 6.32 Constant rate of strain tests on intact sample 2 at NAP -5.70 m from the Achterwaterschap near Alblasserdam interpreted within the sensitivity framework, resulting in $S_\sigma = 3.0$.

The interpretation of the CRS tests mostly resulted in relatively low stress sensitivities. The obtained stress sensitivity values are presented in Paragraph 6.11, in the comparison with other sensitivity results.

The derived stress sensitivities S_σ seem to be uncertain due to uncertainties of the void ratio, intrinsic compression index C_c^* and void ratio e_{100}^* . The void ratio is uncertain because the various ways to determine the void ratio as discussed in Paragraph 4.3 give considerably different results. The intrinsic compression index C_c^* and void ratio e_{100}^* are uncertain too, because the correlations as discussed in Paragraph 6.9 have uncertainty.

6.11 Sensitivity from field vane tests, triaxial tests and constant rate of strain tests

In this paragraph the strength sensitivity S_t as derived from the FVT and triaxial tests and the stress sensitivity S_σ as obtained from the constant rate of strain tests are presented and compared. The determination of the stress sensitivity S_σ from the constant rate of strain tests is discussed in Paragraph 6.10. The strength sensitivity S_t is calculated from the FVT tests as described in Paragraph 4.8. The strength sensitivity S_t of the triaxial test is calculated by dividing the peak undrained shear strength ratios of the intact samples by the approximated values of the remoulded shear strength ratio as derived from the reconstituted samples (see Paragraph 6.6). As in the previous paragraphs the interpretation of the results is based on the estimation of the in situ effective stress.

Figure 6.33, Figure 6.34 and Figure 6.35 give a comparison of S_t from the FVT and triaxial compression tests on intact samples and S_σ from the constant rate of strain tests for the locations at the Lekdijk, Waaldijk and Achterwaterschap respectively. The comparison for the Lekdijk and the Waaldijk shows that S_t from the laboratory tests on intact samples is about a factor 1.5 lower than S_t from the FVT. For the Achterwaterschap S_t from the triaxial tests is in a nice agreement with S_t from the FVT. S_σ from the constant rate of strain tests is relatively low compared to the other tests, however the trend is good. For the Lekdijk and the Waaldijk S_σ from the constant rate of strain tests is low compared to S_t from the triaxial tests.

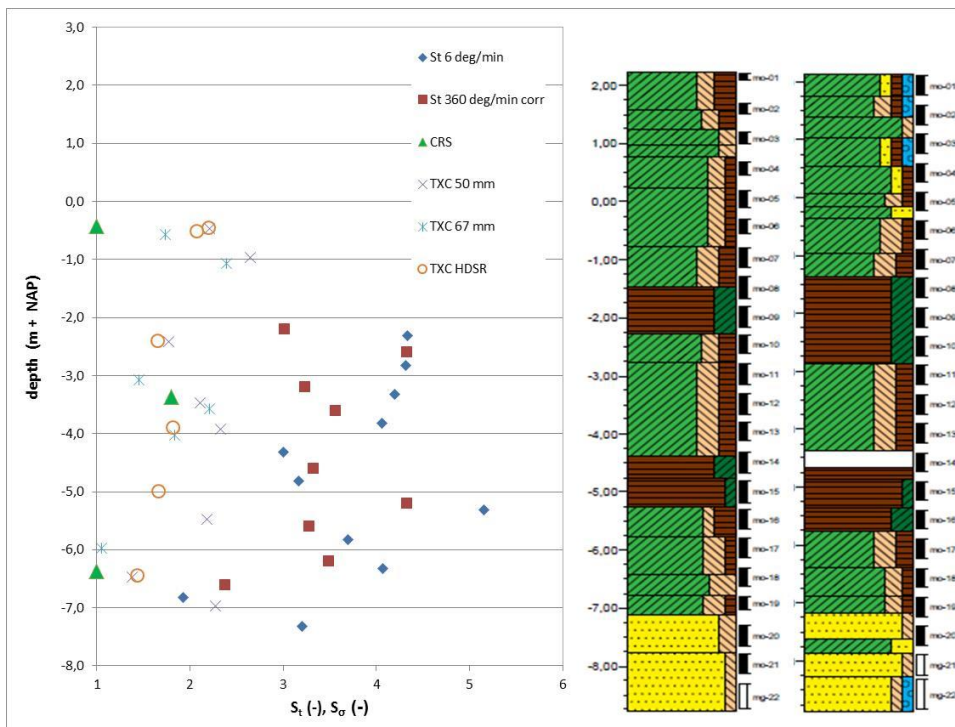


Figure 6.33 Comparison of S_t from the FVT and triaxial compression tests (TXC) on intact samples and S_σ from the constant rate of strain tests (CRS) at the Lekdijk near Schalkwijk. The FVT give systematic higher sensitivity than the laboratory test results. For legend of the borehole descriptions see Appendix B.

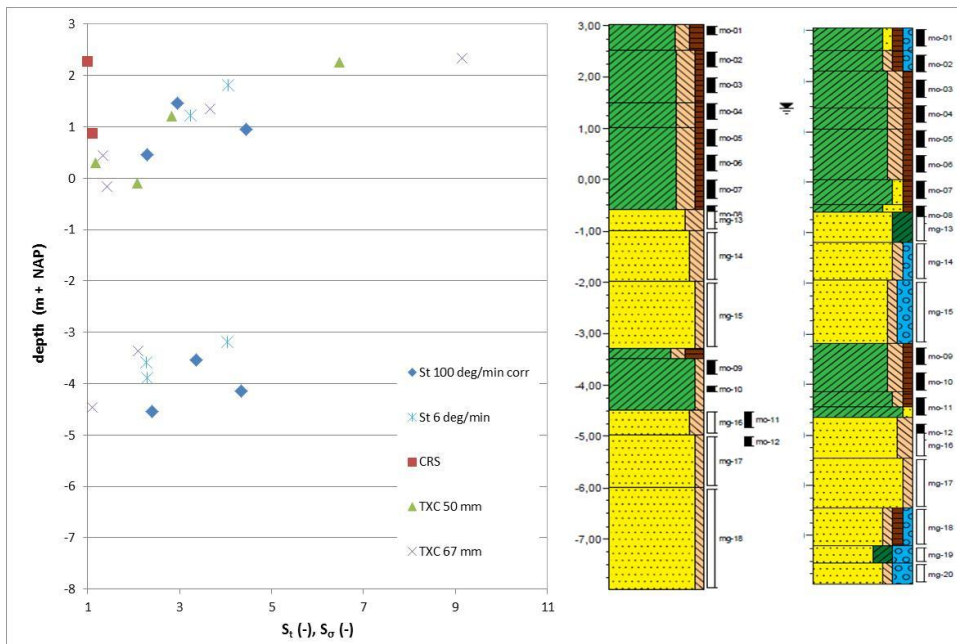


Figure 6.34 Comparison of S_t from the FVT and triaxial compression tests (TXC) on intact samples and S_σ from the constant rate of strain tests (CRS) at the Waaldijk in Waardenburg. For legend of the borehole descriptions see Appendix B.

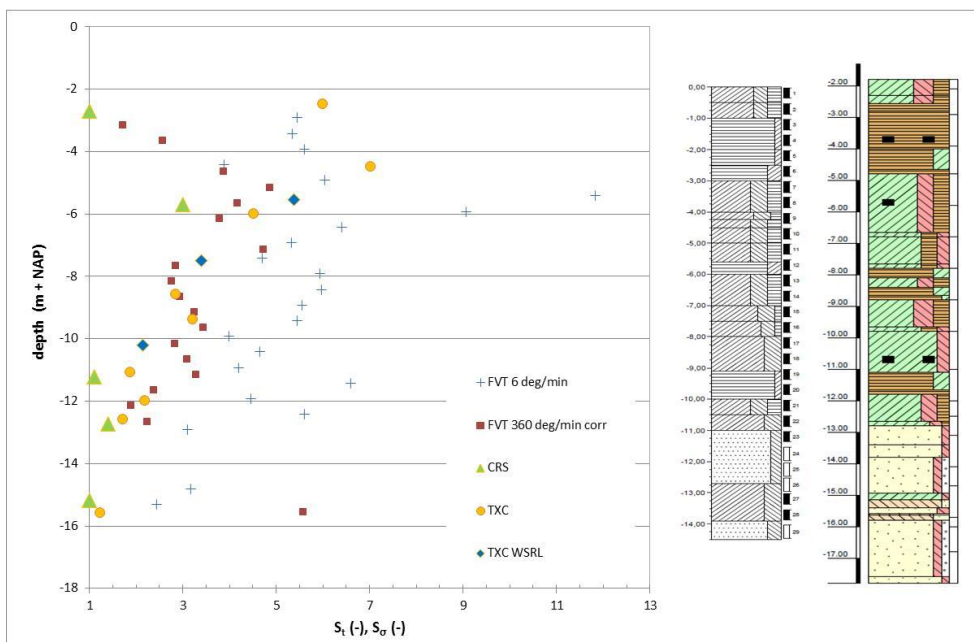


Figure 6.35 Comparison of S_t from the FVT and triaxial compression tests (TXC) on intact samples and S_σ from the constant rate of strain tests (CRS) at the Achterwaterschap near Alblasserdam. The sensitivity from the FVT and the laboratory tests agree well. For legend of the borehole descriptions see Appendix B.

At the Lekdijk and the Waaldijk the strength sensitivity S_t has roughly the same value over the whole profile (see Figure 6.33 and Figure 6.34). For the Achterwaterschap Figure 6.35 however shows that the strength sensitivity S_t increases in upward direction. These trends agree well with the trends of the general soil properties in Figure 6.1, Figure 6.2 and Figure 6.3. It seems that the trend of the strength sensitivity S_t is related to the trends of soil unit weight, plasticity index and organic content. For the Achterwaterschap S_t reflects the more swampy depositional conditions in upward direction.

Figure 6.36 gives an overview of the strength sensitivity S_t for the three measurement locations. In this figure the strength sensitivity S_t from FVT and triaxial tests on intact samples are compared. It is very interesting that the general pattern of this figure compares very well with the general pattern of Figure 6.22, Figure 6.23 and Figure 6.24, where undrained shear strength ratios are plotted. As in these figures also Figure 6.36 shows high values at low soil unit weights and high soil unit weights, but low values at soil unit weights between 14 and 17 kN/m^3 .

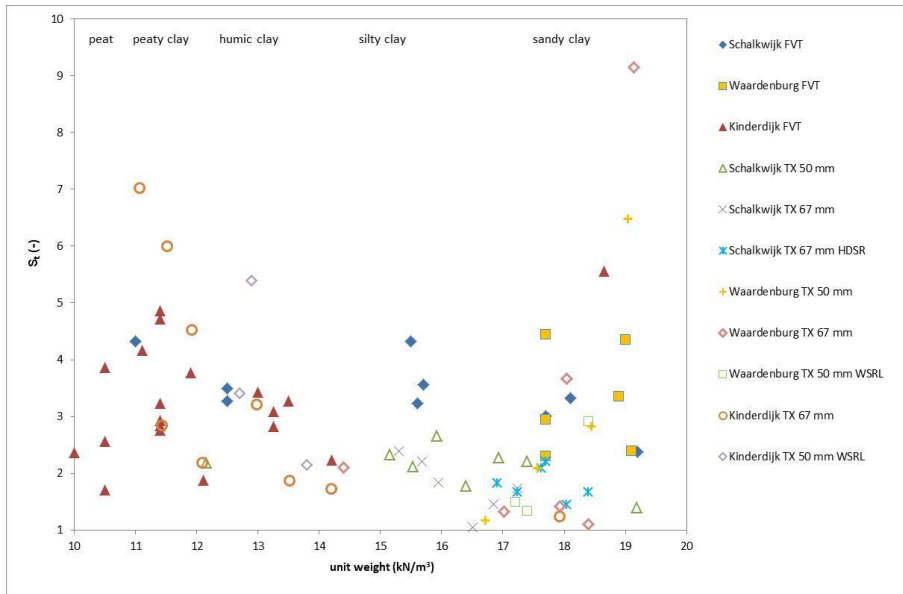


Figure 6.36 Comparison of S_t from the FVT and triaxial compression tests (TX) on intact samples for three sites. S_t from the FVT and triaxial compression tests compare very well for the soil unit weights between 10 and 15 kN/m^3 , but for the higher soil unit weights S_t from the triaxial tests is on average relatively low.

In Figure 6.36 it is also clear that S_t from the triaxial tests on intact samples at the Lekdijk and the Waaldijk are low compared to S_t from the FVT. For the Achterwaterschap the agreement is good.

6.12 Undrained shear strength ratio from field vane tests and triaxial tests

In this paragraph the undrained shear strength ratio of the intact natural soils is assessed based on the results of the triaxial compression tests on intact samples and the results of the field vane tests. The FVT results are corrected with the empirical corrections as discussed in Paragraph 4.8. For the triaxial compression tests on intact samples the ultimate values (25% axial strain) of s_u/σ'_{vi} are plotted. These obtained strength values from the FVT results and triaxial test results are to be conceived as operational shear strength in the context of slope stability.

As discussed in previous paragraphs the analysis is based on an estimation of the in situ effective stress. The in situ effective stress may deviate from the consolidation stress applied in laboratory testing, as in different projects different schematizations are made, with differences in estimates of the phreatic level and soil unit weight, as discussed before.

Figure 6.37 gives a comparison of the undrained shear strength ratio s_u/σ'_{vi} from the FVT and triaxial compression tests on intact samples at the Lekdijk near Schalkwijk. The figure shows much scatter. For some tests there is a good agreement between the FVT and triaxial test results. Most scatter occurs around NAP -2.5 m, around NAP -5.5 m and around NAP -6.5 m. The scatter around NAP -2.5 m and around NAP -5.5 m may be caused by heterogeneity as illustrated by the borehole descriptions. At short distance (about 3.0 m) differences in the soil profiles can be observed. The triaxial tests are performed on clay

samples. The FVT tests may be executed in somewhat more peaty clay material. Around NAP -6.5 m firm clay occurs, which may behave as a transitional soil, exhibiting dilative shear strength at full undrained conditions. As for transitional soils the initial density determines the shear strength this material may be sensitive for disturbances.

Between NAP -3.5 m and NAP -4.0 m also some deviations between the FVT results and triaxial compression test results can be observed. It is not clear what the reason for these deviations might be.

The boreholes for the current project as well as the borehole for the HDSR project are performed with the Ackermann sampling system with hammered samplers. Therefore it can be explained that the triaxial tests results of the present project and the HDSR project compare well.

As noticed earlier no relevant difference can be seen between the undrained shear strength ratios derived from triaxial tests on intact 67 mm samples and undrained shear strength ratios derived from triaxial tests on 50 mm samples which were damaged during transport.

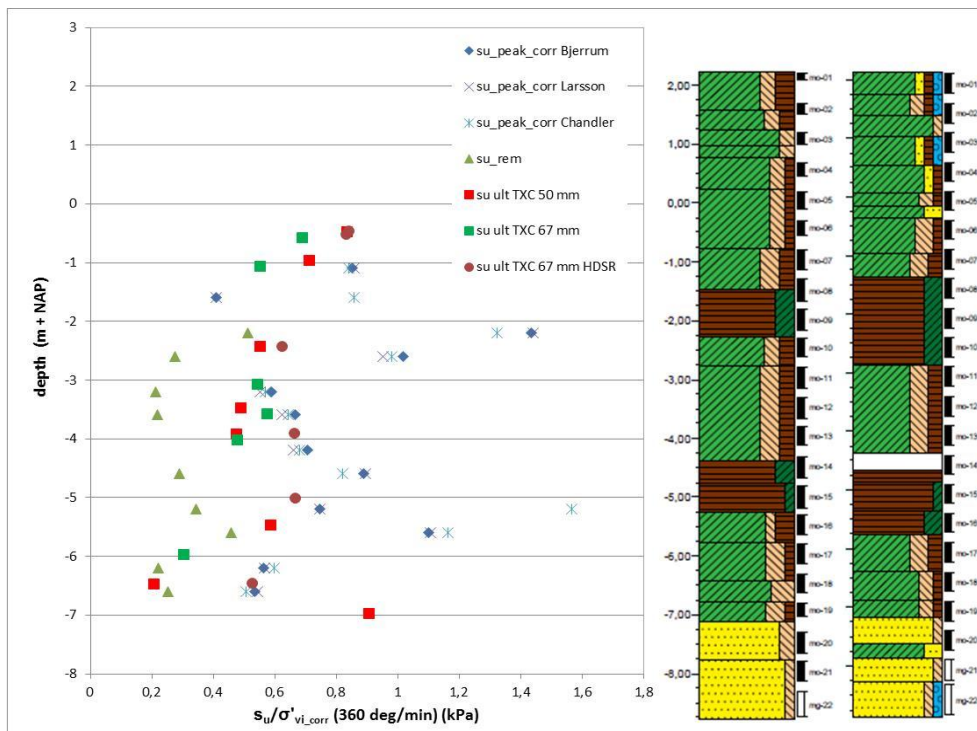


Figure 6.37 Comparison of s_u/σ'_{vi} from the FVT ($s_{u_peak_corr}$) and triaxial compression tests (TXC) on intact samples at the Lekdijk near Schalkwijk. The triaxial compression tests results agree reasonably well with the FVT results, except for the peat layers. For legend of the borehole descriptions see Appendix B.

Figure 6.38 compares the undrained shear strength ratios s_u/σ'_{vi} as derived from the FVT and from triaxial compression tests on intact samples for the Waaldijk at Waardenburg. This figure shows a reasonable agreement between the FVT and triaxial test results. For the results above NAP +1.5 m there are some differences. These differences can be caused by the fact that these samples are around and just above the phreatic level and close to the surface. Some of these samples can be partially saturated, and therefore result in high strength values.

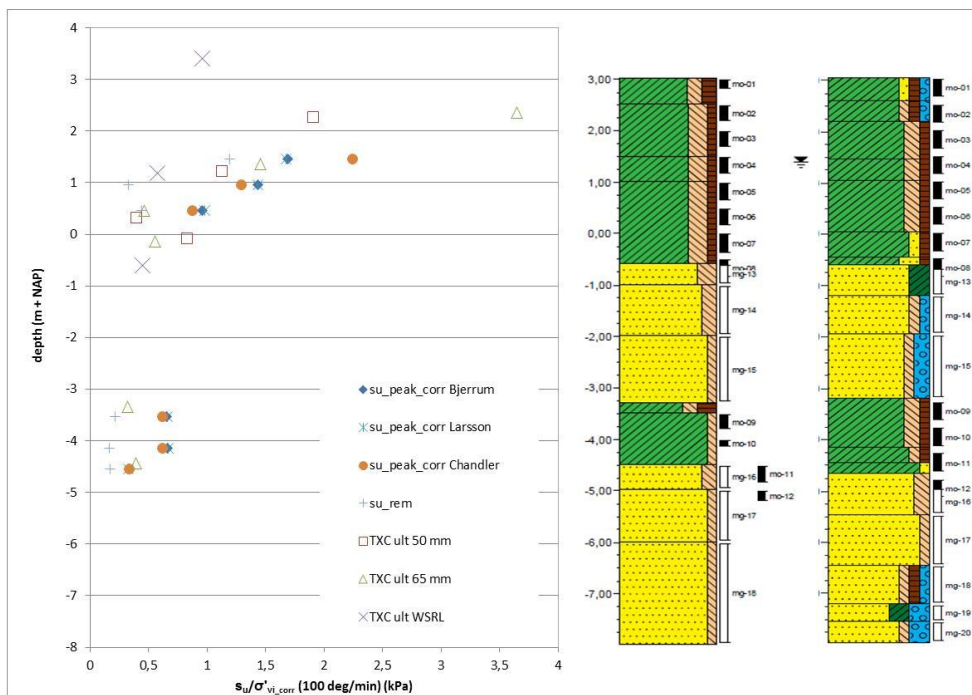


Figure 6.38 Comparison of s_u/σ'_{vi} from the FVT ($s_{u_peak_corr}$) and triaxial compression tests (TXC) on intact samples at the Waaldijk at Waardenburg. The triaxial compression tests results agree reasonably well with the FVT results. For legend of the borehole descriptions see Appendix B.

As reported earlier no substantial differences can be observed between the undrained shear strength ratios derived from triaxial tests on intact 67 mm samples and undrained shear strength ratios derived from triaxial tests on 50 mm samples which were damaged during transport.

For the measurement location at the Achterwaterschap near Alblasterdam Figure 6.39 gives the comparison of the undrained shear strength ratio s_u/σ'_{vi} from the FVT and triaxial compression tests on intact samples. At this site there is generally a good agreement between the corrected FVT results and the triaxial test results when using the ultimate shear strength. The triaxial test results from the WSRL project derived from 50 mm samples from Piston samplers agree well with the triaxial tests results from the present project.

Between NAP -2.20 m and NAP -4.50 m and at NAP -15.50 m there are some deviations between the FVT results and the triaxial tests results. At NAP -2.20 m and NAP -4.50 m the triaxial test results are very high compared to the FVT results. This can be caused by the peaty material, which may result in high undrained shear strength ratios for triaxial compression conditions. This is also indicated by the high friction angles of these triaxial tests ($> 50^\circ$). At NAP -15.50 m the triaxial tests results are low compared to the FVT results. At NAP -15.50 m this can be attributed to the transitional behaviour of the soil, as discussed for the Lekdijk case.

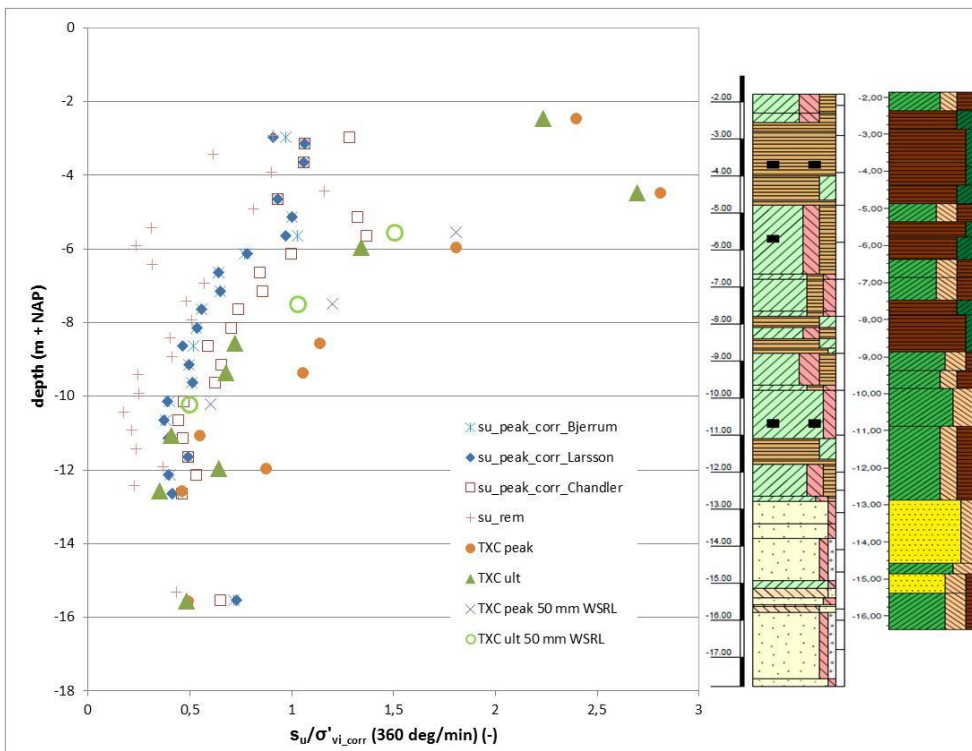


Figure 6.39 Comparison of s_u/σ'_{vi} from the FVT ($s_{u_peak_corr}$) and triaxial compression tests (TXC) on intact samples at the Achterwaterschap near Alblasserdam. The FVT and triaxial compression tests results are in good agreement. For legend of the borehole descriptions see Appendix B.

In Figure 6.40 the intact peak undrained shear strength ratios $s_{u,peak}/\sigma'_{vi}$ and residual shear strength ratios $s_{u,residual}/\sigma'_{vi}$ from the FVT and the ultimate state undrained shear strength ratios $s_{u,ultimate}/\sigma'_{vi}$ (25% axial strain) from the triaxial tests from the three measurement sites are collected and compared with each other. Regarding the FVT results the relevant corrections are applied. As mentioned before the intact peak undrained shear strength ratios $s_{u,peak}/\sigma'_{vi}$ from the FVT and the ultimate state undrained shear strength ratios $s_{u,ultimate}/\sigma'_{vi}$ from the triaxial tests are to be conceived as operational shear strength in the context of slope stability and can therefore be compared with each other.

The high intact peak undrained shear strength ratios from the FVT and the ultimate state undrained shear strength ratios from the triaxial tests compared to the residual undrained shear strength ratios from the FVT is the contribution of the structure of the soil to the shear strength due to various soil forming processes and creep.

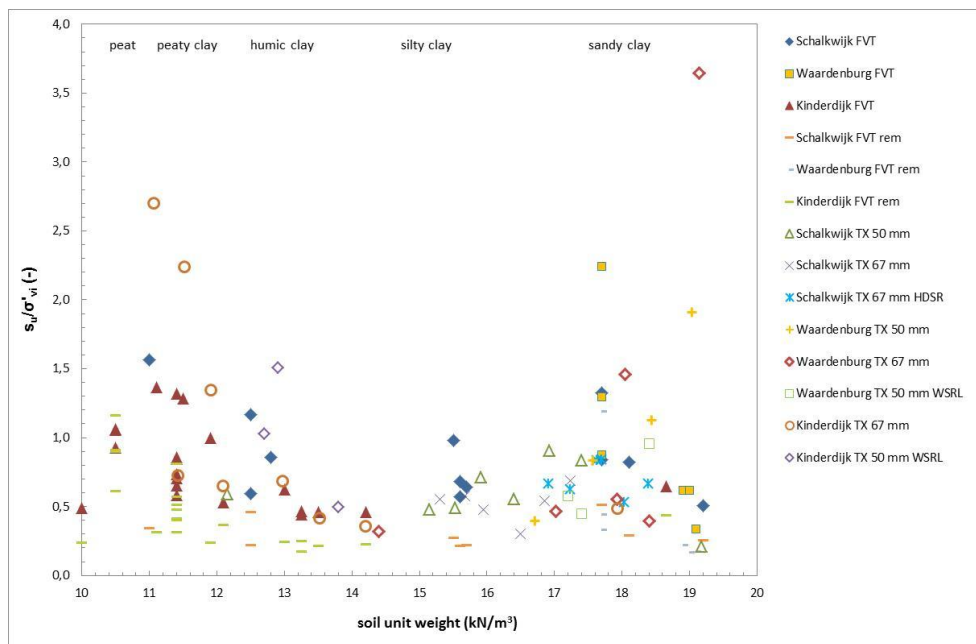


Figure 6.40 Comparison of s_u/σ'_{vi} from the FVT and triaxial tests (TX) for three sites. The FVT and triaxial compression test results compare very well for the soil unit weights between 10 and 15 kN/m^3 . For the higher soil unit weights the triaxial test results are on average relatively low compared to the triaxial compression test results.

Figure 6.40 gives a similar pattern as Figure 6.20 to Figure 6.23, where only the triaxial test results were presented. In all these figures high intact undrained shear strength ratios are present in the soil unit weight ranges between 10 and 13 kN/m^3 and around 17 and 18 kN/m^3 . In the range of soil unit weight between 13 kN/m^3 and 17 kN/m^3 the undrained shear strength ratios of the intact natural soils are relatively low, as also indicated by the triaxial tests in Figure 6.20 to Figure 6.23. The intact peak undrained shear strength ratios $s_{u,peak}/\sigma'_{vi}$ from the FVT result in a similar pattern with generally the same values.

The residual undrained shear strength ratio is relatively constant around 0.21 over a large range of soil unit weights. Higher values of the residual undrained shear strength ratio up to about 1.0 are measured in the range of the soil unit weight between 10 and 11 kN/m^3 . These data points belong to peaty material as can be seen in Figure 6.37 and Figure 6.39.

The triaxial test results of the Lekdijk and Waaldijk sites more often show relatively low $s_{u,ultimate}/\sigma'_{vi}$ values compared to the $s_{u,peak}/\sigma'_{vi}$ values from the FVT than the triaxial tests of the Achterwaterschap site. This trend is in agreement with the results based on S_t , as discussed in Paragraph 6.11 (see Figure 6.36). So there seem to be an effect of sample disturbance on the undrained shear strength as derived from the triaxial tests, especially for soils in the range of soil unit weight between 16 and 19 kN/m^3 . As already mentioned no relevant differences can be observed between $s_{u,ultimate}/\sigma'_{vi}$ obtained from triaxial tests on intact 67 mm samples and $s_{u,ultimate}/\sigma'_{vi}$ derived from triaxial tests on 50 mm samples which were damaged during transport.

Figure 6.41 and Figure 6.42 show the comparison of s_u/σ'_{vi} from the FVT and triaxial tests for three sites. s_u/σ'_{vi} is plotted versus plasticity index I_p and versus organic matter content OC respectively.

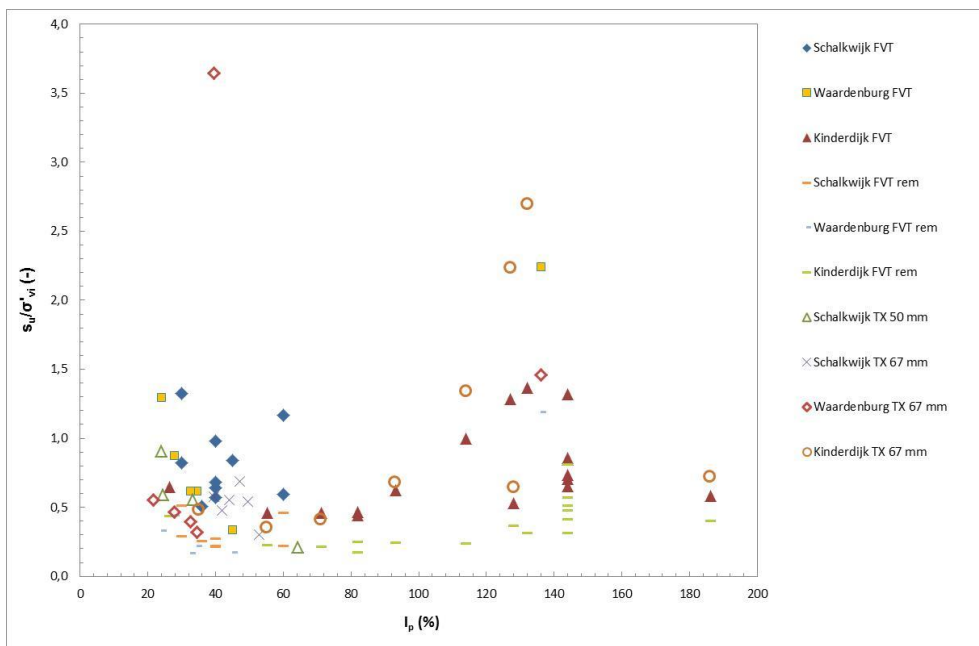


Figure 6.41 Comparison of s_u / σ'_{vi} versus plasticity index I_p from the FVT and triaxial tests (TX) for three sites.

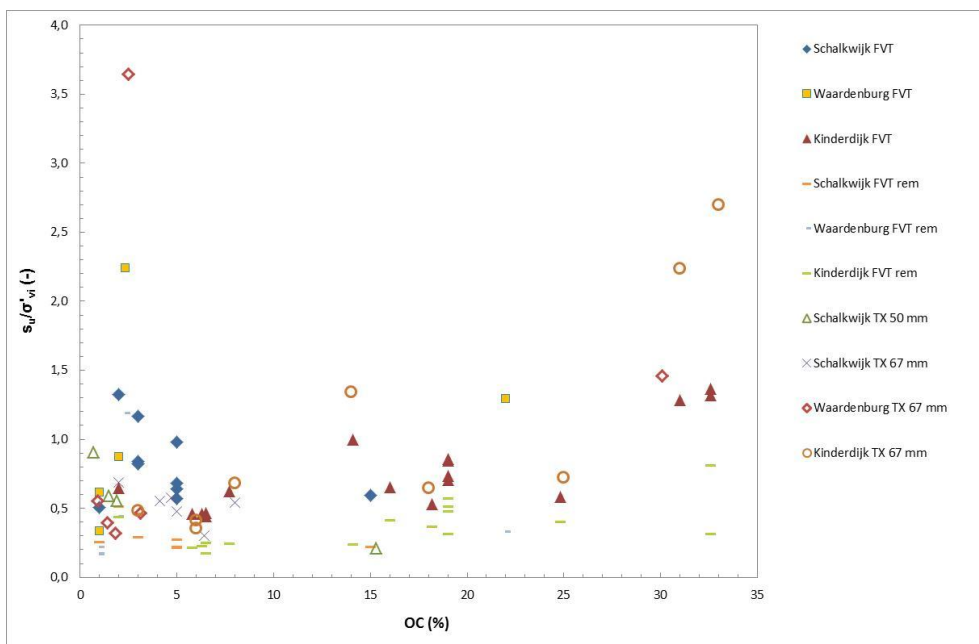


Figure 6.42 Comparison of s_u / σ'_{vi} versus organic matter content OC from the FVT and triaxial tests (TX) for three sites.

6.13 Effect of natural variability

In this paragraph the undrained shear strength s_u as derived from the FVTs and triaxial tests is combined with estimations of s_u from the CPT data in order to determine whether the deviations between s_u from the FVTs and s_u from the triaxial tests on intact samples, which might be caused by sample disturbance, are relevant compared to spatial variability of s_u . For each research site CPT data is plotted from CPTs which are conducted within a very short distance of some meters from the FVTs and boreholes.

The CPT readings are averaged over 15 cm as this is approximately the same size as samples for triaxial tests and the FVT blade. Per research site a N_{kt} value is estimated which gives on average a good agreement of the CPT data with the FVT data and triaxial test data.

The FVT results are presented with errors bars with two times the standard deviation caused by the uncertainty of the required adjustment of the FVT results to the operational undrained shear strength in the field according to Azzouz et al. (1983) (see Paragraph 4.8).

Figure 6.43 gives the comparison of s_u derived from FVT, CPT and triaxial tests for the Lekdijk site. A N_{kt} value of 15 is chosen for all CPTs. The distance between FVT and boreholes is 2.9 m and 6.6 m. The distance between the four CPTs and FVT is 4.2 m (dykecone D-15) to 5.8 m. The distance between the four CPTs and boreholes is 1.8 m to 3.8 m. The in-between distance of the four CPTs is about 1.3 to 1.9 m.

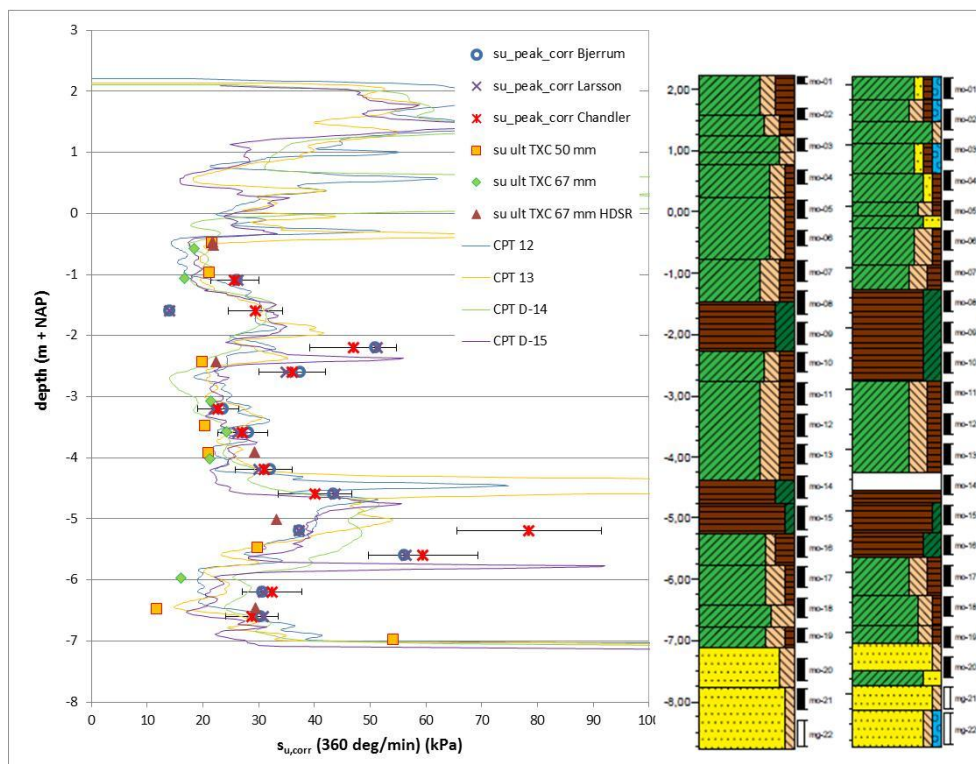


Figure 6.43 Comparison of s_u derived from FVT (su_peak_corr), CPTs and triaxial tests (TXC) for the Lekdijk site. The deviations between the FVT results and triaxial compression test results largely fade away when considering spatial variability as deduced from the CPT results. For legend of the borehole descriptions see Appendix B.

For most FVT and triaxial test results it yields that they fall nicely within the bandwidth of the estimated s_u from the CPTs. The deviations between FVT and triaxial test results also fade away when considering the natural variability as deduced from the CPT results. The differences in s_u based on the CPTs are up to about a factor 1.4 to 1.7 measured on the same reference level.

Most scatter occurs around NAP -2.5 m, around NAP -5.5 m and around NAP -6.5 m as already discussed in the previous paragraph.

The FVT, CPT and triaxial test results of the Waaldijk site are compared in Figure 6.44. For this case the correlation factor N_{kt} is 13. The distance between the four CPTs is about 0.9 to 1.7 m. The distance between the CPTs and FVT is between 3.72 m (dykecone D-03) and 4.95 m. The distance between the FVT and the two boreholes is 2.60 m and 5.60 m.

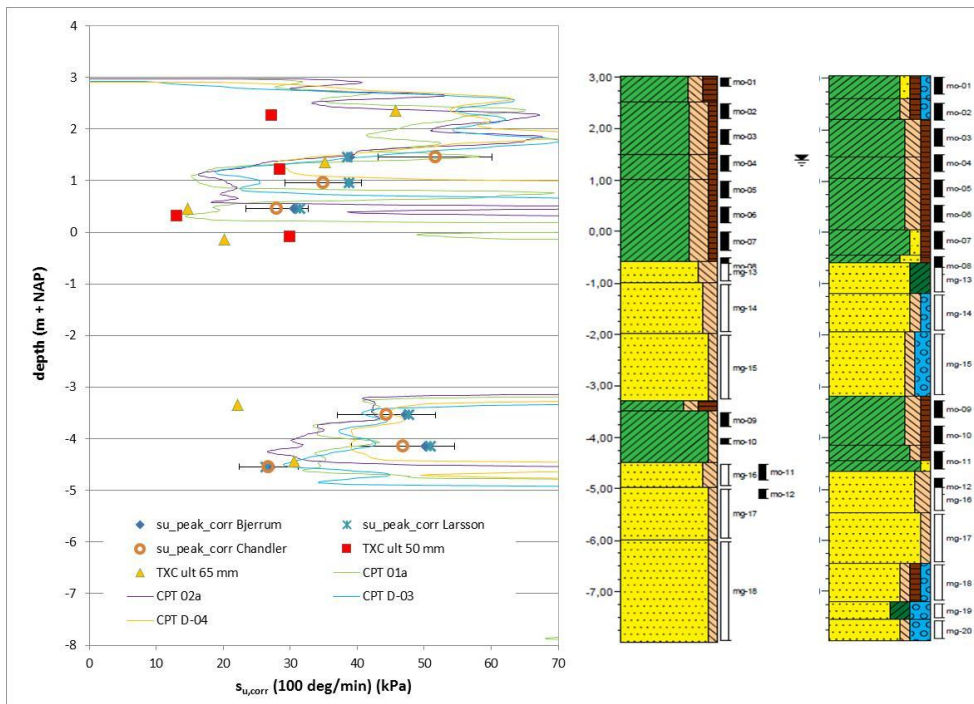


Figure 6.44 Comparison of s_u derived from FVT (su_peak_corr), CPTs and triaxial tests (TXC) for the Waaldijk site. The differences between the FVT results and triaxial compression test results can for a large part be traced back to spatial variability as derived from the CPTs. For legend of the borehole descriptions see Appendix B.

At the Waaldijk site the most striking result is the top of the Holocene sand layer between NAP +1.00 m and NAP +0.20 m. In the four CPTs the top of this sand layer varies considerably. Consequently the FVT and triaxial test results give scatter compared to the CPT results.

Considering the natural variability for this site a reasonable agreement between FVT, CPT and triaxial tests results is found. Some poor triaxial tests results are found at NAP +2.25 m for a 50 mm sample and at NAP -3.30 m for a 65 mm sample.

For the Achterwaterschap AC 251 research location $N_{kt} = 19$ is chosen to compare the CPT readings with the FVT and triaxial tests results. At this site the distance between the FVT and borehole is 1.9 m. The distance between the CPTs and FVT is between 0.5 m (dykecone D-117) and 2.7 m. The distance between the CPTs and boreholes is 2.3 m to 3.9 m. The in-between distance of the CPTs about 0.8 to 4.6 m. The comparison of s_u derived from FVT, CPTs and triaxial tests for the Achterwaterschap AC 251 site is presented in Figure 6.45.

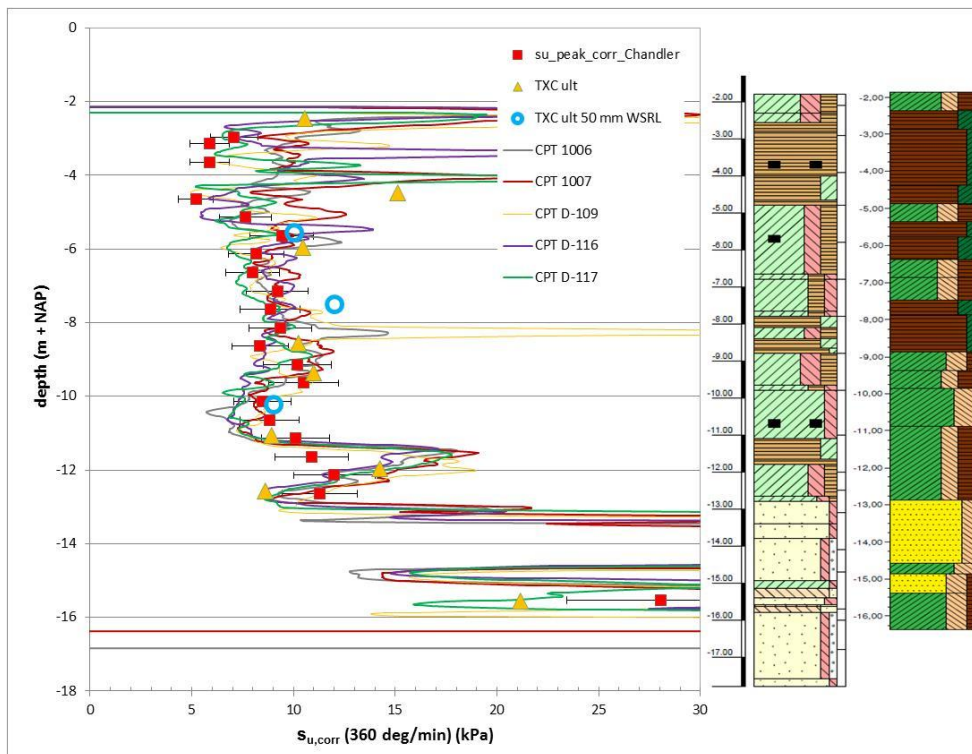


Figure 6.45 Comparison of s_u derived from FVT ($s_{u_peak_corr}$), CPTs and triaxial tests (TXC) for the Achterwaterschap AC 251 site. Considering spatial variability of the shear strength as deduced from the CPTs the deviations between the FVT results and triaxial compression test results can be explained very well. For legend of the borehole descriptions see Appendix B.

The comparison for the Achterwaterschap site also shows that an important part of the deviations between s_u from the FVT and s_u from the triaxial tests can be explained by spatial variability of s_u as deduced from the CPT results. Differences of up to 20% in s_u between the FVT and triaxial tests can be traced back to spatial variability on the meter scale. For this site no indications for sample disturbance are found. So in this case the deviations between s_u from the FVT and s_u from the triaxial tests are thought to be completely the result of spatial variability.

Note that the differences in s_u as obtained from the CPT readings can be very large. In the peaty layers these differences can be a factor of 2 at the same reference level. For the clayey layers these differences are up to a factor of 1.5.

Poor results are found for peaty material at NAP -3.0 m to NAP -5.0 m and at NAP -11.5 m. The relatively low FVT values are corrected with $\mu = 0.5$, which may be too high for this material.

7 Discussion

7.1 Natural variability

The analysis of the CPT data at three locations along the Achterwaterschap shows a large variability in the stratigraphy. Within the same lithological units there is a large variability in the cone penetration resistance. This is the case for the variability in vertical direction within the CPT's as well as for the variability in horizontal direction as derived from the means of the cone penetration resistances of the CPT's within a soil layer. Continuous very soft lithological units are not observed in the data at the three locations along the Achterwaterschap. Many 'outliers' are identified in the cone penetration resistances. These outliers are attributed to fragments of wood in the peat and humic clay layers.

The corrections and normalisation of the CPT data have an important effect on the cone penetration resistances. The coefficient of variation of the corrected cone penetration resistance q_{net} and normalised cone penetration resistance Q_t is much larger than the coefficient of variation of the measured cone penetration resistance q_c . The corrections and normalization will affect the results of the analyses. However the coefficient of variability of the class 1 cone and the class 1+ cone are comparable. So the effect of the uncertainty about stratigraphy when interpreting the class 1+ data seems to be as large as the effect of the differences in measurement accuracy between the class 1 cone and the class 1+ cone. However, the uncertainty about the variability in soil unit weight and pore water pressure within the soil layers affect the analysis of CPT data from both class 1 cone and class 1+ cone.

Correlation lengths between 3 and 33 m are found based on the measured cone penetration resistances q_c from the class 1+ CPT's using the correlation function. The correlation length varies for different soil types but also for the same soil type the correlation length is variable. This is the same with the coefficient of variation of the cone penetration resistance. So the variability within a certain depositional environment is likely to be variable enough to result in very different degrees of variability from one location to another. For peat layers the correlation length is generally shorter than for clay layers. This can be expected based on the very different genesis of these soils; clay layers are a result of sedimentary processes in a certain depositional environment and peat layers are the remains of plants of different species.

Calculating the variance reduction factor I^2 based on the horizontal correlation length (3 - 33 m) as determined for the measured cone penetration resistance q_c results in values between 0.04 and 0.44, with an average value of 0.19. As the horizontal correlation length is calculated based on the mean values of the cone penetration resistances per soil layer and per CPT this variance reduction factor I^2 accounts for the local averaging of the horizontal fluctuation of the cone penetration resistance on the scale of a potential slope instability. Although the approach of TAW (2002) and Calle (2007) differs from the approach of Vanmarcke (1977) the range of the calculated variance reduction factors compare very well with the recommended variance reduction factor I^2 of 0.25 in TAW (2002). Considering that the CPT data at the three locations are local data on the scale of a potential slope failure these results are higher than the variance reduction factor of 0 in TAW (2002).

Using the normalised cone penetration resistance Q_t the calculated horizontal correlation lengths are relatively short (3 - 13 m). Consequently the variance reduction factor (0.04 - 0.17) is lower than the variance reduction factor based on the measured cone penetration resistance q_c . These results may be influenced by the interpretation, corrections and normalisation as mentioned before. On the other hand the normalised cone penetration resistance Q_t is theoretically a more decent parameter to calculate the correlation length and coefficient of variation, because of the corrections and the normalization which removes trends.

7.2 Sample disturbance

The undrained shear strength ratio and sensitivity are derived from FVT, triaxial tests and constant rate of strain tests in order to find out whether sample disturbance plays a role on parameter determination and on the derivation of the empirical correlation factor N_{kt} .

Indications that sample disturbance occurs could also be derived from the recovery ratio and the differences of sample length and soil unit weight in the field and in the laboratory before and after extrusion of the samples. For the Achterwaterschap site the recovery ratio is 1.0, but for the other two sites the average recovery ratio is 0.85 at the Waaldijk and 0.94 at the Lekdijk. Regarding the soil unit weight it is observed in Paragraph 6.5 that soil unit weight shows a high uncertainty. This uncertainty is partly attributed to natural variability of the soil. However, variability of the measured soil unit weight is also caused by volume changes of the samples due to sampling and extrusion of the samples in the laboratory. Sampling as well as extrusion of the samples sometimes requires much energy, which may cause volume changes of samples. Measurement errors may also play a role in the determination of soil unit weight. The volume changes of the samples imply up to about 7% change of the length of the samples. These large volume changes suggest that samples will be disturbed. These changes of the volume are not systematic, but vary strongly per sample.

Undrained shear strength ratio

Concerning the undrained shear strength ratio $s_{u,ultimate}/\sigma'_{vi}$ the results of the triaxial tests on intact samples generally agree reasonably with the FVT results. The triaxial test results of the Lekdijk and Waaldijk sites more often show relatively low $s_{u,ultimate}/\sigma'_{vi}$ values compared to the $s_{u,peak}/\sigma'_{vi}$ values from the FVT than the triaxial tests of the Achterwaterschap site. This trend is in agreement with the results based on S_t , as discussed in Paragraph 6.11 (see Figure 6.36). So there seems to be an effect of sample disturbance on the undrained shear strength as derived from the triaxial tests, especially for soils in the range of soil unit weight between 16 and 19 kN/m³. In this analysis the ultimate state undrained shear strength ratio from the triaxial tests is compared with the peak undrained shear strength ratio of the FVT, applying corrections for strain rate effects and empirical corrections to adjust the FVT results to operational shear strengths which refer to field conditions.

The triaxial test results show uncertainty when normalizing the results for effective stress level. As in the present study results from other projects are included and also in the present project uncertainty about the soil unit weight appeared, the normalization for effective stress level caused discrepancies when using the applied consolidation stresses from the various projects. When using the estimated in situ effective stress these discrepancies could be partly rectified. The estimated in situ effective stress can deviate from the applied consolidation stresses with a factor of 2, at least for the Achterwaterschap near Alblusserdam with the low effective stresses. It must therefore be emphasized that the determination of the in situ effective stress is very sensitive for estimates of soil unit weight and phreatic level.

In this study it is found that no substantial differences appear between the undrained shear strength of samples from Ackermann sampling system with pushed tubes as well as hammered tubes for intact samples and for intact samples which were injured during transport. Because of the damage of some samples these samples are trimmed to 50 mm diameter. Intact samples from an additional borehole are tested with 65 mm diameter. Both series of triaxial tests give on average the same results. It is difficult to understand what the consequences of these findings are, however it seems that these findings are in contradiction to the results of Hight et al. (2003), see Paragraph 2.2.3. It might be the case that trimming the damaged samples was sufficient to get good quality samples for the triaxial tests. Alternatively it can be hypothesized that both series of samples are equally disturbed due to sampling and extrusion of the samples in the laboratory.

Strength sensitivity and stress sensitivity

Regarding the strength sensitivity S_t the agreement between the results from the triaxial tests on intact samples and the results from the FVT is poor. This disagreement is assumed to be

caused mainly by the uncertainty of the remoulded shear strength as derived from the triaxial tests on reconstituted samples. The undrained shear strength ratio from the reconstituted samples shows large variability as discussed in Paragraph 6.6. The mean value and the variability of the remoulded shear strength from the reconstituted samples are however in line with the findings of Chandler (2000). The interpretation of the FVT as discussed before may also introduce some uncertainties in the determination of the sensitivity.

The derivation of the stress sensitivity S_σ from constant rate of strain tests using the sensitivity framework and normalisation with the void index according to Burland (1990) and Chandler (2000) leads to relatively low stress sensitivities compared to the strength sensitivities. The stress sensitivity appears to be uncertain due to uncertainties of the determination of the void ratio, intrinsic compression index C_c^* and void ratio e_{100}^* . To determine the void ratio various methods are available as discussed in Paragraph 4.3. These methods give considerably different results. The intrinsic compression index C_c^* and e_{100}^* are uncertain too, because the correlations as discussed in Paragraph 6.9 have uncertainty. Additionally it may be the case that the intrinsic void ratio e_{100}^* is not a truly intrinsic parameter contrary to Burland (1990). Cerato et al. (2004) showed that the void ratio e_{100}^* may depend on the initial water content of the reconstituted sample. According to these authors the clay mineralogy and the corresponding soil properties may influence the degree to which the initial water content affects the void ratio e_{100}^* . As a consequence the uniqueness of the ICL is questionable.

Uncertainties field vane tests

The FVT and the concerning corrections introduce uncertainties. The FVT measurements have some uncertainty as the tests with different rotation rates did not result in a distinct relation between shear strength and rotation rate. Possibly the natural variability of the shear strength of the soil is more important than the variation of the rotation rate, as can be deduced from Figure 6.11 and Figure 6.12. Additionally the assessment of the drainage conditions of the FVT results with different rotation rates as discussed in Paragraph 6.4 is not fully clear, as there are two approaches in literature for this assessment. In this study the very high rotation rate of 360 degrees per minute combined with a very short waiting time after insertion of the vane is chosen as the test set up which with certainty results in undrained behaviour, because only this test set up could be assessed as undrained according to both approaches. This rotation rate is much higher than the standard rotation rate of 6 degrees per minute and the waiting time much shorter than recommended in the ISO and ASTM codes. The fast rotation rate requires a correction for strain rate effects, which causes additional uncertainty (see Figure 4.3).

The correction for strain rate effects from Biscontin & Pestana (2001) and Schlue et al. (2010) is not verified for Dutch soils, and might therefore be different for Dutch soils. The empirical corrections have a substantial bandwidth as shown in Paragraph 4.8. Furthermore the empirical corrections rely on plasticity index and liquid limit, which are variable within a soil layer (see Paragraph 6.2). Especially for peat the corrections are uncertain.

The coefficient of consolidation as derived from the dissipation tests can also attribute to this FVT uncertainty, as discussed in Paragraph 6.3. At the Lekdijk near Schalkwijk the dissipation tests very often started with very low normalized excess pore water pressures. At the Achterwaterschap near Alblasserdam this phenomenon occurred sometimes. This pattern of the dissipation tests disagrees with the theory as discussed in Paragraph 4.7. Possibly these low values of the normalized excess pore water pressures were caused by desaturation of the porous filter or the chamber behind the filter or pollution of the porous filter by soil particles. As the pore water pressure measurements performed better at Alblasserdam compared to Schalkwijk the dry top layer at Schalkwijk might have influenced the performance of the sensor. This phenomenon of increasing excess pore water pressures at the start of the dissipation tests is also observed by Colreavy et al. (2016) and Carroll et al. (2018). Carroll et al. (2018) performed dissipation tests in a natural silty soil and they also found an increase in excess pore water pressure at the start of some of their tests. In their

tests the increase of pore water pressure occurred within about 20 seconds, whereas in the present project the increase takes about 2 minutes. In this case the difference in time span of the excess pore water pressure increase can be attributed to the different permeabilities of the soils. Colreavy et al. (2016) also found an increase in excess pore water pressure in the first 20 seconds of their dissipation tests. As these tests are conducted in soft clay the permeability of the soil seem to be not the complete explanation of this feature. Colreavy et al. and Carroll et al. suggested that the increase of excess pore water pressure might be caused by pore water pressure redistribution around the cone tip and shoulder. In spite of these uncertainties the derived values of the coefficient of consolidation are deemed to be in the right order of magnitude, as it is expected that the coefficient of consolidation in the field is large compared to laboratory conditions. Therefore the obtained coefficients of consolidation are applied for the FVT interpretations.

Effect of sample disturbance on undrained shear strength and strength sensitivity

Notwithstanding the uncertainties as discussed in this paragraph the agreement between the ultimate state undrained shear strength ratio (25% axial strain) from triaxial tests on intact samples and the peak undrained shear strength ratio from the FVT with corrections to adjust the measured undrained shear strength to the operational undrained shear strength in the field is generally reasonable. There are some exceptions at the Waaldijk and Lekdijk site as mentioned above and discussed in Chapter 6. These exceptions concern often the transitional soils. The triaxial tests results for these soils are often relatively low compared to the FVT results. These transitional soils exhibit dilative shear strength behaviour at fully undrained conditions. As for transitional soils the undrained shear strength depends on the initial density (see Paragraph 4.5) this material may be sensitive for disturbances. However, as the spatial variability of the shear strength on the meter scale is substantially as discussed in Paragraph 6.13, it is difficult to distinguish between sample disturbance and spatial variability. For the Achterwaterschap site the agreement between the results of the triaxial tests and FVT is good. These different results for de Lekdijk and Waaldijk at the one hand and the Achterwaterschap on the other hand corresponds with the findings regarding the recovery ratio.

An interesting result of this study is the pattern of the intact undrained shear strength ratio and strength sensitivity versus soil unit weight. High undrained shear strength ratios are present in the soil unit weight range between 10 and 13 kN/m³ and around 17 and 18 kN/m³. In the range of soil unit weight between 13 kN/m³ and 17 kN/m³ the undrained shear strength ratio of the intact natural soils are relatively low. The same holds for the strength sensitivity. It can be argued that the low clay content and low organic matter content in the range of soil unit weight between 13 kN/m³ and 17 kN/m³ causes the small difference between peak undrained shear strength ratio and remoulded shear strength ratio. In the soil unit weight range between 10 and 13 kN/m³ the clay content and organic matter content are higher. Therefore this material is more susceptible for soil forming processes and creep. In the soil unit weight range around 17 and 18 kN/m³ dilative shear behaviour causes the high undrained shear strength ratios.

7.3 Implications

Regarding the objective of this research several implications from this research for the geotechnical engineering practice and the WBI 2017 approach for the assessment of slope stability can be mentioned.

The present WBI 2017 approach is to estimate the local undrained shear strength based on only one local CPT, with the characteristic lower bound value about 35% lower than the mean value, mainly due to transformation uncertainty (Deltares, 2014). In this research the variation in cone penetration resistance within the rows of CPTs at the Achterwaterschap sites is larger than 35%. This means that the characteristic lower bound of a relatively high cone penetration resistance in one CPT can be higher than the mean value based on a larger

number of CPTs. A relatively low cone penetration resistance in one CPT can be much lower than the characteristic lower bound based on a larger number of CPTs.

Related to the failure mechanism of slope instability of a dike, where the size of a potential slip surface is in the order of 30 to 100 m, and the horizontal correlation length is 3 to 33 m as found in this research (Paragraph 5.5), one CPT is not enough to determine a reliable mean and standard deviation of the shear strength on the scale of a potential slope instability. A second CPT close to the first one can give a very different result for the stratigraphy and cone penetration resistance. For a reliable estimation of the undrained shear strength of a dike section the characteristic lower bound of the cone penetration resistance has to be derived from a series of CPTs within the dike section.

Interpretation of the CPTs and measurement accuracy also determine the variation of the derived stratigraphy, coefficient of variation of the cone penetration resistance and correlation length. When interpreting CPTs there are always difficulties because the information from CPTs is limited. Insufficient information on soil unit weight and pore water pressure for example can have a large influence on the results of the interpretation.

The spatial variability of the shear strength on the meter scale is also relevant. The differences in s_u based on CPTs with a distance of some meters are up to about a factor 1.4 to 2.0, measured on the same reference level (see Paragraph 6.13). These differences in shear strength will also occur when cone penetration resistances from CPTs are correlated to the undrained shear strength from triaxial tests to derive the correlation factor N_{kt} . These differences in shear strength should not be interpreted as transformation uncertainties of the empirical correlation factor as discussed in Paragraph 2.1, as this will lead to conservative estimations of the undrained shear strength when applying the correlation.

The spatial variability of the shear strength on the meter scale seems to mask effects of sample disturbance on the shear strength. In this research a number of indications of sample disturbance are discussed. Especially transitional soils with soil unit weight between 16 and 19 kN/m³ seem to be susceptible for sample disturbance (see Paragraph 6.12), probably because the undrained shear strength of these soils depends on the in situ void ratio, which might be disturbed by sampling. The determination of soil unit weight is also affected by sample disturbance, as discussed in Paragraph 6.5. For these reasons improvement of the Ackermann sampling technique is desirable.

As there are many uncertainties concerning the interpretation of tests and determination of parameters are encountered in this research, it will be helpful to use cross checks in the derivation of the shear strength from field and laboratory tests. In geotechnical engineering practice and the WBI 2017 approach for the assessment of slope stability it is not common to apply cross checks. The Field Vane Test is potentially a useful test to determine the in situ undrained shear strength to be able to verify the results from laboratory tests. When applying the FVT attention has to be given to the drainage conditions of the FVT and the several corrections as described in Paragraph 4.8 and discussed in the previous paragraph. To be able to determine the drainage conditions of the FVT accurately, improvement of the dissipation test is required as discussed in the previous paragraph.

8 Conclusions

The uncertainties of the shear strength of the subsoil due to spatial variability in horizontal direction and sample disturbance are quantified in this research.

The variability of the stratigraphy and cone penetration resistance is found to be considerably. The horizontal correlation length of the cone penetration resistance varies for different deposits and varies also for the same deposit at three locations. The correlation length has been found to be relatively short compared to the scale of a slope failure of a dike. It has to be concluded that one CPT on the scale of a slope failure is only a random sample of the stratigraphy and cone penetration resistance. Therefore the characteristic lower bound of the cone penetration resistance for a dike section has to be derived from a series of CPTs. The variability of the stratigraphy and cone penetration resistance is also very large for CPTs which are carried out within a distance of some meters.

There are a number of indications that sample disturbance occurs during sampling and handling of the samples. Recovery ratios smaller than one and relevant changes of sample volumes occurred due to sampling and extrusion of the samples. Sampling as well as extrusion of the samples sometimes requires much energy, which may cause volume changes of samples. These volume changes affect the determination of the soil unit weight.

Strength sensitivity S_t for the Lekdijk and the Waaldijk shows that S_t from the laboratory tests on intact samples is about a factor 1.5 lower than S_t from the FVT. This disagreement of S_t is deemed to be caused by uncertainties about the remoulded shear strength from triaxial tests on reconstituted samples. Another cause could be the uncertainties on the interpretation of the FVT. For the Achterwaterschap the agreement is good.

The analysis of the undrained shear strength ratio s_u/σ'_v shows that the results of the triaxial tests on intact samples generally agree reasonably with s_u/σ'_v from the FVT results. The triaxial test results of the Lekdijk and Waaldijk sites more often show relatively low $s_{u,ultimate}/\sigma'_{vi}$ values compared to the $s_{u,peak}/\sigma'_{vi}$ values from the FVT than the triaxial tests of the Achterwaterschap site. These exceptions often concern transitional soils, which may be sensitive for sample disturbance as the in situ void ratio determines the undrained shear strength.

The low recovery ratios and volume changes due to sample disturbance are very variable per sample and the undrained shear strength ratios from triaxial tests on intact samples agree mostly reasonably well with the undrained shear strength ratios from the FVT and CPTs. The undrained shear strength varies considerably on the meter scale as mentioned above. These points may indicate that the effect of sample disturbance on the undrained shear strength might be relatively small or the effect of sample disturbance cannot be easily distinguished from the spatial variability of the undrained shear strength.

As the spatial variability of the undrained shear strength on the meter scale is large, it is important to quantify this variability when the empirical correlation factor N_{kt} between the undrained shear strength based on laboratory tests and the cone penetration resistance has to be determined. Considering the spatial variability of the undrained shear strength on the meter scale will lead to an optimization of the characteristic lower bound of the undrained shear strength.

Application of cross checks and improvement of the Ackermann sampling technique will help to improve the reliability of assessments of slope stability of dikes. The FVT can be used for cross checks for the determination of the in situ undrained shear strength. Especially for transitional soils the use of the FVT and improvement of the Ackermann sampling technique will be important.

9 Recommendations

9.1 Natural variability

Based on the observations at the three locations at the Achterwaterschap it is recommended to calculate the characteristic lower bound of the shear strength from a series of CPTs. This series of CPTs represent the variability of the soil much more than one CPT.

When taking the common practice of distances between CPTs as starting point it is recommended to derive the characteristic lower bound of the shear strength from a series of CPTs. These series of CPTs can belong to a dike section or a WBI-SOS segment for example. At least 5 to 10 CPTs have to be combined for the calculation of the characteristic lower bound of the shear strength.

For the assessment of slope stability the extreme values of the shear strength on a potential slip surface are not important but the average strength is important. Therefore the uncertainty of the shear strength can be reduced by accounting for averaging of the uncertainty. The variance reduction factor $\Gamma^2 = 0.25$ from TAW (2002) is recommended as this research generally confirms the suggested values in TAW (2002).

For the statistical analysis to calculate the characteristic lower bound value the corrected cone resistance q_{net} or the normalised cone resistance Q_t can be used. The cone resistance Q_t is normalised for the vertical effective stress. Using the normalised cone resistance Q_t makes it possible to apply straightforward statistical analysis. When using the corrected cone resistance q_{net} the least squares method can be applied to derive the characteristic lower bound values of the relationship between effective stress and corrected cone resistance.

Local optimization

In some cases it is desired to optimize the shear strength of a dike section. Carrying out a series of CPTs can be helpful. The number of CPTs and the distance between the CPTs has to cover the scale of a potential slip surface. This local set of CPTs can be used to calculate a local value of the characteristic lower bound of the shear strength. For this local characteristic value it is allowed to apply the variance reduction factor $\Gamma^2 = 0$ according to TAW (2002).

Optimization of variance reduction factor

In special situations it may be helpful to optimize the variance reduction factor Γ^2 for regional sets of CPT data. Optimization of the variance reduction factor may result in a smaller distance between the mean value of the shear strength and the characteristic lower bound. As illustrated in this study the analyses and the interpretation of the results of the analyses are not straightforward. To optimize the variance reduction factor it is recommended to:

- Perform some series of CPTs at different locations in a project. One series of CPTs has to consist of 5 to 10 CPTs and the distance between the CPTs has to be in the order of 5 m.
- Before performing the Series of CPTs carry out the regular CPTs for the site investigation. Based on the regular CPTs the locations for the series of CPTs can be chosen. To choose the locations of the series of CPTs it is recommended to use as much as possible geological data: WBI-SOS, DINO, and geological maps.
- For the interpretation of the CPTs it is helpful when information of the soil unit weight and pore water pressure is available. This information improves the reliability of the CPT interpretation.
- Based on the regular CPTs the regional variance of the cone penetration resistance can be calculated. The local variance of the cone penetration resistance can be calculated from the series of CPTs. From the series of CPTs also the correlation length can be calculated.

- It is recommended to apply various statistical methods to calculate the correlation length. Preferably the correlation length will be not only determined with the common correlation function, but also with more complex approaches such as Bayesian approach or Maximum Likelihood. These more complex approaches may give more distinct results.
- Based on the ratio of the local variance of the cone penetration resistance and regional variance of the cone penetration resistance the variance reduction factor can be calculated. Calculation of the variance reduction factor is also possible from the correlation length. It can be assumed that the variance reduction factor is the same for s_u , S , m , POP/OCR. It seems to be likely that spatial variability of these parameters result from variability of the basic soil properties, such as clay content and organic content.
- With the results of the previous steps the characteristic lower bound of the shear strength can be calculated. Again the corrected cone resistance q_{net} or the normalised cone resistance Q_t can be applied. In this step averaging of the uncertainty is applied based on the optimized variance reduction factor Γ^2 .

Further research

As this research demonstrates the various uncertainties in processing the CPT data, it is recommended to perform additional research with field and laboratory tests to obtain additional information regarding the variability of soil layers. This research can include boreholes with determination of soil unit weight and organic content and plasticity index or field vane tests. Soil unit weight can be used to improve the analyses of the CPT data in this research. Organic content and plasticity index can be used to determine the variance ratio and correlation length based on these parameters. The advantage of the latter parameters is that they are simple parameters without complex interpretation and they are not susceptible for sample disturbance. However, they give no information about the variability of the state (overconsolidation ratio) of the soil. Field vane tests can also be used to calculate the variance ratio and correlation length. Field vane tests give a direct measure of the undrained shear strength without effects of sample disturbance. As they measure the in situ strength the measurements include the variability of the state of the soil.

9.2 Sample disturbance

In this research it is found that spatial variability is considerably, also on the small scale of several meters. For the engineering practice it is recommended to conduct two or three CPTs near a borehole where samples are taken to determine N_{kt} . Based on the spatial variability between the CPTs the effect of spatial variability on N_{kt} can be taken into account for the derivation of N_{kt} . This will prevent for an overestimation of the transformation uncertainty of N_{kt} .

As various factors can be identified which contribute to the uncertainty of N_{kt} it is very important that the derivation of N_{kt} is carried out carefully. Schematization issues such as the determination of soil unit weight and the assessment of the phreatic level and pore water pressure distribution are very important. It is recommended to use cross checks in the process of the analyses to obtain N_{kt} . The application of the FVT makes it possible to apply cross checks, as the FVT gives an independent measure of the undrained shear strength. These results can be compared with results of laboratory tests. When discrepancies are identified, the analysis has to be adjusted. In this process the cross check will also act as an incentive to improve the quality of sampling and laboratory tests. So, these cross checks will improve the derivation of N_{kt} and therefore also the assessments of flood defences.

Further research

The results of this research indicate that sample disturbance cannot generally be qualified as an important factor which affects the uncertainty of the empirical correlation factor N_{kt} . Conversely it seems to be likely that a large number of factors have an influence on the uncertainty of N_{kt} . Therefore it is recommended to perform an extensive analysis of all the contributing factors to the uncertainty of N_{kt} in order to quantify their influence and whether these factors are systematic or random. The systematic or random character of these contributing factors determine whether they have to be accounted for in the calculation of the characteristic value of the undrained shear strength and yield stress.

Soil unit weight is found to be an uncertain parameter in this research. This is partly caused by natural variability. Changes in the volume of the soil samples are also an important factor on the uncertainty of soil unit weight. Therefore it is recommended to investigate whether an approach can be developed to determine the soil unit weight in situ with sufficient accuracy. As soil unit weight is a very important parameter in geotechnical analyses, accurate information about the soil unit weight is essential. Such an approach can also be helpful for the interpretation of CPTs at locations where no information from boreholes is available, as the correction of the measured cone penetration resistance for total stress can have large influence on the applied undrained shear strength (assuming a known N_{kt}).

From the dissipation tests in this research there are indications that the measurement of the excess pore water pressure u_2 is not reliable. The excess pore water pressures are important for the correction of the measured cone penetration resistance. Therefore the excess pore water pressure influences N_{kt} but also the applied undrained shear strength. Furthermore the excess pore water pressures are used for classification purposes, in order to assess whether a soil layer should be characterised as an undrained soil or a drained soil. Therefore it is recommended to investigate whether the u_2 measurements are reliable and work on improvements when required.

Based on the results of this research sample disturbance is likely to be of minor importance for the uncertainty of N_{kt} . The recovery ratios smaller than one, changes in volume of the samples and consequently the changes in soil unit weight indicate however that sample disturbance play a role. Therefore it is recommended to investigate the possibilities of improvement of sampling methods. Some suggestions to improve sample quality are the use of Teflon lubrication at the inside of the sampling tubes, extruding the samples immediately from the sampling tubes when the tubes arrive in the laboratory, cutting the sampling tubes to release the samples instead of extruding the samples out of the tubes, use the complete sample with the diameter from the sampler instead of trimming the samples to a smaller diameter. Piston samplers may perform better when the sampling tubes are shorter. Consolidation procedures can also have influence on the structure of soil samples (Hight et al., 2003).

References

- A. S. T. M. D5778. (2012). Standard Test Method for Electronic Friction Cone and Piezocone Penetration Testing of Soils. West Conshocken, PA, United States: ASTM International.
- Azzouz, A. S., Baligh, M. M., & Ladd, C. C. (1983). Corrected field vane strength for embankment design. *Journal of Geotechnical Engineering*, 109(5), 730-734.
- Becker, D. E., Crooks, J. H., & Been, K. (1988). Interpretation of the Field Vane Test in Terms of In-Situ and Yield Stresses in Vane Shear Strength Testing in Soils. *Field and Laboratory Studies*, Richards, AF, Editor, ASTM, 71-87.
- Been, K., & Jefferies, M. G. (1992). Towards systematic CPT interpretation. In *Proceedings of the Wroth Symposium*, Oxford, U.K. pp. 44–55.
- Begemann, H. K. (1965). The Friction Jacket Cone as an Aide in Determining the Soil Profile. *Proc. 6th. Int. Conf. on Soil Mechanics and Foundation Engineering*. Montreal. Vol. 1, pp. 17-20.
- Berendsen, H. J., & Stouthamer, E. (2000). Late Weichselian and Holocene palaeogeography of the Rhine–Meuse delta, the Netherlands. *Palaeogeography, Palaeoclimatology, Palaeoecology*, 161(3-4), 311-335.
- Biscontin, G., & Pestana, J. M. (2001). Influence of peripheral velocity on vane shear strength of an artificial clay. *Geotechnical Testing Journal*, 24(4), 423-429.
- Bjerrum, L. (1972). *Embankments on Soft Ground, State-of-the-Art Report*, presented at the June 11-14, ASCE Specialty Conference on Performance of Earth and Earth-Supported Structures, held at Lafayette, Ind., Vol. 2, pp. 1-54.
- Bjerrum, L. (1973). Problems of soil mechanics and construction on soft clays and structurally unstable soils. In *Proc. 8th ICSMFE* (Vol. 3, pp. 111-159).
- Boylan, N., Mathijssen, F. A. J. M., Long, M., & Molenkamp, F. (2008). Accuracy of piezocone testing in organic soils. In *Proceedings of the 11th Baltic Sea Geotechnical Conference*, Gdansk, Poland (Vol. 1, pp. 367-375).
- Burland, J. B. (1990). On the compressibility and shear strength of natural clays. *Géotechnique*, 40(3), 329-378.
- Burns, S. E., & Mayne, P. W. (1998). *Penetrometers for soil permeability and chemical detection*. Report No. GIT.
- Calle, E. O. F. (2007). *Statistiek bij regionale proevenverzamelingen: Het ruimtelijk statistische model*. *Geotechniek*, juli 2007. (in Dutch)
- Calle, E. O. F. (2008). *Statistiek bij regionale proevenverzamelingen*. *Geotechniek*, januari 2008. (in Dutch)
- Campanella, R. G. & Kokan, M. J. (1993). A new approach to measuring dilatancy in saturated sands. *Geotechnical Testing Journal*, ASTM, 16 (4), 485-95.
- Cao, Z., Wang, Y., & Li, D. (2017). *Probabilistic Approaches for Geotechnical Site Characterization and Slope Stability Analysis*. Springer-Verlag GmbH Berlin Heidelberg. ISBN 978-3-662-52912-6.
- Carroll, R., & Paniagua Lopez, A. P. (2018). Variable rate of penetration and dissipation test results in a natural silty soil. In *Cone Penetration Testing IV: Proceedings of the 4th International Symposium on Cone Penetration Testing (CPT 2018)*, June 21-22, 2018, Delft, The Netherlands.
- Cerato, A. B., & Lutenecker, A. J. (2004). Determining intrinsic compressibility of fine-grained soils. *Journal of Geotechnical and Geoenvironmental Engineering*, 130(8), 872-877.
- Chandler, R. J. (1988). The in-situ measurement of the undrained shear strength of clays using the field vane. In *Vane shear strength testing in soils: field and laboratory studies*. ASTM International.
- Chandler, R. J. (2000). The Third Glossop Lecture: Clay sediments in depositional basins: the geotechnical cycle. *Quarterly Journal of Engineering Geology and Hydrogeology*, 33(1), 7-39.

- Colreavy, C., O'loughlin, C. D., & Randolph, M. F. (2015). Estimating consolidation parameters from field piezoball tests. *Géotechnique*, 66(4), 333-343.
- Cohen, K. M. (2003). Differential subsidence within a coastal prism: late-Glacial-Holocene tectonics In The Rhine-Meuse delta, the Netherlands (Doctoral dissertation).
- Coop, M. R. (2015, January). Limitations of a Critical State framework applied to the behaviour of natural and “transitional” soils. In Proceedings of 6th International Symposium on Deformation Characteristics of Geomaterials, IS-Buenos Aires (pp. 115-155).
- Cotecchia, F., & Chandler, R. J. (2000). A general framework for the mechanical behaviour of clays. *Géotechnique*, 50(4), 431-448.
- De Gast, T., Vardon, P. J., & Hicks, M. A. (2017). Estimating Spatial Correlations under Man-Made Structures on Soft Soils. *Geo-Risk 2017 GSP* 284.
- De Gast, T., Vardon, P. J., & Hicks, M. A. (2018). Detection of soil variability using CPTs. In: *Cone Penetration Testing 2018*. Eds.: Hicks, M.A., Pisanò, F., Peuchen, J.
- Deltares (2009). SBW Werkelijke Sterkte, onderdeel Sterkte bij lage spanningen - 02 foutenanalyse. Deltares report 1001463-000-GEO-0001, Versie 2, 18 maart 2009. (in Dutch)
- Deltares (2014). Dijken op Veen II, Eindrapport Heterogeniteit. Report 1208254-019-GEO-0001, Version 01, 30 april 2014, concept. (in Dutch)
- Deltares (2016a). Protocol sonderen voor Su-bepaling. Projectnummer 1220083-010-GEO-0006, 1 juni 2016, definitief. (in Dutch)
- Deltares (2016b). Protocol laboratoriumproeven voor grondonderzoek aan waterkeringen. Report 1230090-019-GEO-0002, Versie 03, 25 mei 2016, definitief. (in Dutch)
- Den Haan, E.J. (1994). Vertical compression of soils. PhD-thesis Delft University of Technology.
- Edil, T. B. (2001). Site characterization in peat and organic soils. Proceedings of the international conference on in situ measurement of soil properties and case histories (eds P. P. Rahardjo and T. Lunne), pp. 49–59. Bali, Indonesia: Parahyangan Catholic University.
- Fenton, G. A. (1999). Estimation for Stochastic Soil Models. *Journal of Geotechnical and Geoenvironmental Engineering*, Vol. 125, No. 6, June, 1999.
- Gouw, M. J. P., & Erkens, G. (2007) Architecture of the Holocene Rhine-Meuse delta (the Netherlands) – A result of changing external controls. *Netherlands Journal of Geosciences — Geologie en Mijnbouw* | 86 – 1 | 23 - 54 .
- L'Heureux, J. S., Gundersen, A. S., D'Ignazio, M., Smaavik, T. F., Kleven, A., Rømøen, M., ... & Hermann, S. (2018). Impact of sample quality on CPTU correlations in clay—Example from the Rakkestad clay. In *Cone Penetration Testing IV: Proceedings of the 4th International Symposium on Cone Penetration Testing (CPT 2018)*, June 21-22, 2018, Delft, The Netherlands.
- Hight, D. W., Paul, M. A., Barras, B. F., Powell, J. J. M., Nash, D. F. T., Smith, P. R., Jardine, R. J., & Edwards, D. H. (2003). The characterisation of the Bothkennar Clay. In: *Characterisation and Engineering Properties of Natural Soils – Tan et al. (eds.)*. Swets & Zeitlinger, Lisse, ISBN 90 5809 537 1.
- Hijma, M. P., Cohen, K. M., Hoffmann, G., Van der Spek, A. J. F., & Stouthamer, E.. (2009). From river valley to estuary: the evolution of the Rhine mouth in the early to middle Holocene (western Netherlands, Rhine-Meuse delta). *Netherlands Journal of Geosciences — Geologie en Mijnbouw* | 88 – 1 | 13 - 53 .
- Hijma, M. P., & Cohen, K. M. (2011). Holocene transgression of the Rhine river mouth area, The Netherlands/Southern North Sea: palaeogeography and sequence stratigraphy. *Sedimentology*, 58(6), 1453-1485.
- Houlsby, G. T. & Teh, C. I. (1988). Analysis of the Piezocone in Clay, *Penetration Testing*, Vol. 2, Balkema, Rotterdam, 1988, pp. 777-783.
- I&M (2017). Schematiseringshandleiding macrostabiliteit. WBI 2017. Ministerie van Infrastructuur en Milieu. 15 november 2016.

- Jardine, R. J., Gens, A., Hight, D. W., & Coop, M. R. (2004). Developments in Understanding Soil Behaviour. In *Advances in geotechnical engineering: The Skempton conference: Proceedings of a three day conference on advances in geotechnical engineering*, organised by the Institution of Civil Engineers and held at the Royal Geographical Society, London, UK, on 29–31 March 2004 (pp. 103-206). Thomas Telford Publishing.
- Jefferies, M. G. & Davies, M. P. (1991). Soil classification by the cone penetration test: Discussion. *Canadian Geotechnical Journal*, 28, 1, 173–468.
- Kimura, T., & Saitoh, K. (1983). Effect of disturbance due to insertion on vane shear strength of normally consolidated cohesive soils. *Soils and foundations*, 23(2), 113-124.
- van der Krogt, M. G., Schweckendiek, T., & Kok, M. (2018). Uncertainty in spatial average undrained shear strength with a site-specific transformation model. *Georisk: Assessment and Management of Risk for Engineered Systems and Geohazards*, 1-11.
- Ladd, C. C. (1991). Stability evaluation during staged construction. *Journal of Geotechnical Engineering*, 117(4), 540-615.
- Ladd, C. C., & DeGroot, D. J. (2004). Recommended practice for soft ground site characterization: Arthur Casagrande Lecture, 12th Panam. In *Conf. on Soil Mechanics and Geotechnical Engineering*.
- Ladd, C. C., & Foott, R. (1974). New design procedure for stability of soft clays. *Journal of Geotechnical and Geoenvironmental Engineering*, 100 (Proc Paper 10064).
- Larsson, R., Bergdahl, U., & Eriksson, L. (1987). Evaluation of shear strength in cohesive soils with special reference to Swedish practice and experience. *Geotechnical Testing Journal*, 10(3), 105-112.
- Larsson, R., & Åhnberg, H. (2005). On the evaluation of undrained shear strength and preconsolidation pressure from common field tests in clay. *Canadian geotechnical journal*, 42(4), 1221-1231.
- Lu, Q., Randolph, M. F., Hu, Y. & Bugarski, I. C. (2004). A numerical study of cone penetration in clay. *Géotechnique* 54, No. 4, pp. 257–267.
- Lunne, T., Berre, T., Andersen, K. H., Strandvik, S., & Sjørusen, M. (2006). Effects of sample disturbance and consolidation procedures on measured shear strength of soft marine Norwegian clays. *Canadian Geotechnical Journal*, 43(7), 726-750.
- Mayne, P. W. (2007). *Cone penetration testing* (Vol. 368). Transportation Research Board.
- Mitchell, J. K., & Soga, K. (2005). *Fundamentals of soil behavior* (Vol. 3). New York: John Wiley & Sons.
- Morris, P. H., & Williams, D. J. (2000). A revision of Blight's model of field vane testing. *Canadian geotechnical journal*, 37(5), 1089-1098.
- NEN 5104 (1989). *Geotechniek - Classificatie van onverharde grondmonsters*. Nederlands Normalisatie Instituut.
- NEN-EN-ISO 22476-1. (2013). *Geotechnisch onderzoek en beproeving – Veldproeven – Deel 1: Elektrische sondering*. Nederlands Normalisatie Instituut.
- Nocilla, A., Coop, M. R., & Colleselli, F. (2006). The mechanics of an Italian silt: an example of 'transitional' behaviour. *Géotechnique*, 56(4), 261-271.
- Peuchen, J., & Terwindt, J. (2014). Introduction to CPT accuracy. In *International symposium on cone penetration testing* (Vol. 3, pp. 12-14).
- Robertson, P. K. (1990). "Soil classification using the cone penetration test." *Can. Geotech. J.*, 27 (1), 151–158.
- Robertson, P. K. (1999). "Estimation of minimum undrained shear strength for flow liquefaction using the CPT." *Proc., 2nd Int. Conf. On Earthquake Geotechnical Engineering*, Balkema, Rotterdam, The Netherlands.
- Schlue, B. F., Moerz, T., & Kreiter, S. (2010). Influence of shear rate on undrained vane shear strength of organic harbor mud. *Journal of geotechnical and geoenvironmental engineering*, 136(10), 1437-1447.
- Schnaid, F. (2008). *In situ testing in geomechanics: the main tests*. CRC Press.

- Schoeneberger, P.J., Wysocki, D.A., Benham, E.C., and Soil Survey Staff. (2012). Field book for describing and sampling soils, Version 3.0. Natural Resources Conservation Service, National Soil Survey Center, Lincoln, NE.
- Shipton, B., & Coop, M. R. (2015). Transitional behaviour in sands with plastic and non-plastic fines. *Soils and Foundations*, 55(1), 1-16.
- Skempton, A. W. (1970). The consolidation of clays by gravitational compaction. *Q. J. Geol. Soc. Lond.*, 125, 373-412.
- Skempton, A. W & Northey, R. D. (1952). The sensitivity of clays. *Géotechnique*, 3, 30-53.
- Smith, P. R. (1992). Properties of high compressibility clays with reference to construction on soft ground. PhD Thesis, University of London.
- Spry, M. J., Kulhawy, F. H., & Grigoriu, M. D. (1988). Reliability based foundation design for transmission line structures: Geotechnical site characterization strategy, Report EL-5507(1). Palo Alto, CA: Electric Power Research Institute.
- Tanaka, H. (2000). Sample quality of cohesive soils: lessons from three sites, Ariake, Bothkennar and Drammen. *Soils and foundations*, 40(4), 57-74.
- TAW (2002). Technisch Rapport Waterkerende Grondconstructies. Technische Adviescommissie voor de Waterkeringen. Juni 2001. ISBN 90-369-3776-0.
- Teh, C. I. & Houlsby, G. T. (1988). Analysis of the cone penetration test by the strain path method. In: *Numerical Methods in Geomechanics*. Innsbruck. Swoboda (ed.). Balkema, Rotterdam.
- Vanmarcke, E. H. (1977). Reliability of Earth Slopes. *Journal of the Geotechnical Engineering Division*. Vol. 103, No. GT11, November 1977.
- Zhang, G., Robertson, P.K., & Brachman, R.W.I. (2002). "Estimating liquefaction induced ground settlements from CPT for level ground." *Can. Geotech. J.*, 39 (5), 1168–1180.
- Zwanenburg, C. & Jardine, R. J. (2015). Laboratory, in situ and full-scale load tests to assess flood embankment stability on peat. *Géotechnique* 65, No. 4, 309–326.

A Measurement sites

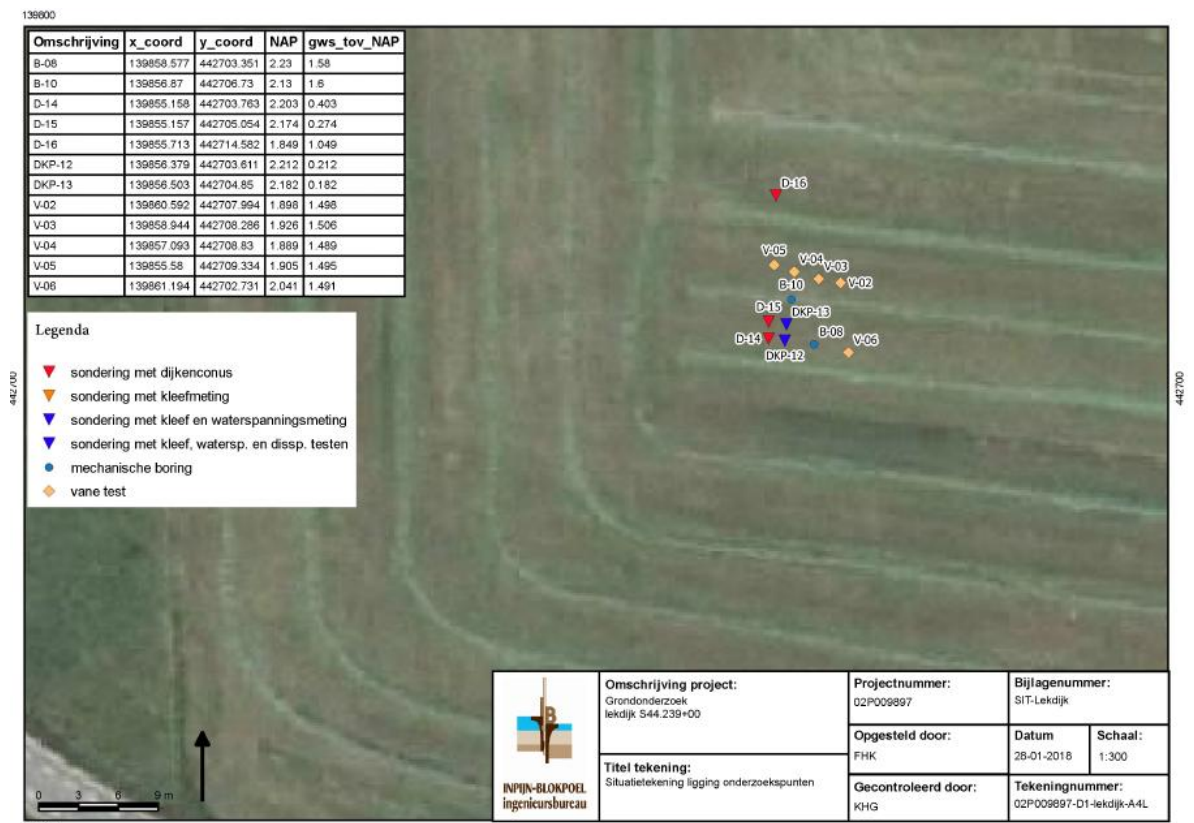


Figure A.1 Location Lekdijk at S44_239_00 near Schalkwijk in the dike trajectory Amerongen – Schoonhoven.

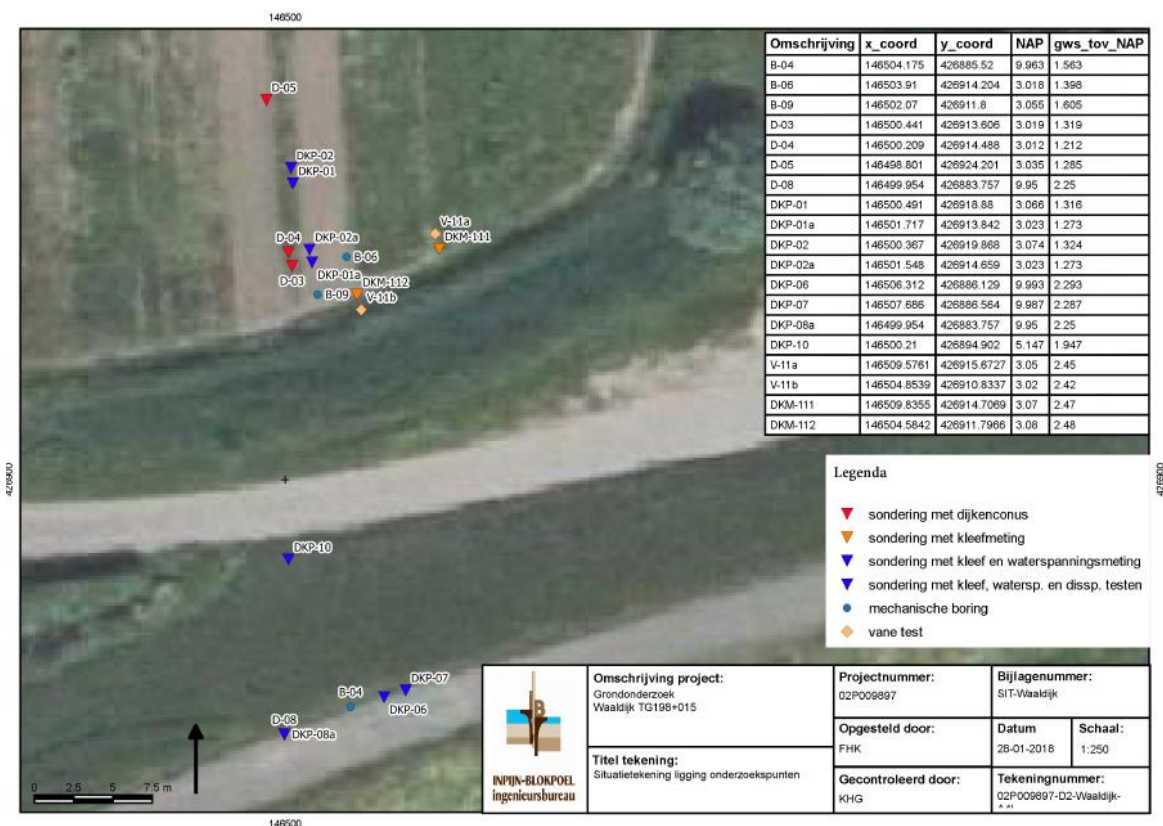


Figure A.2 Location Waaldijk at TG198+015 in Waardenburg in the dike trajectory Tiel – Gorinchem.



Figure A.3 Location Achterwaterschap at AC 251 near Alblasserdam with the locations of the class 1+ cones (red points) and class 1 cones (blue points).



Figure A.4 Location AC 075 at the north dike of the drainage canal Achterwaterschap with the locations of the class 1+ cones (red points) and class 1 cones (blue points).










Figure A.5 Location AC 090 at the north dike of the drainage canal Achterwaterschap with the locations of the class 1+ cones (red points) and class 1 cones (blue points).






B Legend borehole descriptions

Legend of borehole descriptions with color codes according to the Dutch NEN 5104 classification system and texture definitions according to the USDA classification system (Schoeneberger et al., 2012).


Clay

	Clay
	Clay, silty clay
	Clay loam, silty clay loam
	Loam, silt loam
	Sandy clay loam, sandy loam
	Sandy loam, loamy sand
	Loamy sand, sandy loam



Sand

	Sand, loamy sand
	Sand
	Sand, loamy sand
	Loamy sand, sandy loam
	Sandy loam







Peat

	Peat
	Peat, clayey
	Peat, very clayey
	Peat, sandy
	Peat, very sandy

Loam

	Silt loam
	Silt loam, silt

Additives

	Organic
	Moderate organic
	Very organic
	Gravel
	Moderate gravel
	Many gravel

